Politecnico di Torino

Master of Science in Civil Engineering

Master's Degree Thesis

Tunneling in complex soft Bimrock formations: Numerical analyses

Supervisors

PROF. MONICA BARBERO

DR. MARIA LIA NAPOLI

Candidate

RIDA ASIM

JULY, 2023

Acknowledgements

First of all, I would like to thank my creator, for giving me the stamina and health to finish this. Secondly my immense gratitude goes out to Prof. Monica Barbero and Dr. Maria Lia Napoli. Without their continuous guidance and suggestions in the face of hurdles it would not have been possible for me to achieve this milestone. Last but not the least my family especially my husband who has been my rock throughout the whole process.

INDEX

Abstract

Geotechnically complex formations include materials such as conglomerates, agglomerates, glacial tills and melanges, which are very common geological units and are often defined to be "bimrocks" (block in matrix rocks), "bimsoils" (block in matrix soils) and "SRM" (soil-rock mixtures) in the literature. The term bimrock (block in matrix rocks) was coined by Medley in order to identify heterogeneous materials with hard rock blocks enclosed in a softer matrix of finer texture.

Bimrocks are of great importance as the strength contrast that exists between the rocks and the matrix deems them quite significant in the geotechnical context. There are various case histories in which their presence has caused severe economic challenges during construction works, because of their poor characterization. It is therefore vital to have a geometric and mechanical characterization of these formations in the development stages of building works to avoid facing unnecessary economic issues and safety risks in the future during construction works.

While there has been previous analysis done on Bimrocks, not much work has been done on the presence of an interface between the rock and matrix. While analyzing Bimsoils also, the presence of such interfaces and how their properties can affect underground excavations and other earthworks has not been taken into account.

In this dissertation in order to more deeply understand the differences in the behavior of bimsoils with respect to bimrocks, numerical analyses were carried out by introducing an interface at the block-matrix contacts. The underground excavation of a tunnel having a diameter of 10 m in complex heterogenous bimsoil formations with different Volumetric Block Proportions (VBP) is simulated through FEM numerical analyses with the RS2 code, and the interfaces are represented by Joint boundaries. An arbitrary extraction of the Block distribution that characterizes the geomaterial is made via a statistical approach. Such an approach is based on the Monte Carlo strategy. In this way how the size distribution influences the overall results can be evaluated. For 25% VBP, 8 random block distributions were extracted via a Matlab code in which the blocks are elliptical, and hypothetical in-situ conditions are defined for the analysis. The results of the

analyses are compared with bimrock models, investigated in a previous thesis work and lacking any interfaces. Moreover, with the aim of analyzing bimsoils with different block-matrix interface strength, the properties of the joints are decreased gradually from 100% to 25% of the matrix properties in order to evaluate the effects on tunnel convergence during excavation. So in total 32 model analysis were run. The results showed that joint boundaries had little to no effect on the tunnel excavation.

The same analysis is also carried out for 1 model each of 40% and 70% VBP in order to evaluate if the results were different if the VBP was increased, but it was not the case. The properties of the Joints were then decreased up to 25% of the matrix properties also in order to evaluate the effects. The increase in VBP did not produce significant differences in the results.

Since many heterogeneous block-in-matrix formations are characterized by the presence of joints/schistosity, some of the tunnel models analyzed in the first part of the work (one model for each VBP considered) were modified to incorporate a Joint Network, and novel analyses were carried out both with and without the rock-matrix interfaces. The results were then compared and an increase in the overall radial displacements along the tunnel contour was observed in the case in which along with the Joint network, rock-matrix interfaces were also present. The difference in the displacement was more pronounced for less VBP percentage at 25% as compared to 70%.

Lastly, the equivalent homogenous approach proposed by Lindquist (1994) was modelled assuming different VBPs (25%, 40%, 55% & 70%) with and without the presence of a Joint network, to compare the results. As expected, an anisotropic behavior is observed in the models with joints, with a decreasing trend of displacements and yielding zones with the increase of VBP.

List of Figures

List of Tables

1. Bimsoils/ Bimrocks

1.1 Introduction

In 1984, Raymond adopted the terminology “block-in-matrix rocks” to indicate melanges and olistostromes. The term "melange" comes from the French word mélange meaning a mixture in which various blocks are embedded in an inferior sheared matrix. They are mostly found in mountainous areas linked to tectonic plate movements and subductions. Later on Medley (1994) was the one who then introduced the definition of Bimrock.

For geological formations containing rock blocks embedded in a soil-like matrix, Medley (1994) coined the term "bimsoil" (block-in-matrix soil) (Medley E. , 1994; Kalender A., 2014; Sonmez H. E., 2016. ; Medley, EW and Goodman, RE,, 1994). These are complex materials including rock pieces encircled by soil-like matrix material, such as colluvium and glacial tills. These formations are similar to bimrock, but with an uneven matrix and subpar mechanical properties.

Bimrocks and Bimsoils are found in around 60 countries including the USA, Italy, Turkey, and Iran (Medley E. , 1994) Northern Greece and many Greek Isles as shown in Figure-1.

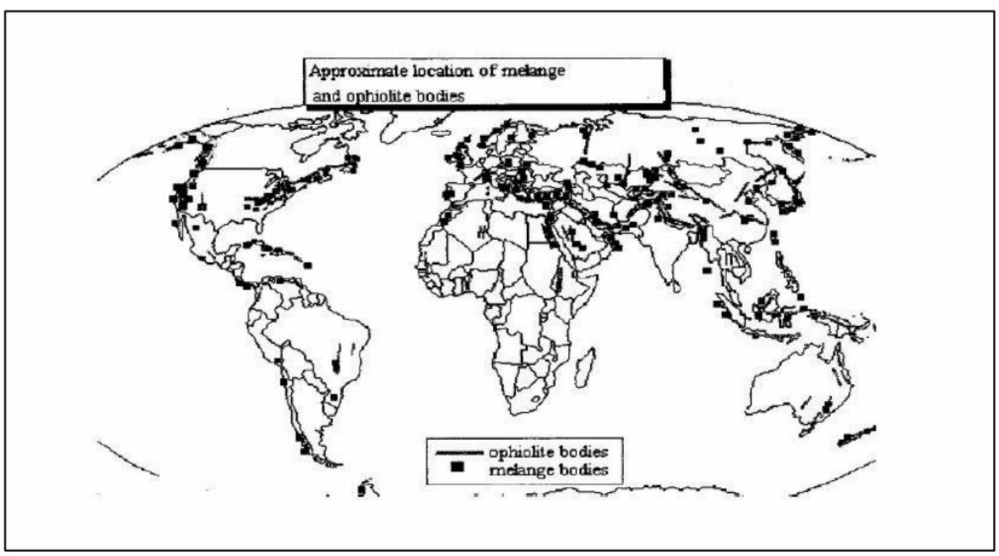

Figure 1- Worldwide mapping of mélanges (Medley E. , 1994)

They are basically a mixture of rocks having superior mechanical properties than the matrix they are embedded into. Since a strength contrast exists between the rocks and the matrix, the blocks are termed "geotechnically significant" which according to (Medley E. , 2002), should be of the order of two or greater i.e. $\tan \varphi_{block} / \tan \varphi_{matrix} \geq 2$ and $E_{block}/E_{matrix} \geq 2$ which is the minimum requirement of strength contrast between the two. Some examples of Bimrocks can be seen in Figure-2.

(a) (b)

Figure 2- Pictures of Different kinds of BimRocks (a) Decomposed granite: a weathered rock located in the Sierra Nevada mountains of California. (Medley E. , 2007a) (b) Wall of a quarry showing Sheared rock surrounding hard blocks of relatively intact rock in California. (E. Medley 1994).

The strength contrast is what can influence the mechanical characterization of the whole. For this reason, it is necessary to have a threshold to differentiate between the two components (matrix and blocks). This is based on the scope of the engineering problem under study. In other words, the characteristic engineering dimension is what decides this threshold (Paragraph 1.3.2).

They are a hot topic of research nowadays because there is a high degree of mechanical, lithological and spatial variability associated with them which leads to challenges in their characterization. Mischaracterizations often occur and can lead to difficulty in design and construction in such complex formations deeming them necessary to be studied more closely.

1.2 Problems associated with Bimrock identification

While carrying out survey and mapping works in the early design stages it is extremely necessary to have correctly characterized the presence of Bimrocks and to understand their characteristics during the exploration phases. Lack of adequate knowledge can lead to disastrous results and to severe economic consequences if for example large rocks blocks are encountered in the excavation activities and works need to be stopped as appropriate steps were not taken initially to tackle this sort of a problem.

Mischaracterizations of such materials can often occur as it is difficult to obtain undisturbed samples due to the different mechanical strength of the blocks and the matrix. The boreholes may not record the entire picture of the strata underneath if no rocks are encountered along the depth of the borehole. The driller can also misinterpret the presence of a large rock block as a bedrock leading to wrong subsoil characterization.

Moreover, since drillings may not necessarily pass through the largest block dimension, rather chords are measured which may significantly underestimate the block sizes. Figure-3 shows how the depth of the borehole can affect the interpretation of the subsoil.

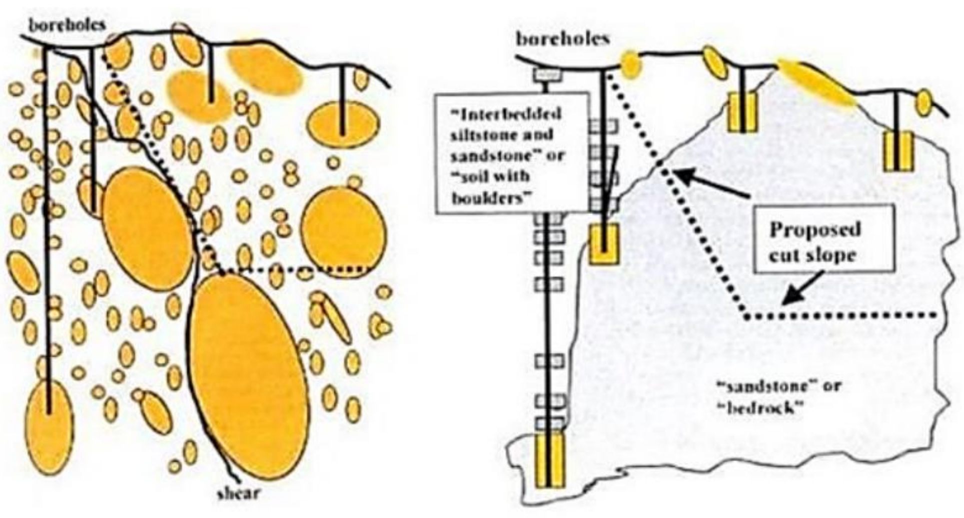

Figure 3- Rock Mass in Bimrock formation with soil profile based on Bore hole log data (Medley E. , 1999)

In such a material the Borehole data cannot be connected to obtain continuous strata as it is not a representative picture of the whole soil underneath. There is a possibility of field tests also but they are an unconventional and costly venture. Hence there is a tendency to underestimate the size of the geometrically larger inclusions and to overestimate the geometry of the smaller ones, with 1D (one-dimensional) analysis using boreholes, due to an incorrect interpretation of the extracted samples.

1.3 Bimrocks Characteristics

While studying such a material it is of utmost importance to examine the material in detail particularly the arrangement, dimensions and percentage of blocks in the matrix. As the arrangement of blocks and their presence is what differentiates the material from a continuum matrix. Potential irregular failure surface trends can occur due to redistribution caused by external stresses dependent on the blocks arrangement in the material under study. (Irfan, T.Y., Tang, K.Y, 1995; Lindquist, E.S., Goodman, R.E., 1994; Medley E. , 1994; Medley E. , 2004; Medley E. , 2007a; Medley E., 2007b; Medley, E., Sanz Rehermann, P.F., 2004).

1.3.1 Block Size Distribution & scale invariance

Bimrocks can be composed of blocks having significant geometric variations from millimeters to tens of kilometers (Medley, E., Lindquist, E.S., 1995). From the start, the self-similarity of melanges was apparent after observing the outcrops of Franciscan melange (located in Mendoncino, California, in the Franciscan coastal belt) and the Geological mapping of complex block-in-matrix formations, focusing on California mélanges and ophiolites.

Scale invariance and self-similarity are typical properties of *fractals,* a term which comes from a latin word *frangere* meaning “to break”. Which essentially means that regardless of the scale of observation of the problem, the geometrical properties remain the same.

Studies have indicated Bimrocks Block size distribution to be fractal (Medley E. , 1994; Medley, E., Lindquist, E.S., 1995; Riedmueller G., 2001; Medley E. , 2002). They are defined by the negative power law (Turcotte, 1986) given as follows:

$$N = n^{-D} \tag{1}$$

Where N is the number of elements and n is the size of the elements and D is a fractal dimension (Mandelbrot, 1983; Turcotte, 1986) by which the fractals are defined, where D (Peitgen, 1992):

$$D = \frac{logN(n)}{\log(n)} \tag{2}$$

Theoretically the power law means the frequency of smaller blocks in the heterogeneous material is higher than that of the larger blocks.

Quantitative measurements to indicate the self-similarity of Mélanges were first carried out by (Lindquist E. , 1991) measuring mélange outcrop dimensions referring to more than 1900 blocks recording d_{mod} for each as shown in Figure-4.

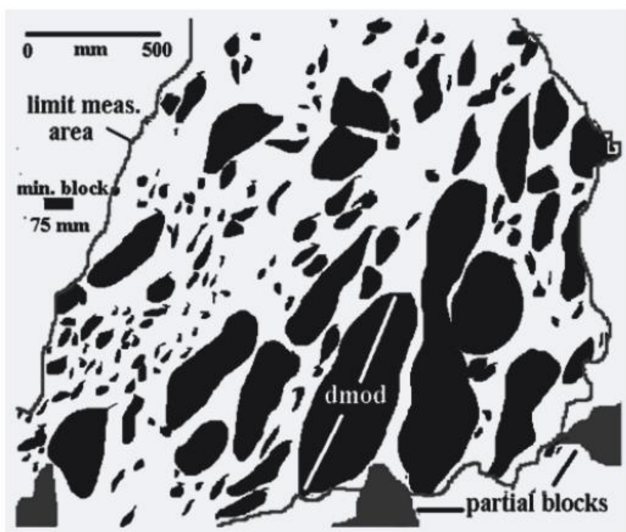

Figure 4- Franciscan mélange outcrop at Caspar Headlands, Mendocino Co., Northern California showing d_{mod}: maximum visible dimension (Medley, E., Lindquist, E.S., 1995)

His works were later on continued by Medley who, by defining several block size classes, plotted log histograms of block sizes and relative frequencies at different scales. Two of those histograms can be seen in Figure-5. The node end class was taken as a representative of each class interval and was calculated by taking 5% of the square root of the relative analyzed area ($0.05\sqrt{A}$).

Photogrammetric methods were used to determine the d_{mod} of all the blocks in the area.

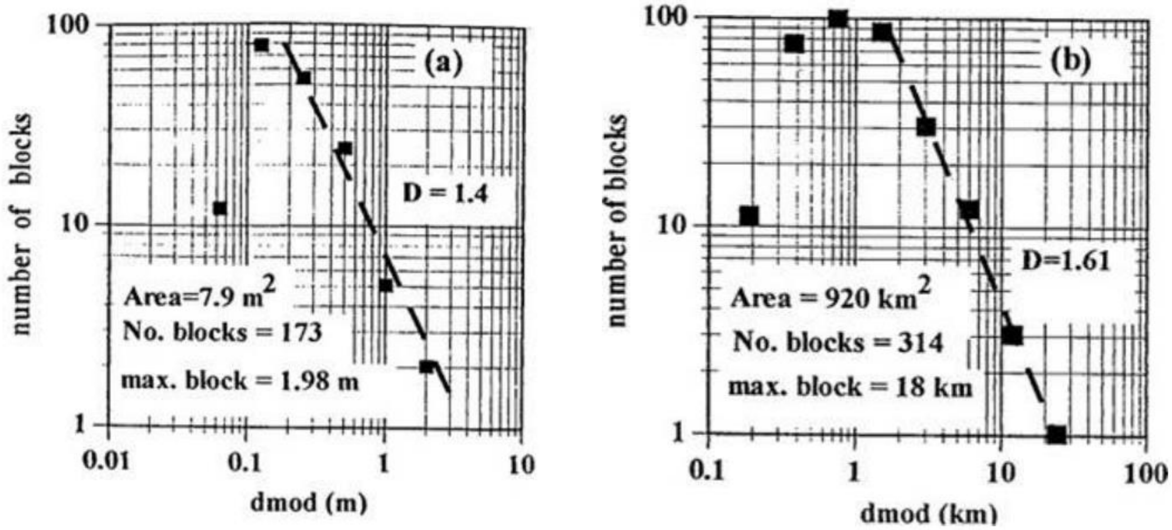

Figure 5- Examples of Histograms of 2 areas prepared by medley (Medley E. , 1994)

The results clearly showed a self-similarity despite there being a large difference in the areas of the two. Using such histograms, size and the number of blocks in a mélange can be obtained.

Medley (1994) normalized many such histograms including data from all the measurement areas and outlined the main characteristics of a bimrock as a function of the blocks sizes.

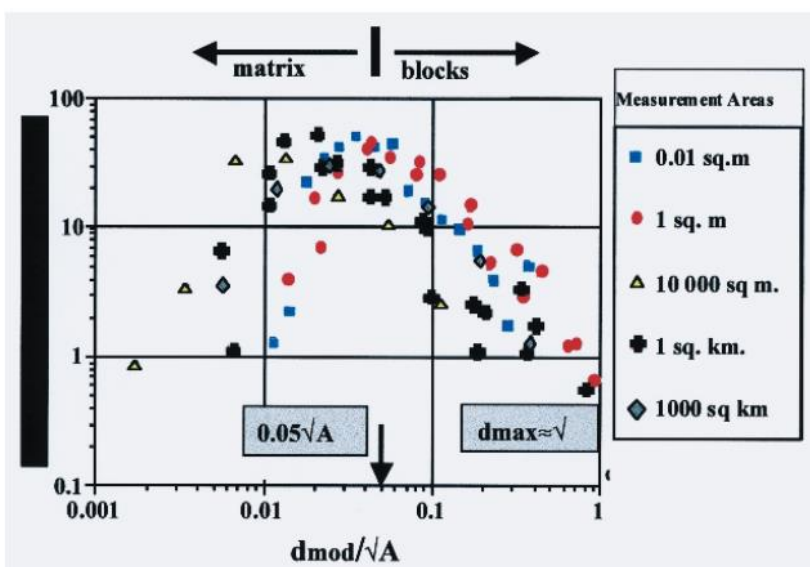

Figure 6- Normalized block size distribution curves for 1,928 blocks measured from outcrops and geological maps of several Franciscan mélanges ranging over seven orders of magnitude in scale, ranging from centimeters to kilometers (Medley E. , 1994)

As apparent from Figure-6, all block size distributions had a parabolic shape with the largest block size being equal to $\sqrt{A}$ where A is the characteristic Engineering dimension. The peak relative frequency was obtained at $5\%\sqrt{A}$ and 99% of the blocks were smaller than $75\%\sqrt{A}$. Hence this in turn gave a threshold that now allows us to approximately differentiate between a block and the matrix.

Material smaller than $0.05\sqrt{A}$ would be characterized as part of the matrix and $0.75\sqrt{A}$ regarded as the largest block dimension d_{max} above which the complex formation would be considered as a fractured rock mass. (Riedmueller G., 2001; Medley E. , 2001; S. Kahraman, 2006).

1.3.2 Characteristic Engineering Dimension

The characteristic Engineering dimension, Lc, is a measure that describes the geometry of the problem under consideration (Medley E. , 1994). Being aware of the type of work in question, we can evaluate the part of the work that interacts with the rock mass; which in different cases can be either the diameter of a tunnel (Button, 2001), the width of a dam foundation (Goodman, RE, Ahlgren, CS, 2000) the average depth over the length of a slip surface slope (Medley E. S., 2004), or the height of the soil sample subjected to in situ mechanical tests (Xu W. Y., 2008).

Hence the scale of interest can range from millimeters in case of laboratory testing to meters in engineering works. And since blocks can occur at any scale, owing to their nature of being scale independent, this dimension needs to be defined each time.

The block/matrix threshold can be described in many ways $0.05Lc$, $0.05\sqrt{A}$ or $0.05d_{max}$ where A can be a project site or excavation area, and d_{max} the largest block dimension.

Medley (2001) considered a project area of 100 mq containing Francisian Mélange. He took the reference engineering dimension as $\sqrt{A} = 100\ m$. On the basis of this size, the block/matrix threshold would be $0.05\sqrt{A} = 5\ m$ with the largest block equal to $0.75\sqrt{A} = 75\ m$. Hence working at this scale any block smaller than 5m will be considered a part of the matrix.

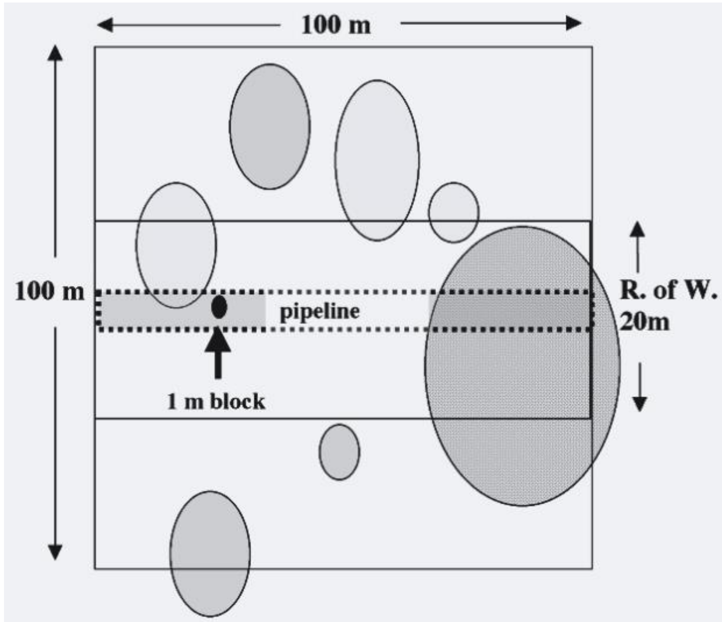

Figure 7- Sketch of Bimrock showing Influence of different engineering works on the scale dimension of interest (Medley E. , 2001)

Taking the example of Figure-7, if we consider the construction of a Road our Lc is 20 m which is the right of way. At this scale the 1 m block is at the block/matrix threshold (0.05 Lc) and the largest significant block is 15 m (0.75 Lc). So in this case blocks greater than 1m can create construction difficulties.

Similarly, at the scale of 2m wide pipeline, the Lc is the depth of the trench (2m). The matrix/block threshold in this case is 0.1m and the largest geotechnically significant block is 1.5m. Hence 1 m block will now be considered as a rock block to the scale of pipeline and the block to the right as a massive rock body.

1.3.3 Estimation of Volumetric Block Percentage (VBP)

The ratio between the volume of the blocks and the total volume of the heterogeneous mass is expressed by the VBP Percentage. The presence of blocks with a range of sizes adds strength to a bimrock by forcing tortuous failure surfaces to tortuously negotiate around blocks. (Irfan, T.Y., Tang, K.Y, 1995; Lindquist E. , 1994; Lindquist, E.S., Goodman, R.E., 1994; Goodman, RE, Ahlgren, CS, 2000; Sonmez H. A., 2006a; Sonmez H. G., 2006b; Sonmez H. K., 2009).

The mechanical resistance values of the bimrocks/bimsoils formations are strongly influenced by the volumetric percentage of the blocks if the VBP ranges between 20-25% up to 70-75%. Hence their accurate estimation is of vital importance.

It can be estimated via geological surveys carried out in two dimensions through mapping and analysis of photographs, by measuring the areal block proportions from outcrops. Manual and computer-aided image analyses were used by Medley and Goodman (1994) for VBP estimation. One dimensional methods such as explorative drilling or a sieve analysis of a sample in the laboratory, involving separation of the block and the matrix, can also be used to estimate the VBP. The latter method is not feasible on site.

Problems with using one-dimensional analysis (Linear Block Proportion, LBP) is that through drilling it cannot be said with absolute certainty that we're able to intersect the maximum dimension of a block within the bimrock/bimsoil formation under examination, as the block size is indicated by the chord length, the intercept between the boring and the block, which is rarely equal to the actual diameter or the maximum block dimension (Figure-8). This can lead to under estimations up to 33% and 55% of the maximum block size (Lindquist, E.S., Goodman, R.E., 1994; Medley E. , 1997; Medley E. , 2001; Medley E. , 2002).

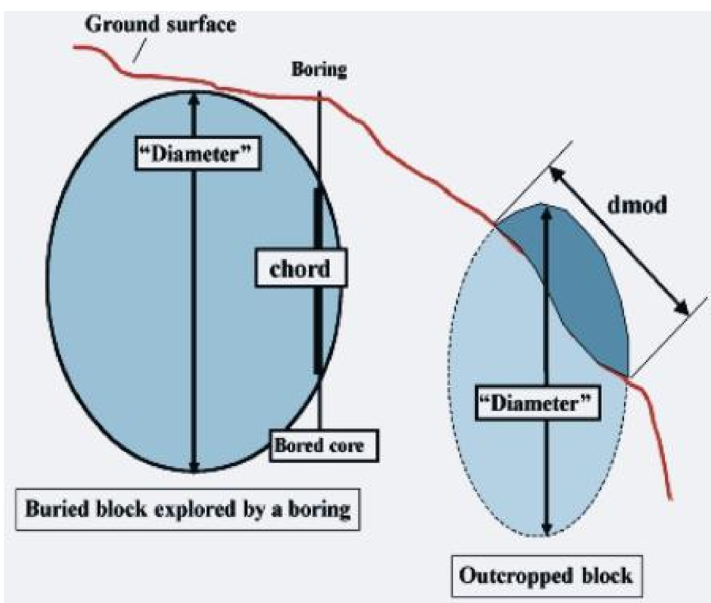

Figure 8- Comparison of two-dimensional and one-dimensional analysis; dmod is the maximum observable size and chord which is the intersection length between the hole and the block itself (Medley E. , 2001)

Two-dimensional analysis relies on image analysis hence it is closely linked to a good chromatic representation, and if the color contrast between the blocks and the matrix is not well defined it might lead to inaccurate VBP estimations.

Medley (2001) established an experimental approach by drawing scanlines on the specimen side or image analysis of their exteriors, to be able to carry out a description of the estimate of the volume percentage of the blocks in the considered domain based on the assumption that they are the same as the measured linear block proportions. He fabricated physical models of mélange with known block size distributions and volumetric block proportions and explored the models with hundreds of model boreholes. The experiments showed that measured linear block proportions had to be adjusted by an uncertainty factor to yield an appropriate estimate of the volumetric block proportion.

Medley (1994a) described methods of approximating block proportions from scanlines drawn on the side of specimens or image analysis of specimen exteriors, although these measures are generally not the same as volumetric proportions.

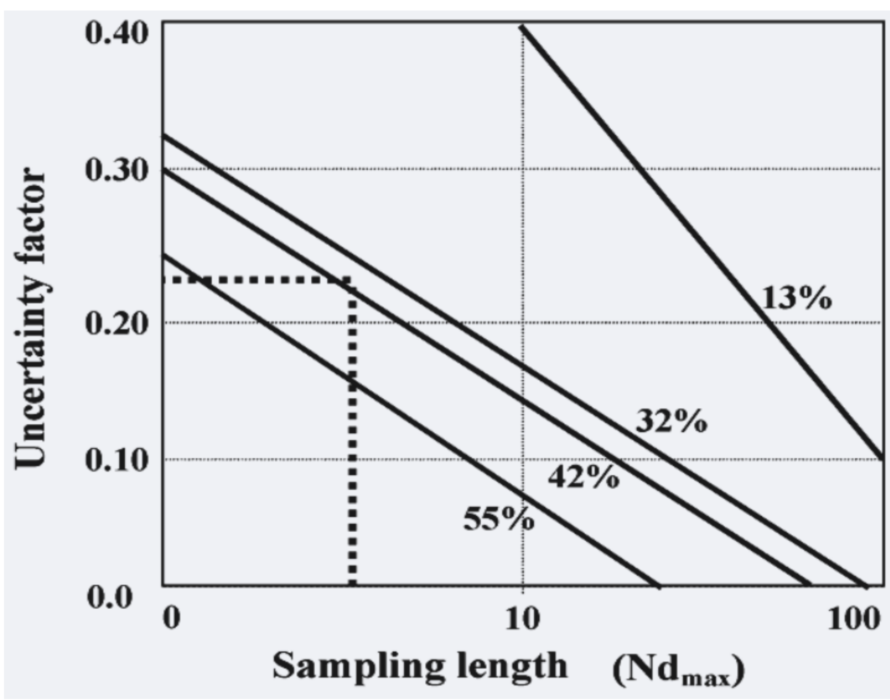

Figure 9- Uncertainty in estimates of VBP as a function of the length of linear measurement (LBP), expressed as a multiple (N) of the length of the largest block (d_{max}), and the measured linear block proportion (13 to 55 %). (Medley E. , 2001)

In the Figure-9 the uncertainty factor is a ratio between Standard deviation and actual Volumetric proportions. N^*d_{max} is the total sampling length as a multiple of the largest block dimension d_{max}. The plot indicates that as volumetric proportion increases from 13-55% the uncertainty decreases and it also decreases with an increase in sampling length.

Hence chord length distributions can be converted to 3D block size distributions considering the statistical uncertainties. This uncertainty chart of Medley (2001) has been used by geo-practitioners for VBP estimations.

2. Mechanical Characterisation of BimRocks

Bimrock formations have a significant amount of structural variety owing to their chaotic heterogeneous structure containing blocks immersed within a matrix. This makes it difficult to characterize them mechanically. Researchers have found that the strength of the matrix increases with the number of block inclusions (Fig. 1.16) and also that the mechanical characteristics of bimrocks are influenced not only by VBP but also by the position, size, shape, and orientation of the blocks in the weak matrix. They cause the mixture to stiffen, the frictional strength of the bimrock to rise, the cohesion to decrease/increase, and tortuous failure surfaces to negotiate around the blocks.

According to Lindquist (Lindquist E. , 1994; Lindquist, E.S., Goodman, R.E., 1994), the volumetric block proportion is closely correlated with the overall rise in strength in the matrix-only model. The strength and deformation are independent of the block strengths.

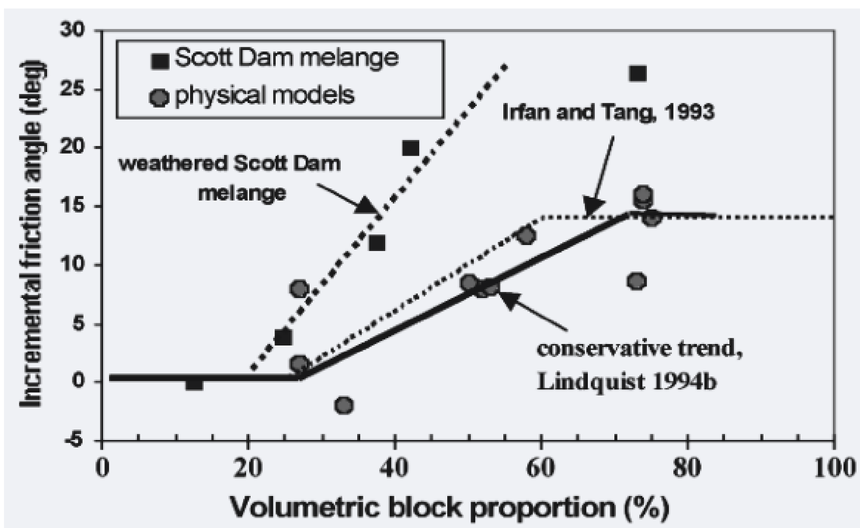

Figure 10- Bimrocks strength increased with increase of VBP. Marked similarity between the data of Lindquist (1994), for physical model melanges, and that of Irfan and Tang, for Hong Kong boulder colluvium with increased frictional strength.

Hence investigations needed to be conducted to ascertain the mechanical properties of bimrocks. Results of various researches are compared in Figure-10.

They were carried out using man-made physical models in laboratories, extensive in-situ testing and finally numerical analyses on fictitious laboratory samples (Barbero M., 2007; Barbero, 2008).

2.1 In-Situ Tests

In Italy at the Santa Barbara abandoned open-pit mine there is Shale-Limestone Chaotic Complex (SLCC) bimrock, whose defining feature is a dark-grey clayey matrix containing calcareous rock pieces of varying sizes. As testing at laboratory scale was not possible due to the variable block dimensions, six unconventional in situ shear tests were conducted to examine it's strength characteristics.

The findings indicated a decent linear positive association between the VBC and the bimrock friction angle, although a crucial VBC threshold (20–25%) appeared to have a significant impact on cohesiveness. Additionally, in line with the typical mechanical behavior of bimrock, the bimrock strength parameters exhibited a general increase in friction angle and a decrease in cohesion when compared to those of the SLCC clayey matrix. (Coli, 2011).

2.2 Laboratory Tests

Since Bimrocks are substantial heterogeneous materials, investigating them on a small scale is not easy. Therefore, researchers in the past have created artificial bimrock samples in the lab which had a particular block composition surrounded by a weaker matrix. This allowed them to study the effects of block content, their orientation, etc., on the mechanical characteristics of the overall Bimrock. Results indicated the failure trends, deformability and strength mainly depend on the VBP when it ranges between 25% to 75% (Lindquist, E.S., Goodman, R.E., 1994; Sonmez,, H., 2004b; Sonmez H. A., 2006a; Barbero, 2012; Coli N., 2012; Afifipour M. M., 2014; Napoli M. B., 2018; Napoli M. B., 2021).

One such example is of Lindquist & Goodman (1994). They carried out triaxial compression tests on synthetic samples with elliptical inclusions, with VBP ranging from 25-75% and 4 different block orientations; 0°,30°, 60° and 90° shown in Figure-11.

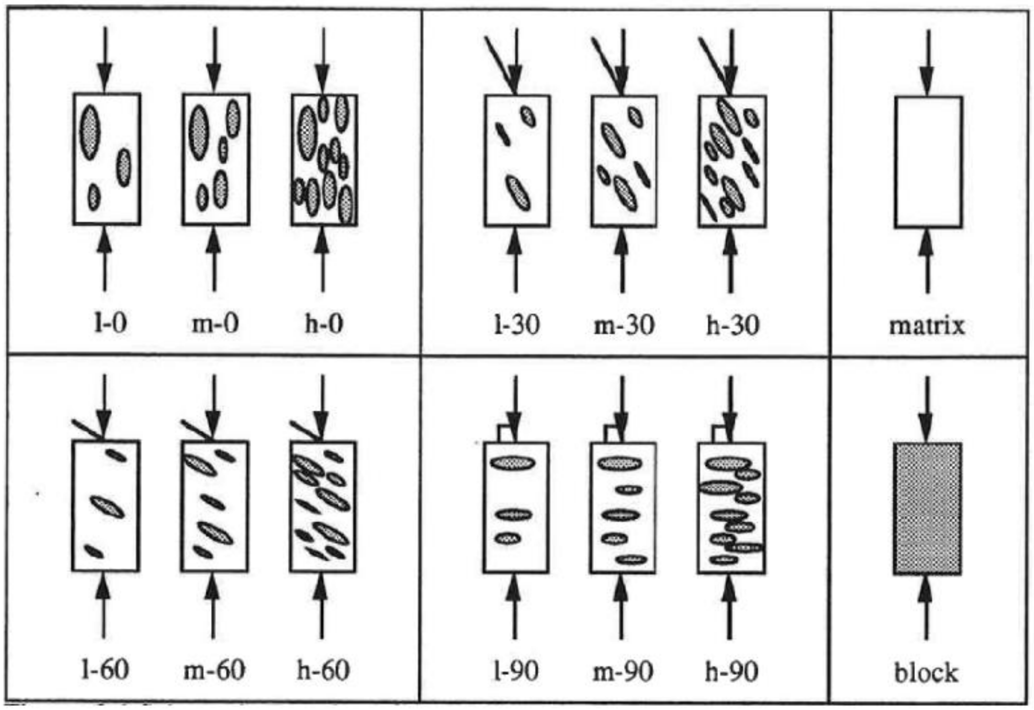

Figure 11- Lindquist's fabricated specimen (Lindquist E. , 1994)

Lindquist (1994) discovered that the angle of friction between the material and the matrix increased by about 15°–20° as a result of the increase in volumetric percentage due to a greater tortuosity of the failure surface. Cohesion, meanwhile, tended to decline as VBP increased. The configuration of the blocks in the reference domain as well as their impact on size and form, needed to be taken into account. The design of the blocks with the main axis at a 30° angle with regard to the direction of application of the axial stress had the lowest values for cohesiveness, in particular. Results are reported in Figure-12.

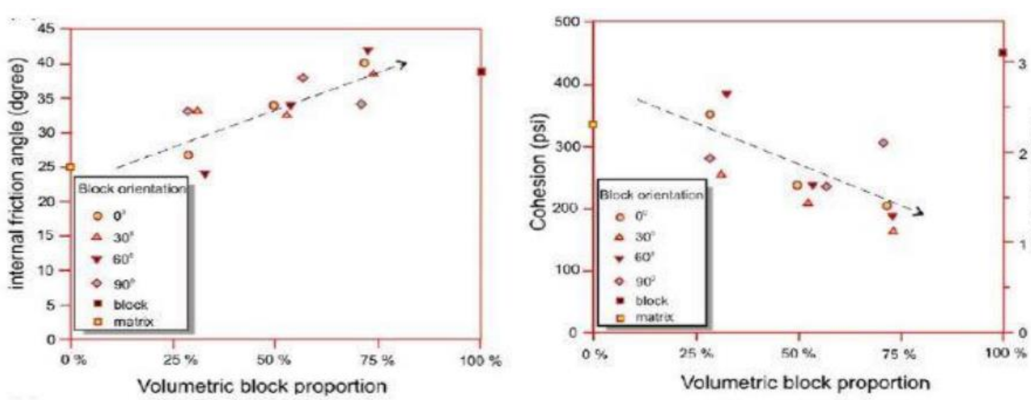

Figure 12- Variation of friction angle (left) and cohesion (right) with VBP (Lindquist E. , 1994)

This led to the development of one such empirical approach to predict the strength parameters (c and φ).

2.2.1 Lindquist Empirical approach

Lindquist gave an expression to determine the shear strength value representable of a mélange, based on the Mohr-Coulomb failure criterion;

$$\tau_p = c_{matrix} \cdot (1 - VBP) + \sigma \; \cdot \tan\big(\varphi_{matrix} + \Delta\varphi_{matrix}(VBP)\big) \tag{3}$$

where;

τ_p represents equivalent shear strength of the Bimrock

c_{matrix} & φ_{matrix} are cohesion and internal friction angle of the matrix

$\Delta\varphi_{matrix}(VBP)$ represents the increase of friction angle 3° for every 10% VBP increase above 25%

It provides the most conservative value of internal friction angle w.r.t VBP as compared to other studies. The approach allows us to model heterogeneous complex formations by taking the presence of blocks into account via the modified mechanical properties considering the complex formation in turn as an equivalent homogenous material.

2.3 Numerical Methods

Numerical modelling is a tool via which we can test samples with sizes ranging to meters. Studies were carried out for the mechanical characterization of bimrocks via such modelling softwares so that the numerical and physical outcomes could be contrasted. One such numerical study in the literature is of M. Barbero (Barbero, 2008) in which a 2D & 3D numerical analyses were carried out to understand the mechanical behavior of the bimrock and to individuate strength and deformability laws suitable for the bimrock as an equivalent continuum. On laboratory samples of bimrock, uniaxial and triaxial compression tests were simulated taking various volumetric ratios of the blocks into account.

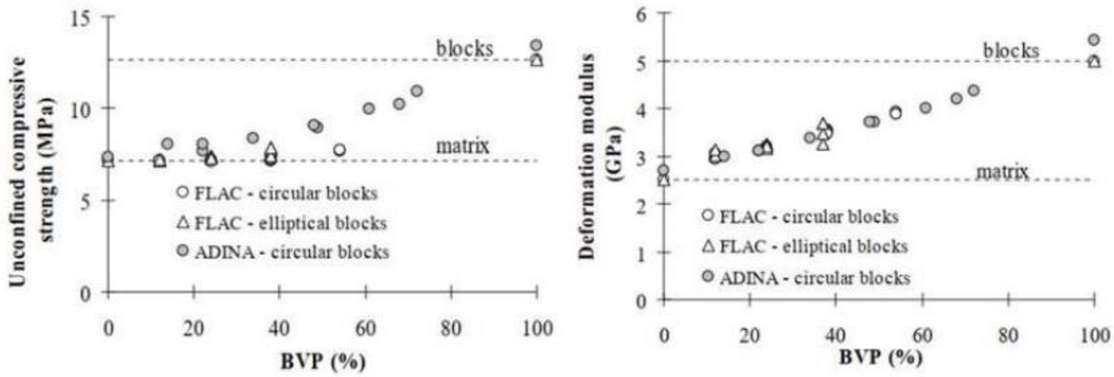

Figure 13- Relationship between VBP and UCS (left) and deformation modulus (right) for 2D analysis. (Barbero, 2008)

Results reported in Figure-13 indicated that for Low VBP (for e.g, 10%) behavior corresponded to that of the matrix and above 20% block influence grew and compressive strength of the bimrock rose linearly with increasing VBP as well as the deformation modulus. Similar results were found for 3D analyses.

Other prominent numerical studies carried out on bimrocks include (Pan, 2008; Xu W. Y., 2008; Xu W. W., 2016).

3. Analysis of Tunneling in Heterogeneous Formations with Rock-Matrix Interface

3.1 Introduction

As not much research is aimed at studying the behavior of the interface between the matrix and the blocks, this dissertation aims to study how such interface material can influence the behavior of bimsoils or soft bimrocks with respect to hard bimrocks. Moreover, since in reality there is a possibility of discontinuities in the displacement field around the blocks, appropriate contact elements should be added to the model to simulate the interaction. (Barbero, 2008)

This thesis is an extension of a previous thesis work of Dadone in which the excavation of a deep tunnel with diameter equal to 10m was analyzed in complex Bimrock formations with varying volumetric block Proportions (VBPs). In this dissertation interfaces between the rock and the matrix are added in those original Bimrock models keeping rest of the material properties the same. The interfaces are assigned the properties equal to that of the matrix in the beginning. The interface strength is then gradually decreased in order to understand the difference in behavior of soft bimrocks with respect to bimsoils via numerical analysis.

3.2 Model Implementation

3.2.1 Block Distribution Generation

In order to take the VBP, block size, shape, location, orientation, and eccentricity of the blocks into account, the stochastic method of (Napoli M. B., 2021) was used to generate random block distributions via a Matlab code. It generated different models with random block distribution for each VBP under study. The Matlab code generated a .txt file containing the coordinates of the elliptical block inclusions which was then used in AutoCAD in order to make a .dxf file of the blocks geometry to be imported in the numerical modeling software RS2.

3.2.2 Numerical Modeling in RS2

The domain of interest (shown in Figure-15) is a square area of 50x50m in which we have randomly placed blocks in the matrix with a tunnel placed at the center having a diameter of 10m. The external domain (Figure-14) is extended 50m on each side of the area of interest in order not to influence the results. A material boundary separated the two and the material outside the area of interest is taken as elastic homogeneous material with same the properties as that of the matrix. The mesh is discretized with a triangular mesh having mid-sized nodes.

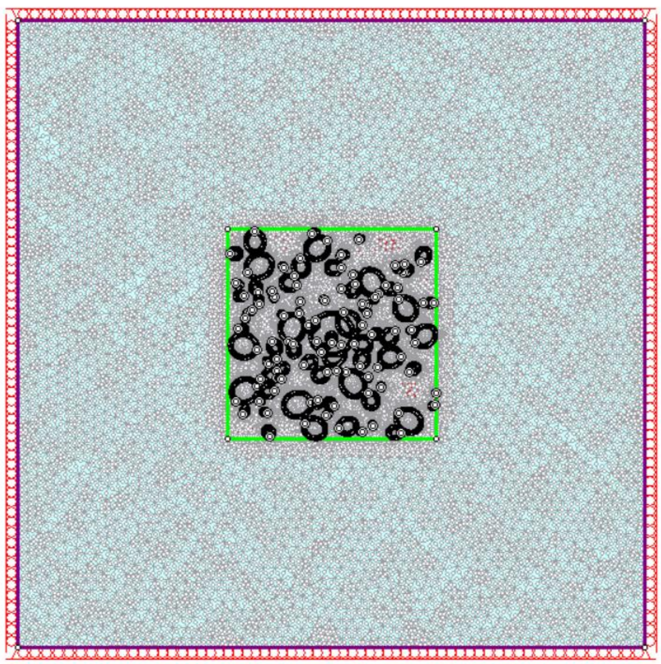

Figure 14- Model 0.25_4 (4th random draw of block orientation with VBP = 25%, Definition of model)

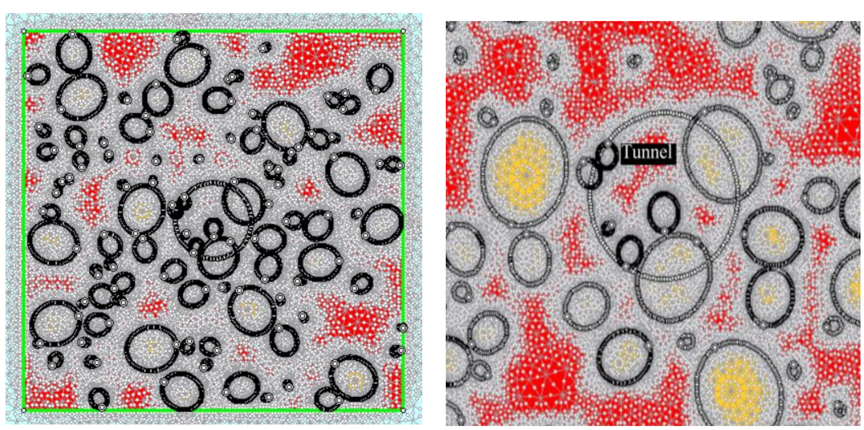

Figure 15- Model 0.25_4 (Detailed geometry of inclusions, Excavation zone)

12 model stages are considered, the first in which elastic properties are assigned and the rest with elastic plastic model. A stress reduction of 10% takes place in each stage as the excavation of the tunnel is simulated.

The field stress type is taken constant as it is the case of deep tunnel excavation. The stress state value is obtained for different VBPs (Table-1) which is directly proportional to the areal percentage of the inclusions hence the stress state increases with increasing volumetric percentage of the blocks.

VBP	σ_1 [MPa]	σ_3 [MPa]	σ_z [MPa]
25%	1.68	1.68	1.008
40%	1.70	1.70	1.02
55%	1.72	1.72	1.032
70%	1.74	1.74	1.044

Table 1- Isotropic In-situ stress state w.r.t VBP

The density values for the block and the matrix were taken equivalent to those in the research of (Li, 2004) who conducted in situ shear tests with hydraulic jacks on bimrock material in the vicinity of the Three Gorges Dam in China as they also carried out numerical modeling through a stochastic procedure of analysis of the test samples and obtained consistent results. The rest of the properties were presumptive based on (Adam, 2014) characterization of laboratory experiments on the bimrock complex encountered while building the bypass tunnel of Waidhofen an der Ybbs (Austria). An Elastic perfectly plastic Mohr Coulomb failure criteria is adopted. The material properties assigned are reported in Table-2.

Property	Matrix	Blocks
Density ρ[kg/m^3]	2200	2700
Young's Modulus E [MPa]	40	40700
Cohesion c [MPa]	0.065	11
Angle of Internal friction φ [°]	28	50
Tensile Strength [MPa]	0.02	6
Poisson ratio ν [-]	0.3	0.3
Uniaxial Compressive strength [MPa]	0.22	60

Table 2- Assigned Material Properties

The rock-matrix interface is simulated by converting the boundary of each rock block from a material boundary to a Joint Boundary using the convert boundary command. The Joint Boundary is assigned both ends open to allow rotation. Initially the properties of the joints are equal to that of the matrix.

Firstly models for 25% VBP with rock-matrix interfaces were analyzed and compared with models without rock-matrix Interface (i.e., bimrocks). Then the interfaces properties were decreased from 100% to 25% of the matrix properties as reported in Table-3, in order to investigate the effects on the tunnel convergence, if any.

Property	Strength of the Interface as a Percentage of the Matrix Strength			
	25%	**50%**	**75%**	**100%**
Cohesion c [MPa]	0.01625	0.0325	0.04875	0.065
Angle of Internal friction φ [°]	28	28	28	28
Tensile Strength [MPa]	0.005	0.01	0.015	0.02

Table 3- Assigned Interface Properties

3.3 Results of 25%VBP models with Rock-Matrix Interface

The results are interpreted using the definition of the characteristic curves (convergence-confinement) for each individual model referring to three points identified as the crown, the left and the right side wall of the excavation area in order to compare it with previous model results. The dimensional distribution of the blocks and their positioning occur randomly associated with a particular VBP. 8 models in total were analyzed for 25%VBP. Random extraction numbered 1 and 3 were skipped as their file sizes were not compatible to be run in the latest available version of RS2 software used for the purpose of this dissertation. All the results reported below are at total relaxation.

The following figures show the overall radial displacement along the tunnel boundary with the strength of the rock-matrix interface increased from 25% of the matrix properties (Figure-16) to having properties exactly the same properties as that of the matrix (Figure-19):

The x-axis corresponds to the linearized tunnel contour with the origin at the crown and subsequently moving along the tunnel circumference in clockwise direction.

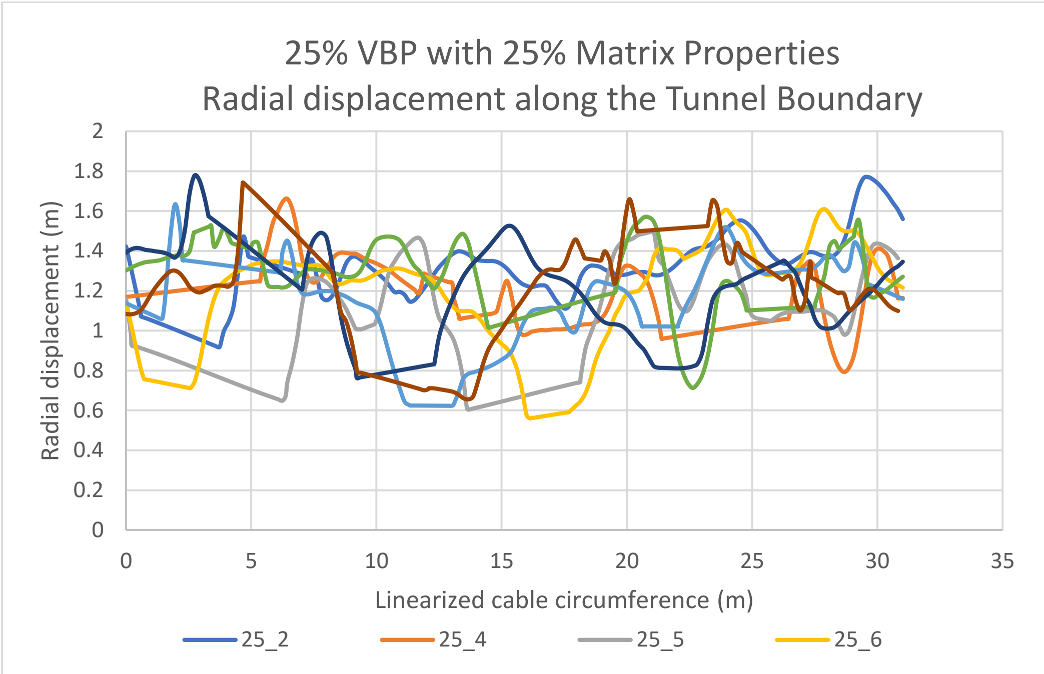

Figure 16- Trend of the convergence displacements of the linearized cable contour, according to eight stochastic extractions associated with VBP = 25% having Rock-matrix interface with 25% matrix properties

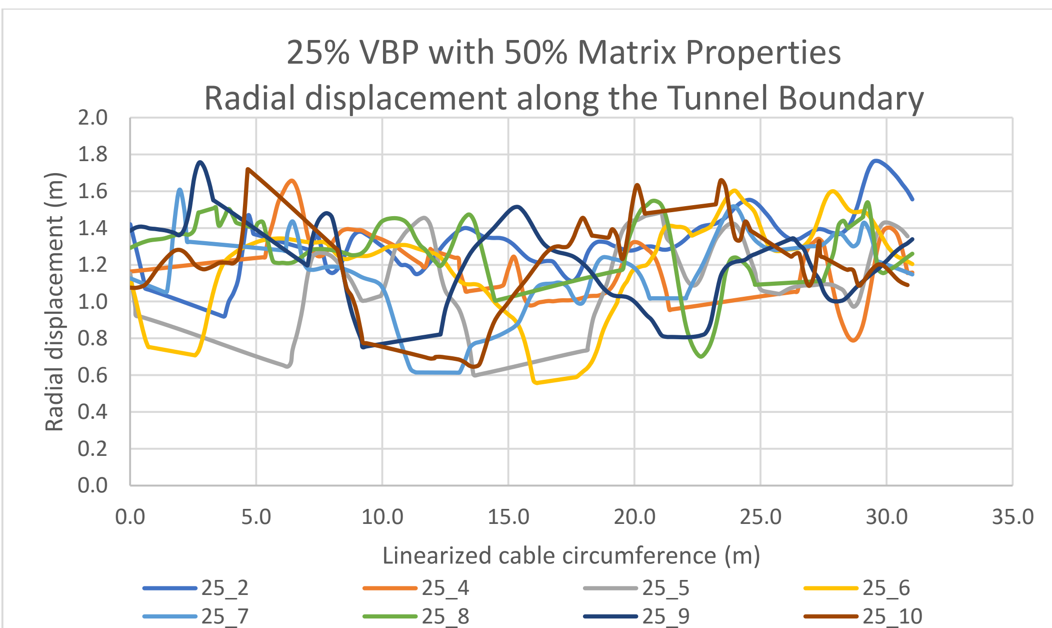

Figure 17- Trend of the convergence displacements of the linearized cable contour, according to eight stochastic extractions associated with VBP = 25% having Rock-matrix interface with 50% matrix properties

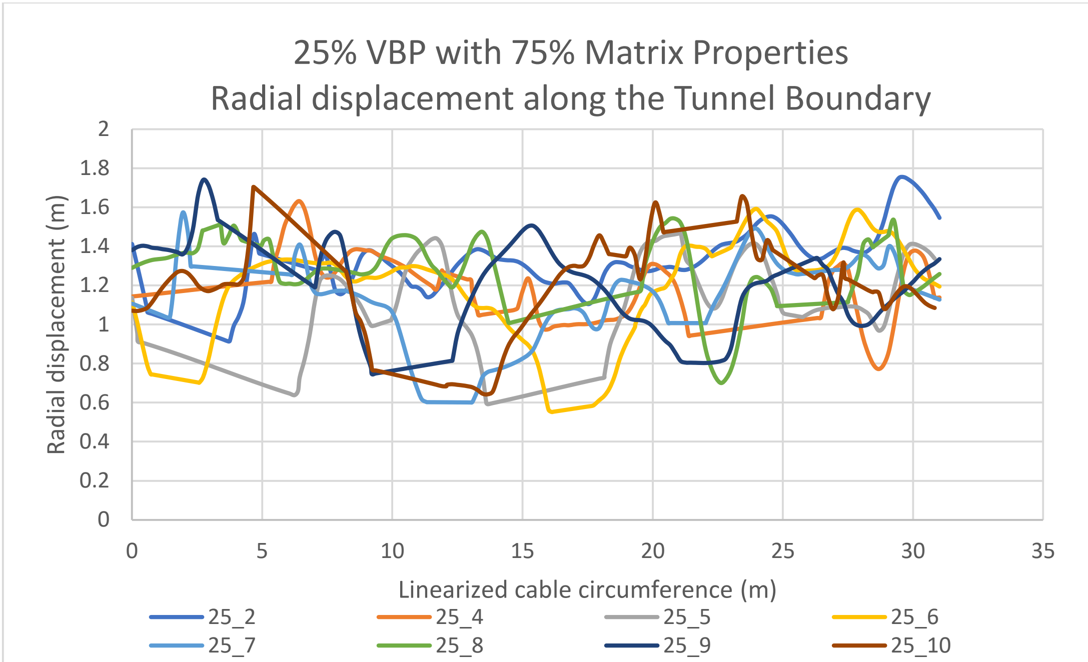

Figure 18- Trend of the convergence displacements of the linearized cable contour, according to eight stochastic extractions associated with VBP = 25% having Rock-matrix interface with 75% matrix properties

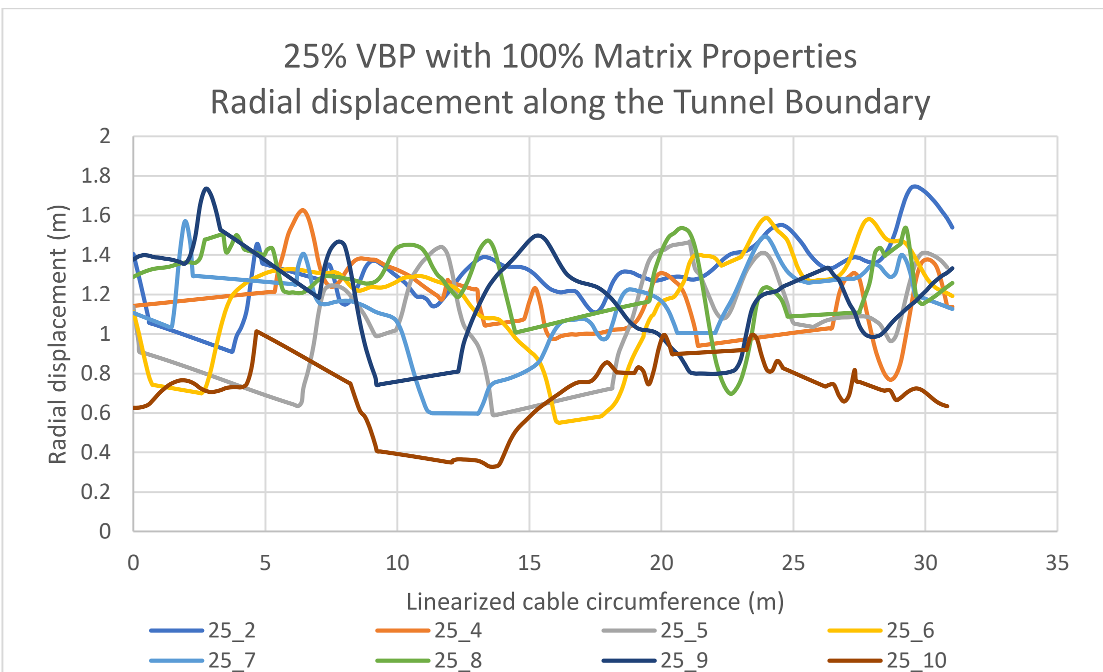

Figure 19- Trend of the convergence displacements of the linearized cable contour, according to eight stochastic extractions associated with VBP = 25% having Rock-matrix interface with 100% (same as) matrix properties

The results obtained showed that the decrease in the overall radial displacement along the tunnel boundary with the increase in the strength of the rock-matrix interface was very minute, almost negligible, except in the case of random extraction number 10 which showed decreased radial displacement when the properties (strength and cohesion) of the Rock-matrix interface were increased to be equal to those of the surrounding matrix. This can be owed to the fact that in all the extractions we have a different placement of blocks which would explain why they all have different displacement patterns around the tunnel contour as can be seen in Figure-20. In the case of model 25%_10 the number of blocks intersecting the tunnel zone is the highest as compared to other models, which can explain it having a different trend as compared to the rest. The random block placements of all the models is reported below for reference.

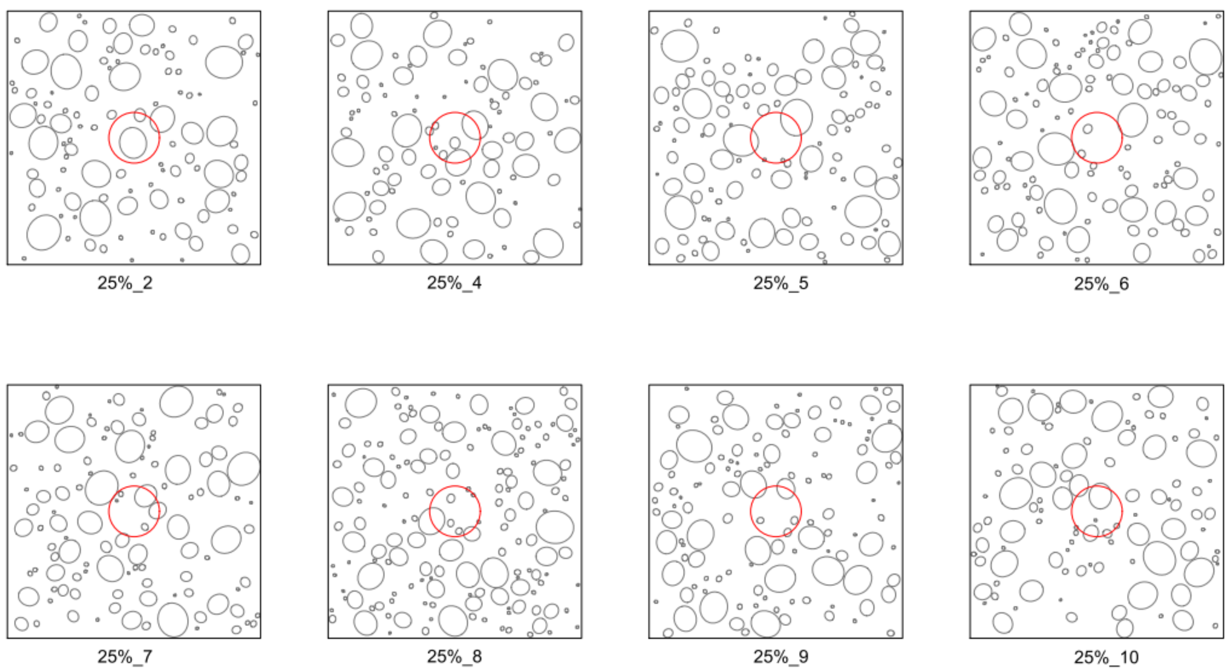

Figure 20- Random Block distributions for 25% VBP extracted from Matlab code

The plasticization around the tunnel contour for all the models was also analyzed and compared with each other, but no visible difference in the plastic zones could be detected. The results are reported in Annex A.

The results were also interpreted using characteristic curves as the previous model results referred to three points identified as the crown and the left and right side wall of the excavation area. So for each individual model these curves were obtained at these 3 points. This led to the development of such graphs where the trend of displacement could be observed owing to the ratio of the properties of the Joint boundary of the rock inclusions. The properties are gradually decreased moving from soft bimrocks to bimsoils having ratio equal to 1, indicating that the interface strength is equal to that of the matrix. The ratio is depicted as:

$$\frac{c_{interface}}{c_{matrix}}$$

where $c_{interface}$ indicates the properties (namely tensile strength and cohesion) of the matrix with respect to c_{matrix} , that of the matrix.

The results are shown below at the left (Figure-21) and the right tunnel side wall (Figure-22), and the crown (Figure-23):

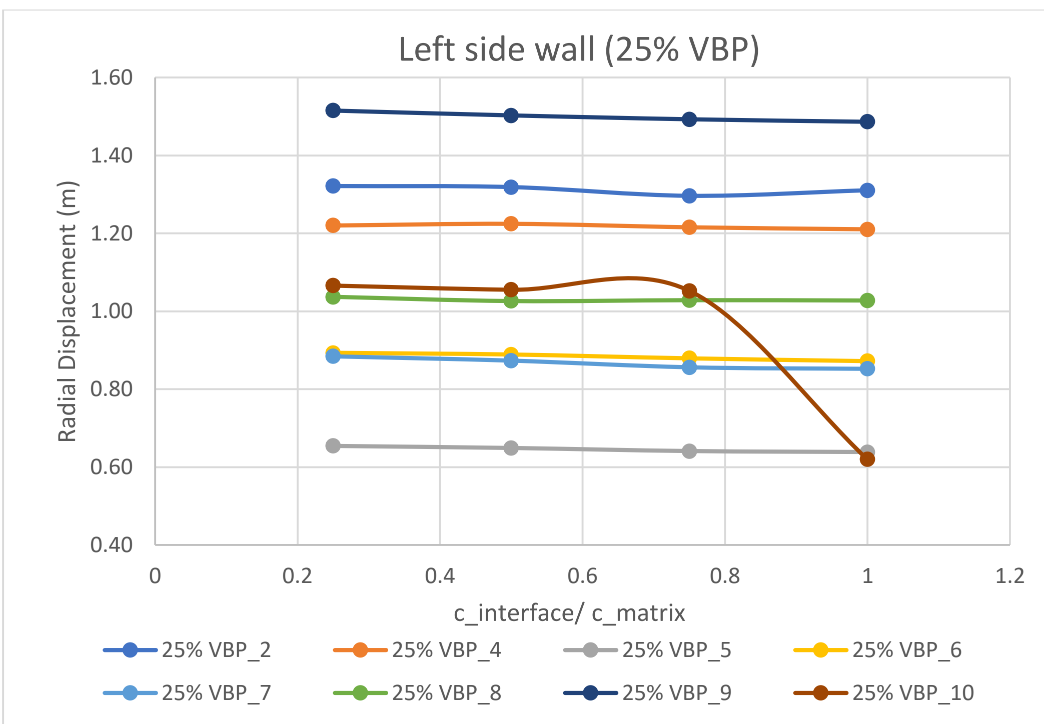

Figure 21- Trend of Radial Displacement at Left tunnel wall with increase in Interface strength, 25% VBP. $c_{interface}/c_{matrix}$ represents ratio of the interface and the matrix properties, equal to 1 when they are the same

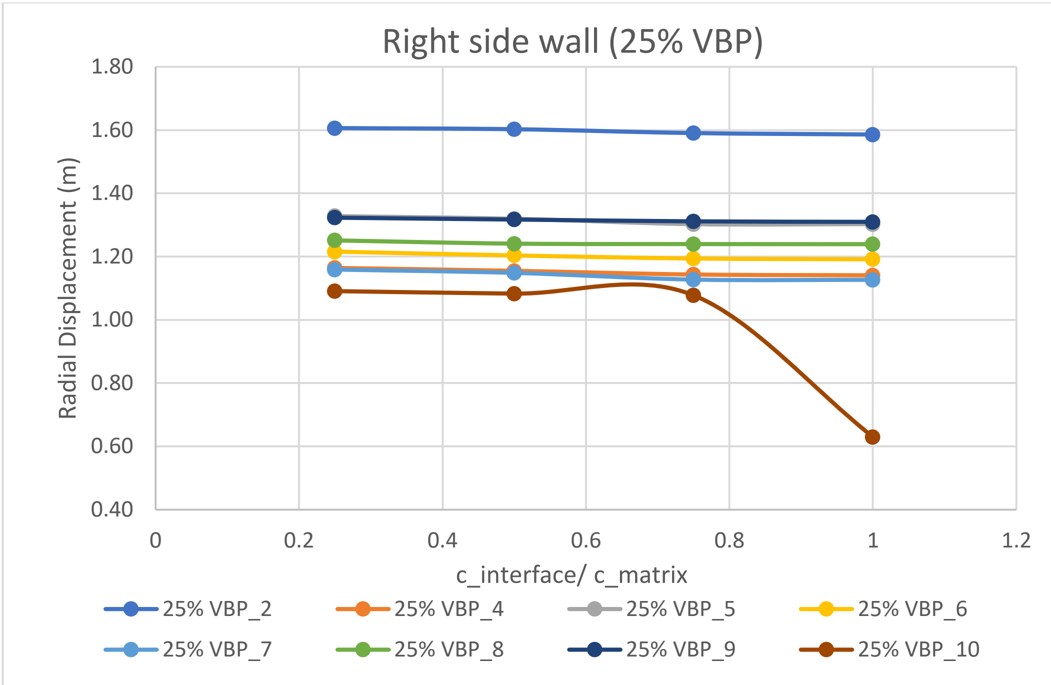

Figure 22- Trend of Radial Displacement at Right tunnel wall with increase in Interface strength, 25% VBP. $c_{interface}/c_{matrix}$ represents ratio of the interface and the matrix properties, equal to 1 when they are the same

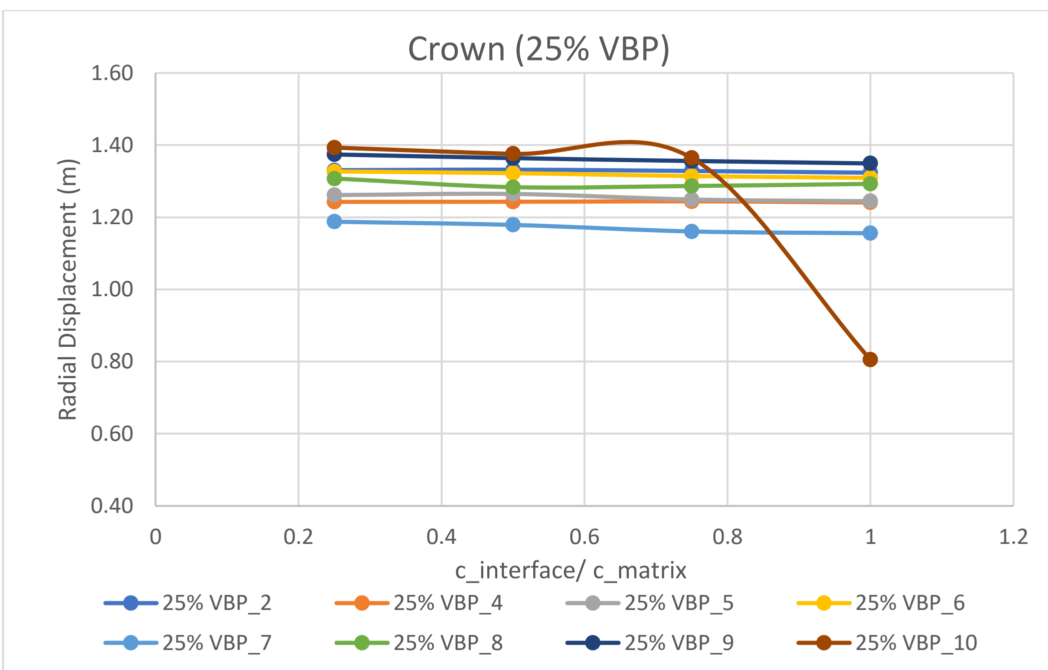

Figure 23- Trend of Radial Displacement at Crown of the tunnel wall with increase in Interface strength, 25% VBP. $c_{interface}/c_{matrix}$ represents ratio of the interface and the matrix properties, equal to 1 when they are the same

The results are consistent with what has already been observed in the linearized tunnel contour graphs of Figures 16-19, which shows that the decrease of displacements achieved with increasing the strength of the interface does not have much effect on the overall tunnel displacements and the reduction is still very minute if any, with the exception of the random extraction 10 already discussed above. The difference in the Figures 21-23 is due to the fact that at these 3 points the block placements are not the same owing to the fact that they are random stochastic extractions from Matlab.

These results led to the conclusion that adding joint boundaries to the rock inclusions with a VBP of 25% in order to simulate Bimsoils did not have much effect on the tunnel excavation even after changing their strength properties. So the analysis was moved on to Higher VBPs.

3.4 Results of 40% & 70% VBP models with Rock-Matrix Interface

Since the models with 25% VBP and rock-matrix Interfaces did not yield any substantial change in the radial displacements of the tunnel or in other words the presence of interface showed little to no effect on the overall excavation, one model from 40% and 70% VBP from Dadone’s models was analyzed in order to see if something changed by increasing the Volumetric Percentage of Blocks.

For this reason, one extraction each was chosen at random for both 40% VBP and 70% VBP, and each model was run four times again decreasing the properties of rock-matrix interface from same as that of the matrix to 25% of the matrix properties. The results obtained are discussed below.

3.4.1 40% VBP Model Results

The fourth random extraction of the Dadone’s work was chosen for 40% VBP with the model detail shown in Figures 24,25. All the rest of the model properties were kept the same as those used for the 25% VBP models.

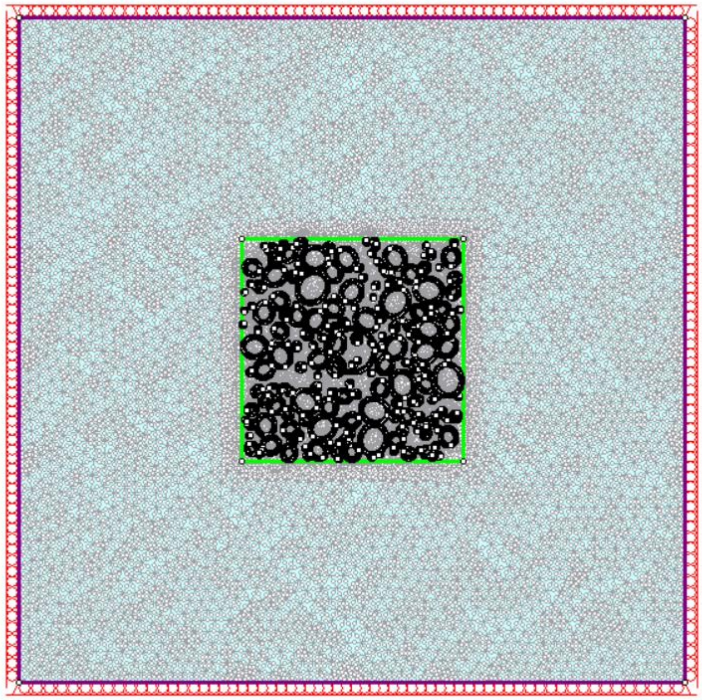

Figure 24- Model 0.40_4 (4th random draw of block orientation with VBP =40%, Definition of model)

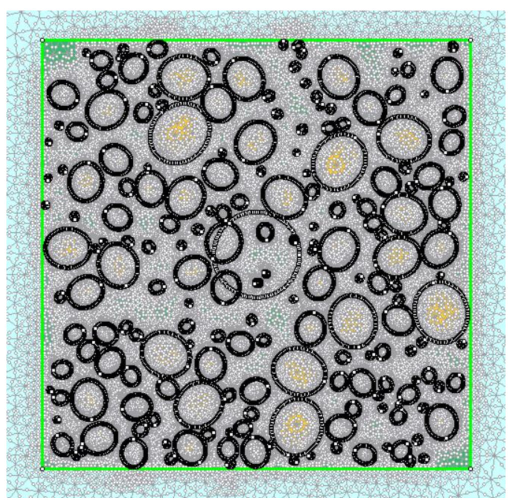

Figure 25- Model 0.40_4 (Detailed geometry of inclusions)

It can be seen in Figure 26 that the trends obtained were more or less similar with very minute changes in the overall displacement with the increase in the interface strength.

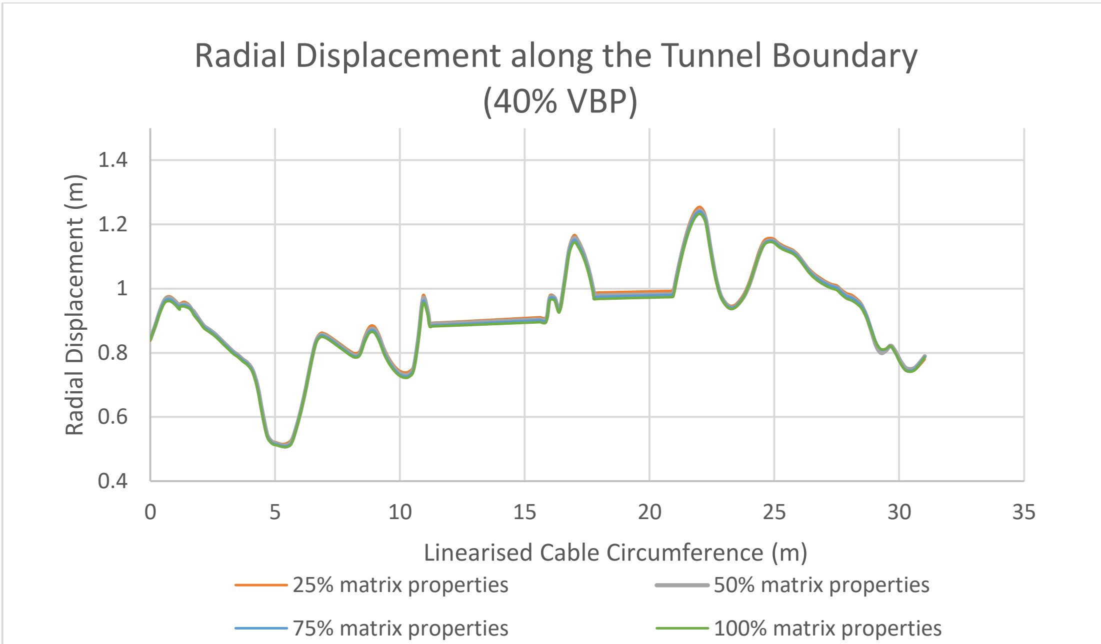

Figure 26- Trend of Radial Displacement around the tunnel contour for 40% VBP model with increase in Interface strength from 25-100% of matrix properties.

Displacements in the last quadrant are high as we have more blocks there intersecting the excavation zone as compared to the first quadrant.

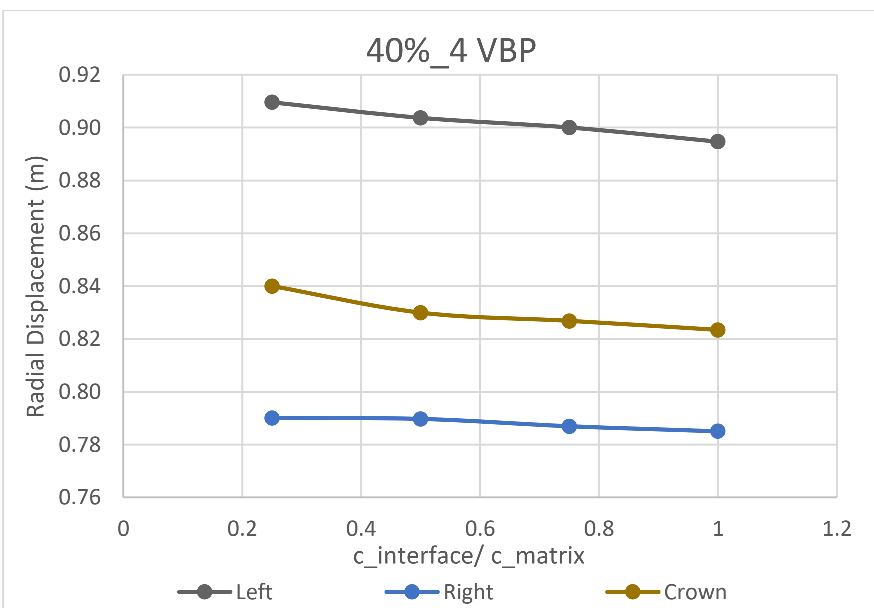

Figure 27- Trend of Radial Displacement at the crown, left and right tunnel wall with increase in Interface strength, 40% VBP. $c_{interface}/c_{matrix}$ represents ratio of the interface and the matrix properties, equal to 1 when they are the same (i.e. bimrock models)

The results of the radial displacements around the tunnel contour and the plasticization for all the 40% VBP models with increasing interface strength were also compared in Figure-27 and were found to be quite similar to each other. The model results are attached as Annex B.

3.4.2 70% VBP Model Results

The First random extraction from the Dadone's work was chosen for 70% VBP with the model detail shown in Figures 28,29. All the rest of the model properties were kept the same as those used for the 25% VBP models.

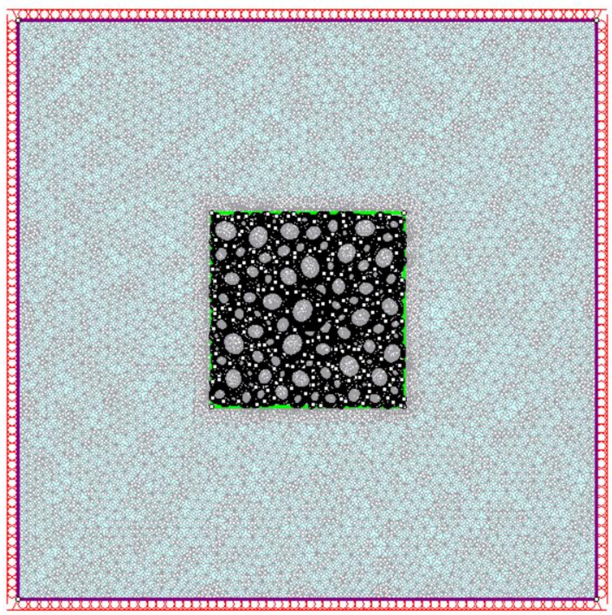

Figure 28- Model 0.70_1 (1st random draw of block orientation with VBP =70%, Definition of model)

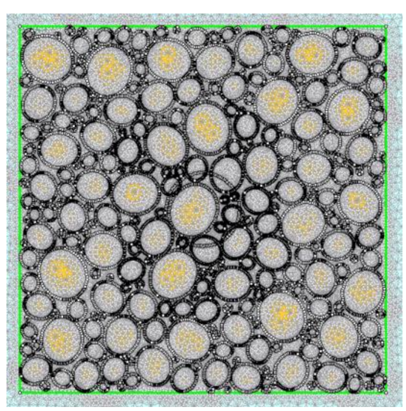

Figure 29- Model 0.70_1 (Detailed geometry of inclusions)

As expected again the trends obtained were more or less similar with very minute changes in the overall displacement with the increase in the interface strength as shown in Figures 30.

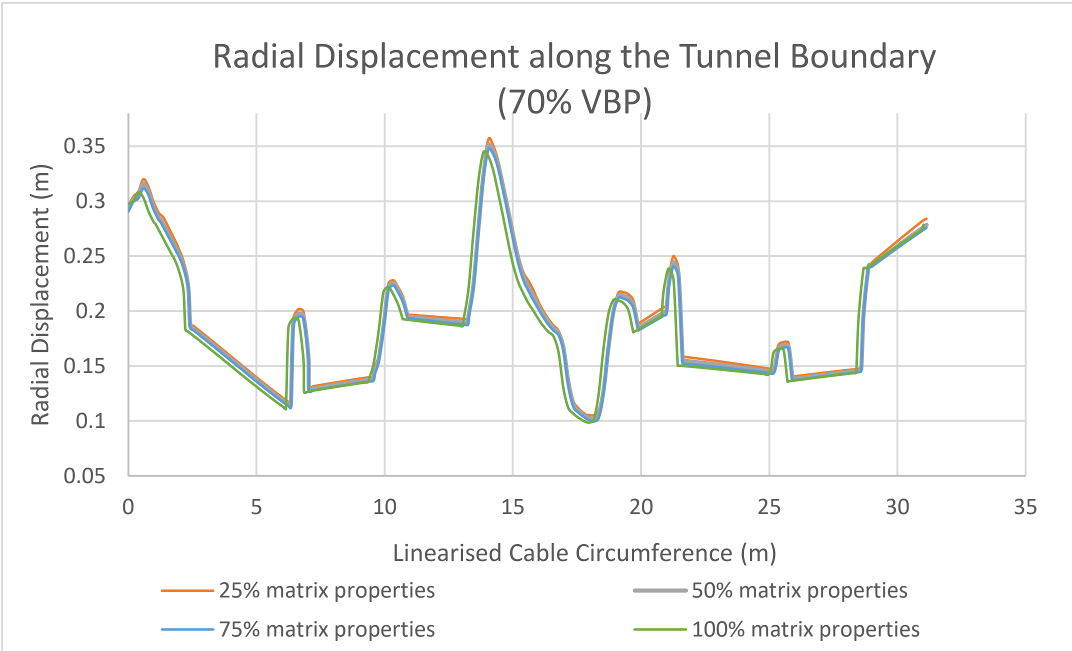

Figure 30- Trend of Radial Displacement around the tunnel contour for 70% VBP model with increase in Interface strength from 25-100% of matrix properties

Displacements in the second quadrant are higher as we have more blocks there intersecting the excavation zone as compared to the last quadrant. The trends obtained were more or less similar with very minute changes in the overall displacement with the increase in interface strength with the displacement being the highest in case of weak interface having only 25% of the matrix properties.

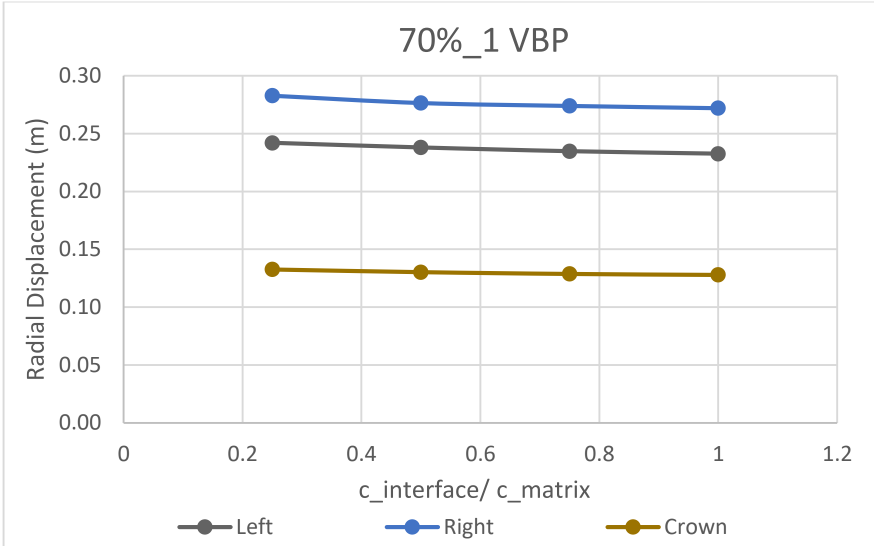

Figure 31- Trend of Radial Displacement at the crown, left and right tunnel wall with increase in Interface strength, 70% VBP. $c_{interface}/c_{matrix}$ represents ratio of the interface and the matrix properties, equal to 1 when they are the same (i.e. bimrock models)

The results of the radial displacements around the tunnel contour and the plasticization for all the 70% VBP models with increasing interface strength were also compared in Figure-31 and were found to be more or less similar also. Model results are attached as Annex B.

These results led to the conclusion that adding joint boundaries to the rock inclusions does not have much effect on the tunnel excavation even after changing their strength properties. And the trend did not change even when the VBP was increased from 25% up till 70%.

4. Analysis of Tunneling in Heterogeneous Formations with Joint Networks

Another series of analyses was carried out by simulating natural joints in the Bimrock mass using the Joint Network feature of RS2. Two models each for 25%, 40% and 70% VBP were modelled, one with Joint Network only and one with Joint Network along with rock-matrix interfaces in the same model in order to see the change in trend with increasing VBP. The results were also compared with Dadone's Bimrock models lacking any joints or interfaces.

4.1 Model Properties

A joint network was added in the region with Bimrock inclusions (Figure 32) leaving the rest of the properties of the model same as the models analysed above.

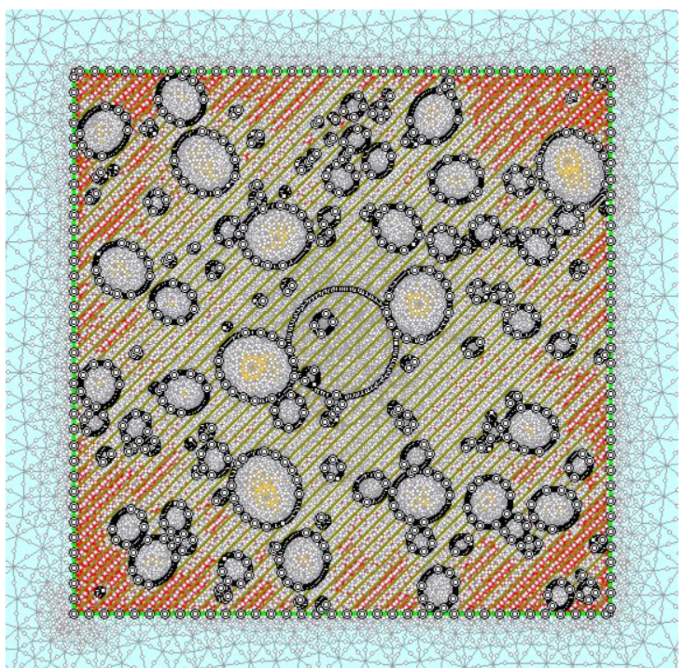

Figure 32- Example of model 0.25_6 (Joint Network, Detailed geometry of inclusions)

A Parallel Deterministic joint network model was used. It defined a series of parallel joints in the model which were assigned a spacing of 1m and an orientation of 45°.

The spacing, length and persistence of the joints is assumed to be constant in the deterministic method but it does allow randomness of the joint location.

Use Trace Plane was turned off in order for the inclination and spacing of the joints to be measured in 2D cross-sectional plane of the model and Joint ends are all assigned as open.

The Joints were assigned a material dependent slip criterion meaning that the strength of the Joint will be determined on the basis of the type of rock or soil it is passing through. The interface co-efficient of 0.5 was used which determined the cohesion and friction angle of the joint from the cohesion and friction angle of the matrix.

4.2 Results of Joint Network model of 25% VBP

The sixth random extraction with 25% VBP (25%_6 VBP) was chosen and analyzed with the above mentioned properties and it yielded the following results reported in Figure 33.

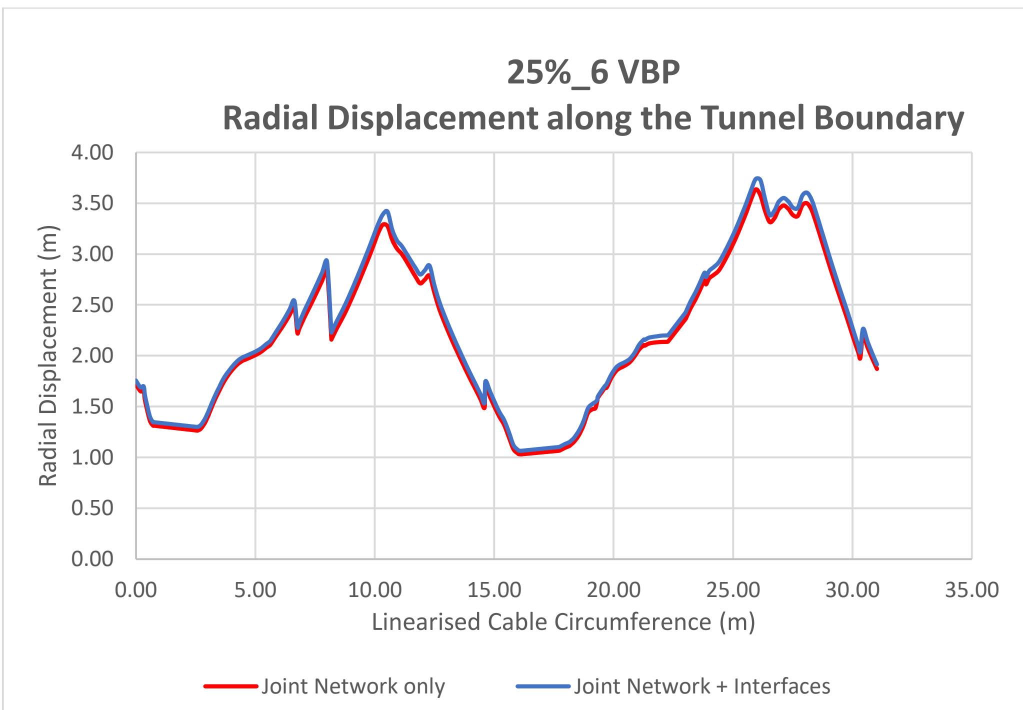

Figure 33- Comparison of the trend of radial displacements on the linearized hollow contour of the tunnel, for the sixth random stochastic extraction associated with VBP = 25% in the presence of a Joint network only and with Joint network + Rock Matrix Interfaces.

The results of total displacement at the total relaxation stage of the model is shown below:

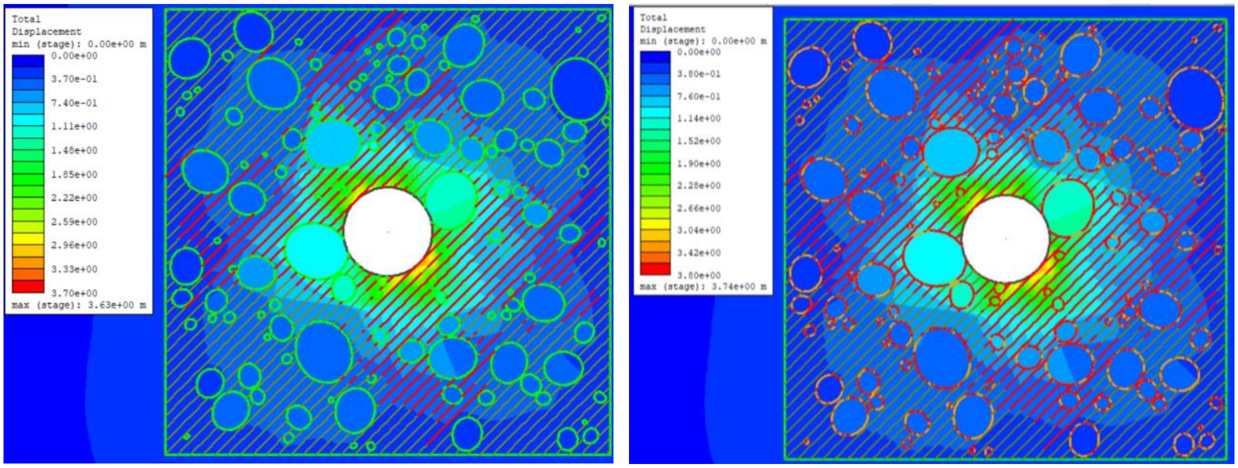

Figure 34- Model 0.25_6 with Joint Network on left Total Displacement with yielded joints shown in purple. On right Model 0.25_6 with Joint Network + Rock-Matrix Interface (Total Displacement with yielded joints and interfaces shown in purple)

The trend of displacement (Figure 34) is more or less the same in both the cases with a slight increase in the overall displacement around the tunnel contour in the presence of both the Joint network and the rock-matrix interfaces, with yielding also visible in the rock matrix interfaces.

The positioning of yielded elements (Figure 35) was the same in both the cases with the ultimate strength condition reached by shearing within the matrix, with a tortuous pattern of failure following the presence of the inclusions.

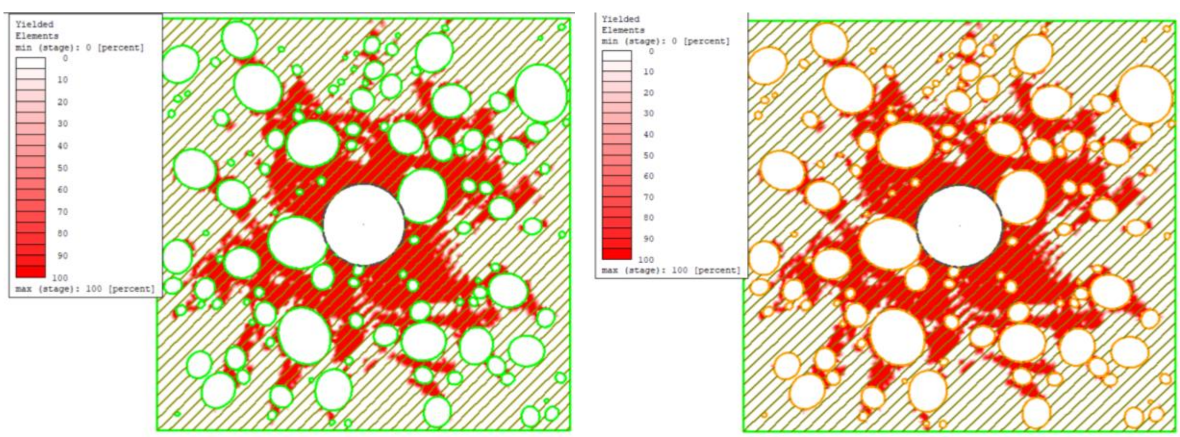

Figure 35- Yielding trend around the tunnel of model 0.25_6 with Joint Network only (left) Joint Network + Rock-Matrix Interface (right)

When these results were compared with Dadone’s Bimrock models results (Figure-36) without any interfaces or Joint networks, the yielded zones and the displacement around the tunnel contour were observed to be significantly less than in the two cases discussed above.

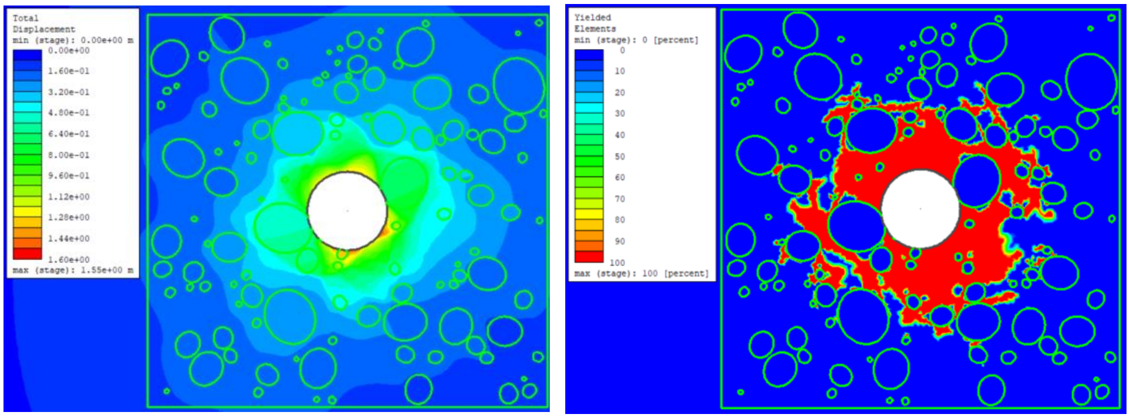

Figure 36- Original Bimrock Model 0.25_6 without any Joint Network or Interfaces. On left Total Displacement and yielded zones around the tunnel contour on the right.

4.3 Results of Joint Network model of 40% VBP

The third random extraction with 40% VBP (40%_3 VBP) was chosen and analyzed with the properties mentioned previously and yielded the following results reported in Figure 37.

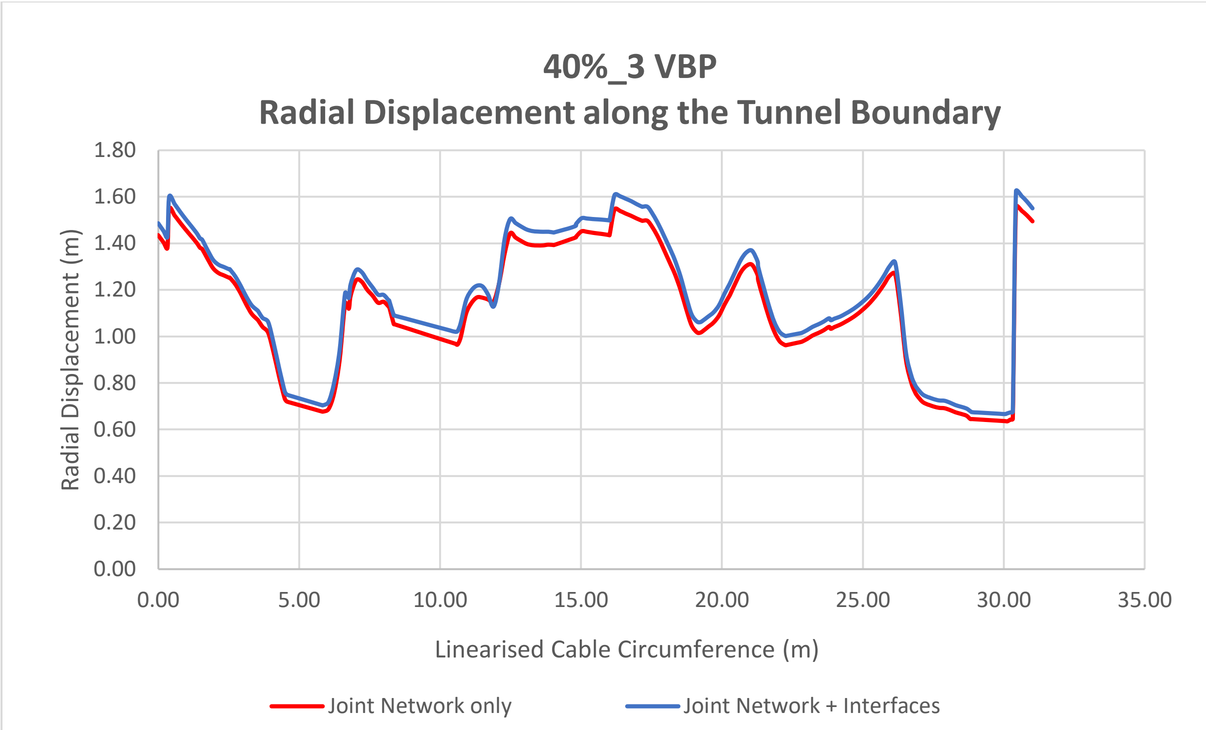

Figure 37- Comparison of the trend of radial displacements on the linearized hollow contour of the tunnel, for the third random stochastic extraction associated with VBP = 40% in the presence of a Joint network only and with Joint network + Rock Matrix Interfaces.

Both the analysis results showed a similar trend of radial displacement. It is a little higher in the scenario where we have both the Rock-matrix interfaces and the Joint network and this result is slightly less pronounced for 40% VBP as it was in the case of 25% VBP.

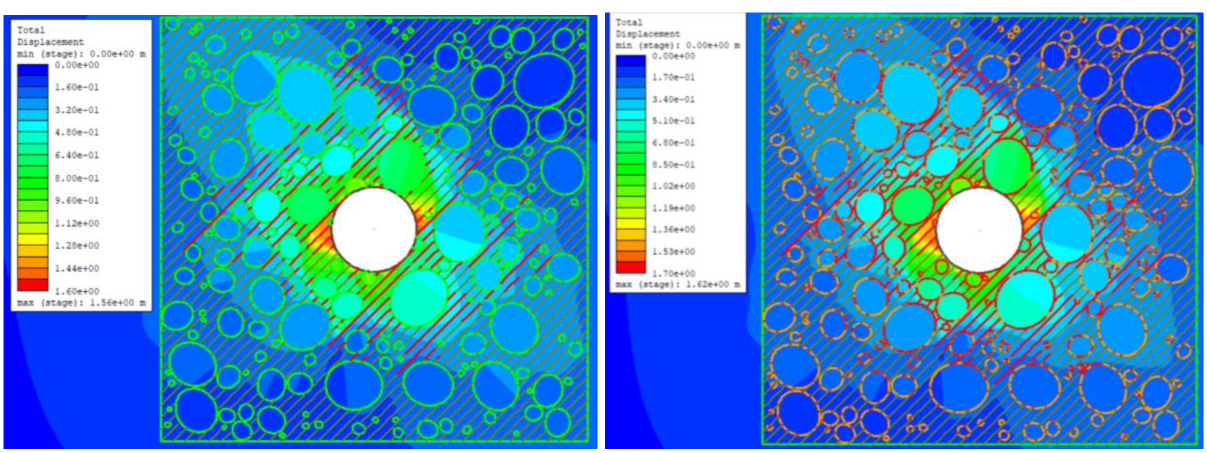

Figure 38- Model 0.40_3 with Joint Network on left Total Displacement with yielded joints shown in purple. On right Model 0.40_3 with Joint Network + Rock-Matrix Interface (Total Displacement with yielded joints and interfaces shown in purple)

A slight increase in the overall displacement around the tunnel contour with yielding, also visible in the rock matrix interfaces, can be seen in the second scenario on the right (Figure-38).

The positioning of yielded elements was the same in both the cases (Figure-39) with the ultimate strength condition reached by shearing within the matrix, with a tortuous pattern of failure following the presence of the inclusions.

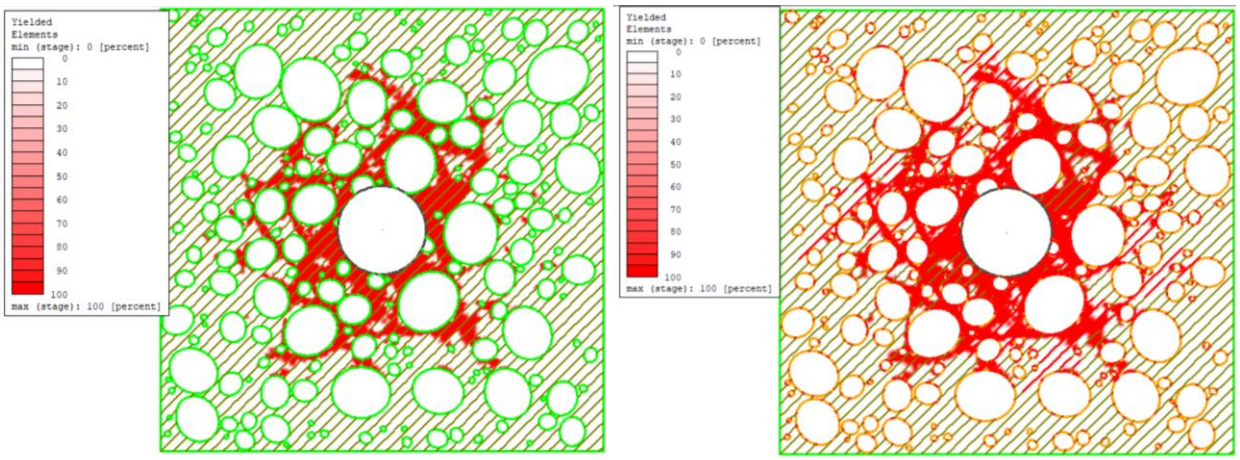

Figure 39- Yielding trend around the tunnel of model 0.40_3 with Joint Network only (left) Joint Network + Rock-Matrix Interface (right)

Comparing with Dadone's Bimrock models results (Figure-40) without any interfaces or Joint networks, the yielded zones and the displacement around the tunnel contour was observed to still be less than the two cases discussed above, but the difference was less pronounced than it was in the case of lower 25% VBP.

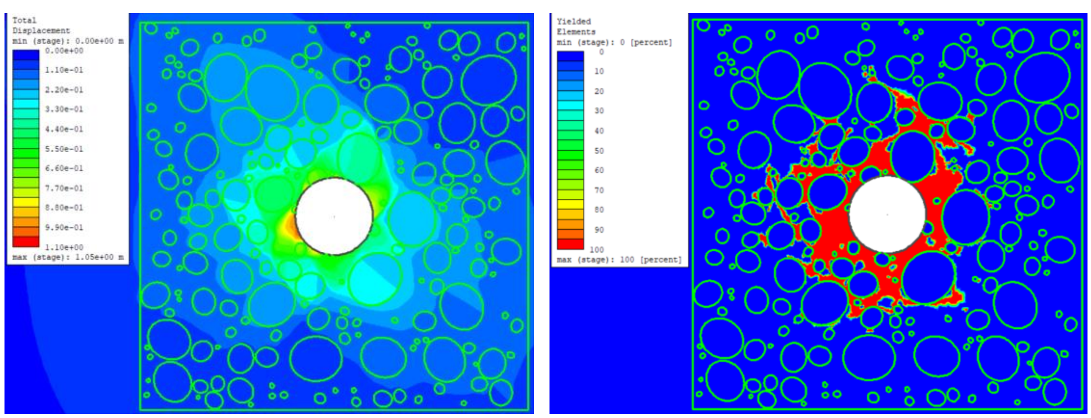

Figure 40- Original Bimrock Model 0.40_3 without any Joint Network or Interfaces. On left Total Displacement and yielded zones around the tunnel contour on the right.

4.4 Results of Joint Network model of 70% VBP

The second random extraction with 70% VBP (70%_2 VBP) was chosen and analyzed with the properties mentioned previously and yielded the following results reported in Figure-41.

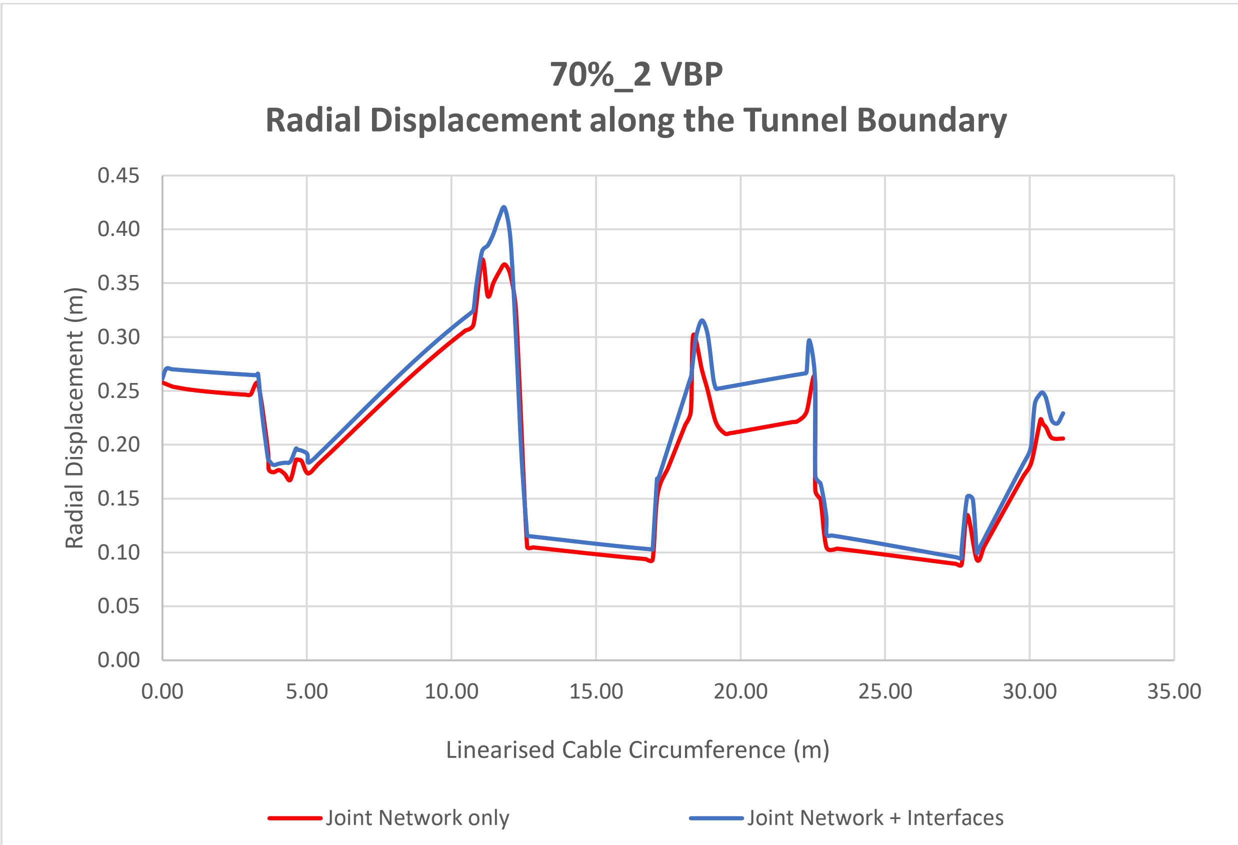

Figure 41- Comparison of the trend of radial displacements on the linearized hollow contour of the tunnel, for the second random stochastic extraction associated with VBP = 70% in the presence of a Joint network only and with Joint network + Rock Matrix Interfaces.

Similarly to the 40% VBP analysis results, the displacement is a little higher in the scenario where we have both the Rock-matrix interfaces and the Joint network with the trend being more or less similar.

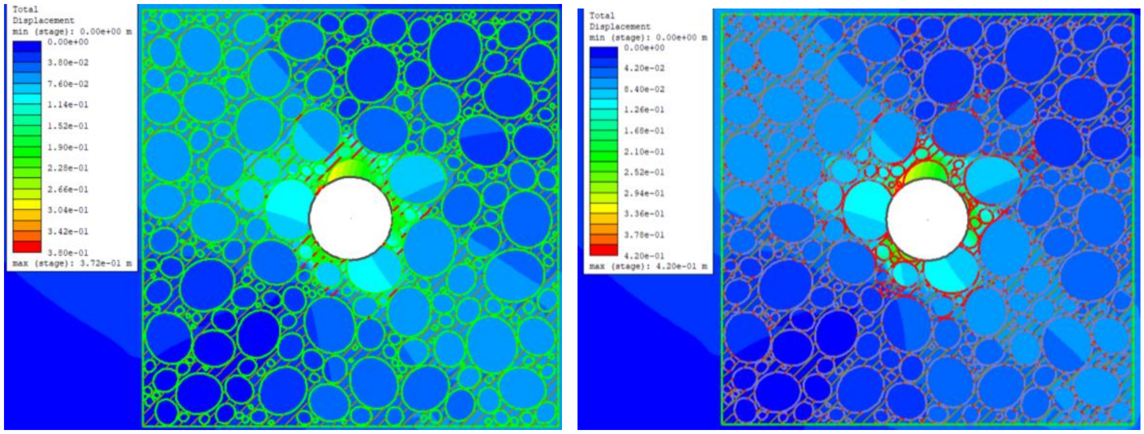

Figure 42- Model 0.70_2 with Joint Network on left Total Displacement with yielded joints shown in purple. On right Model 0.70_2 with Joint Network + Rock-Matrix Interface (Total Displacement with yielded joints and interfaces shown in purple)

A slight increase in the overall displacement around the tunnel contour, with yielding also visible in the rock matrix interfaces, can be seen in the second scenario on the right of Figure-42.

The positioning of yielded elements (Figure-43) was the same in both the cases with the ultimate strength condition reached by shearing within the matrix, with a tortuous pattern of failure following the presence of inclusions.

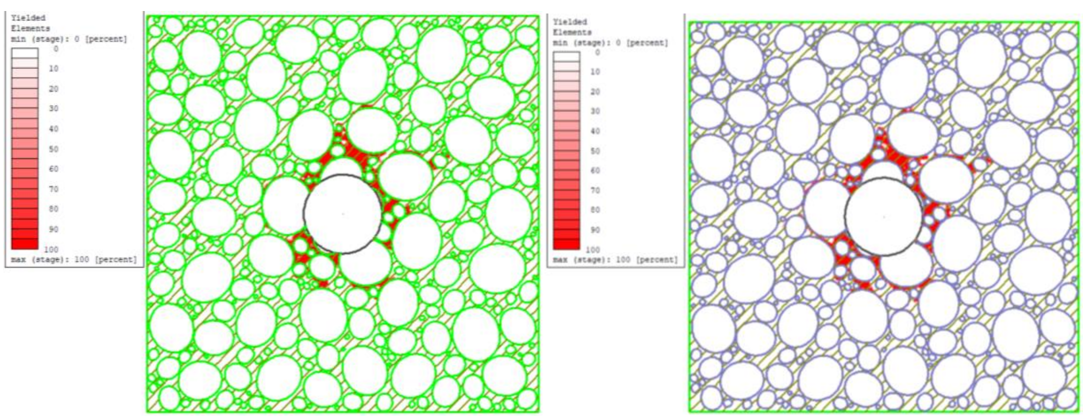

Figure 43- Yielding trend around the tunnel of model 0.70_2 with Joint Network only (left) Joint Network + Rock-Matrix Interface (right)

Comparing with Dadone's Bimrock models results (Figure-44) without any interfaces or Joint networks, the yielded zones and the displacement around the tunnel contour were observed to be quite similar to the case of the model with a Joint network and slightly less as compared to the model with both the Joint network and interfaces.

Nevertheless, it can still be said that the differences are not noteworthy in the case of high VBP.

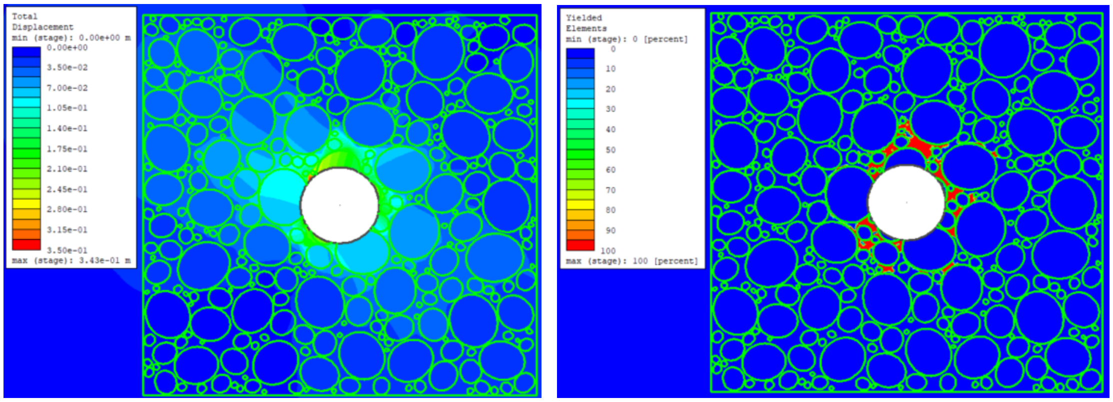

Figure 44- Original Bimrock Model 0.70_2 without any Joint Network or Interfaces. On left Total Displacement and yielded zones around the tunnel contour on the right.

Table-4 Compares the results for the three VBPs analysed with and without the presence of joint networks and interfaces and Dadone's original Bimrock models lacking any interfaces and Joint network.

	Max Displacement (m)		
VBP	No Joint Network or interfaces (Dadone's)	Joint Network only	Joint Network+Rock-Matrix Interface
25%	1.55	3.63	3.74
40%	1.05	1.56	1.62
70%	0.34	0.37	0.42

Table 4- Comparison of Maximum displacement obtained in the 3 cases i.e Dadone's models without Joint Network or Interfaces, Models with only Joint Network and Models with Joint Network+Interfaces for each VBP

To summarise we can say that as we move from 25% to 70% VBP the differences between the results of the models having Joint network + Interfaces and Joint network only, decreases. The increase of radial displacement around the tunnel contour is more pronounced for 25% VBP and it is almost negligible when the VBP is quite high such as 70%.

Comparing the results also with Dadone's bimrock models which lacked any joint network or interfaces it can be observed that the displacement along the tunnel contour and the yielded zones were much less as compared to the cases of Bimsoils where Joint networks and interfaces were present for lower VBP, whereas for high VBP, the results were almost the same.

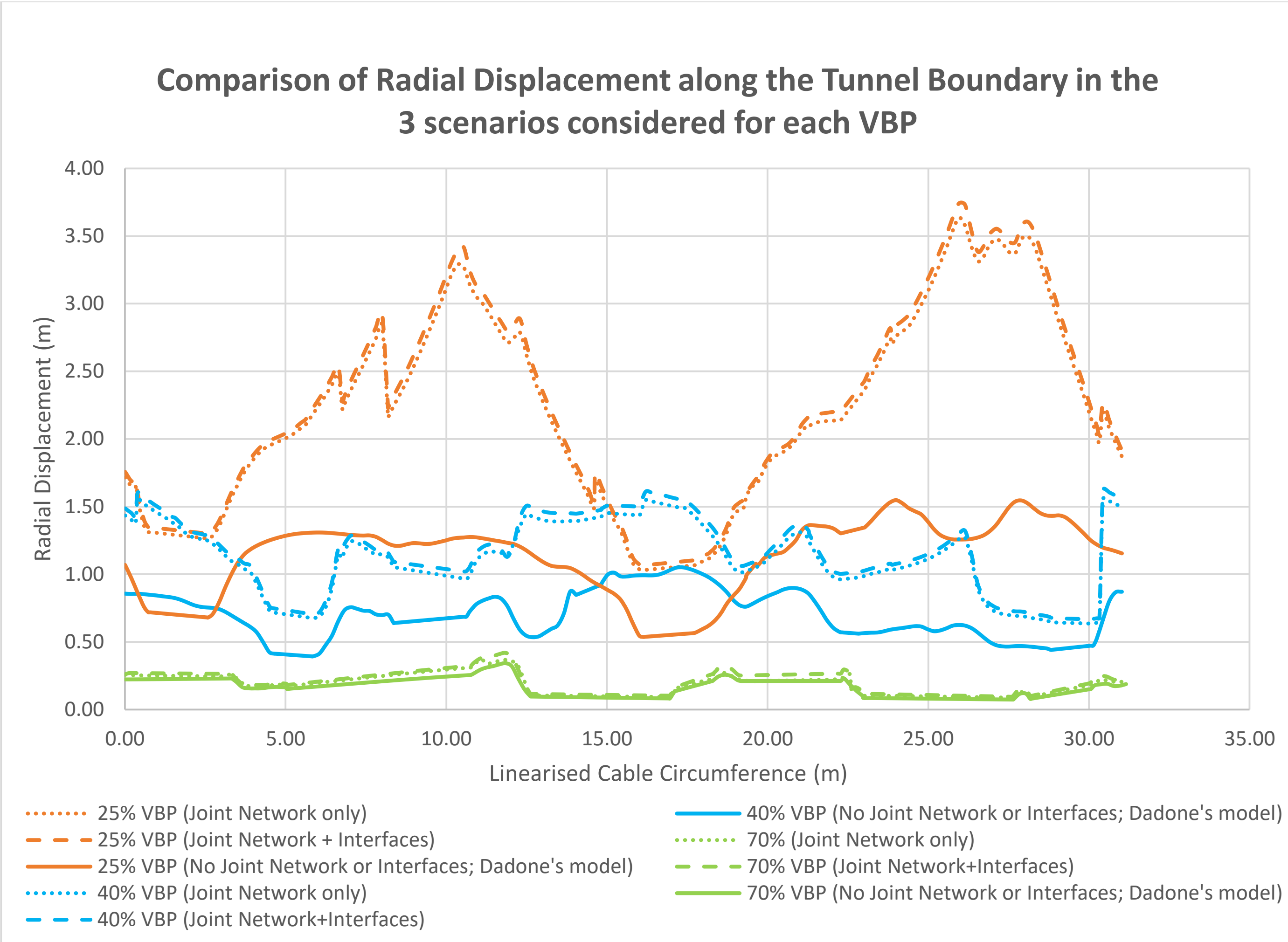

Figure 45- Comparison of Radial Displacement along the Tunnel Boundary for the 3 scenarios; Joint Network only, Joint Network+Interfaces and No Joint Network or Interface (Dadone's Bimrock Models) for each VBP (25%, 40% and 70%) considered.

Hence the presence of rock-matrix interfaces is comparatively more important while dealing with lower VBPs. This fact is showcased in the Figure 45 by superimposing the results of all the three scenarios discussed above in detail, for each VBP (25%, 40% and 70%) considered.

5. Analysis using the Lindquist equivalent homogenous approach

In this part of the thesis the empirical approach given by Lindquist (1994) is applied to determine the mechanical characteristics of Bimrocks (Paragraph 2.2.1).

As shown in Chapter 2, Paragraph 2.2.1, it is based on the Mohr-Coulomb failure criterion and uses the following material expression.

$$\tau'_{\text{bimrock}} = c'_{\text{bimrock}} + \sigma'_{\text{bimrock}} * \tan\varphi'_{\text{bimrock}} \tag{3}$$

where

$\tau_{bimrock}$ = shear strength

$c'_{bimrock}$ = cohesion

$\varphi'_{bimrock}$ = friction angle

The cohesion and the friction angle are obtained using suitable formulations based on the VBP. The criterion is applied using the homogeneous model (VBP = 0%), where the aforementioned parameters are modified from the original homogeneous model properties, while the matrix's specific weight, Young's modulus of elasticity, and Poisson's coefficient remain the same. In this way the equivalent homogenous model under consideration takes into account the percentage of areal presence of inclusions assumed to be equal to VBP. For each value of VBP considered (25%, 40%, 55%, and 70%), two analyses are carried out, (for a total of eight models), one with a joint network and one without it, in order to investigate the effects of the presence of Joints. The properties of the Joint network remain the same as those already mentioned in Paragraph 4.4. The basic properties of the matrix, listed in Table-5 are the following.

Property	Matrix
Density ρ[kg/m 3]	2200
Young's Modulus E [MPa]	40
Cohesion c [MPa]	0.065
Angle of Internal friction φ [°]	28
Tensile Strength [MPa]	0.02
Poisson ratio ν [-]	0.3
Uniaxial Compressive strength [MPa]	0.22

Table 5- Mechanical parameters of the matrix

Using equations (3) and (4) the values of cohesion and friction angle are determined for each Volumetric Block Percentage analysed.

The values obtained are reported in Table-6.

Lindquist empirical approach (1994)			
VBP	$c_{bimrock}$ **[MPa]**	**Δφ [°]**	**Φ [°]**
25%	0.05	0	28
40%	0.04	4.5	32.5
55%	0.03	9	37
70%	0.02	14.5	42.5

Table 6- Mechanical parameters of equivalent strength according to the empirical model of Lindquist (1994)

The trend of increase of friction angle and decrease of cohesion with increasing VBP highlighted by Lindquist can be clearly observed.

The model had the same RS2 settings as in the previous analysis with just the removal of blocks being simulated by the properties of a homogenous equivalent material. An example image of the model is shown in Figure 45.

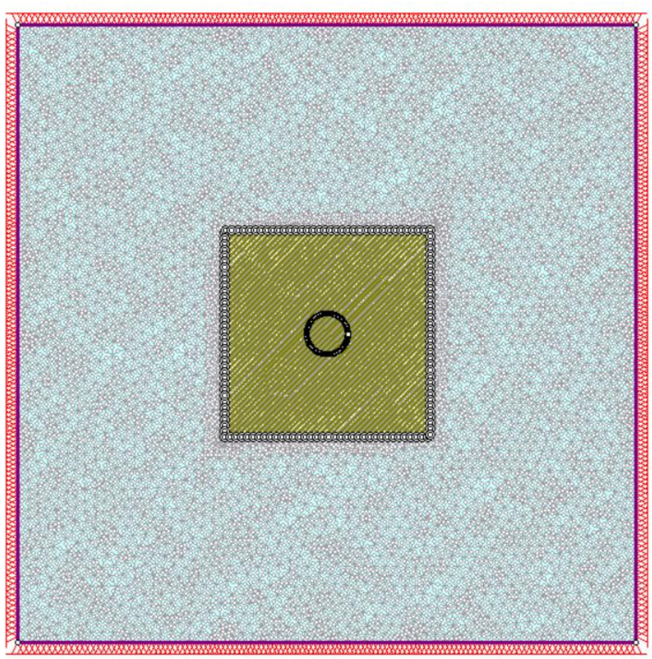

Figure 46- Model based on Lindquist Empirical approach (Joint Network shown in green in the domain of interest).

5.1 Results of 25% VBP models

The radial displacements obtained around the hollow of the tunnel contour for 25% VBP models are shown and compared in the following Figure-46:

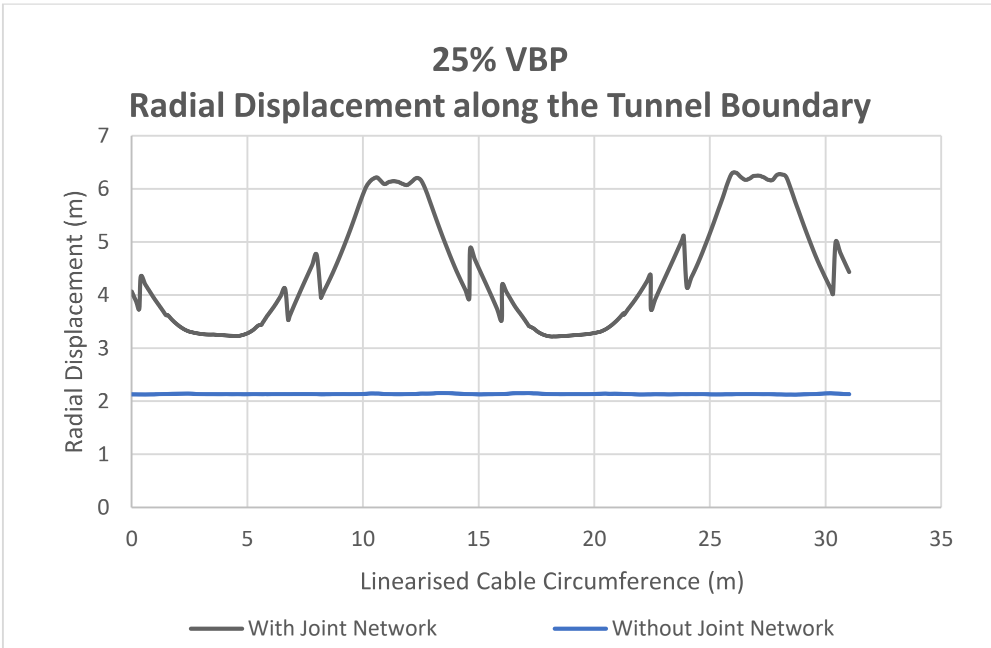

Figure 47- Comparison of the radial displacements on the linearized hollow contour of the tunnel, for the model with strength properties obtained on the basis of the Lindquist empirical approach (Lindquist 1994) with VBP = 25% in the presence of a Joint network and without it.

In the absence of a Joint network an isotropic behavior can be observed where the displacement around the tunnel contour is **2.13 m** approximately.

The direction-dependent characteristics of the rock mass, known as its anisotropy, have a significant impact on the stress re-distribution and displacements. It often results in reduced stiffness in the direction normal to the discontinuities and higher stiffness in the direction parallel to the rock mass structure and is related with weak planes in the rock mass structure (foliation, bedding planes, faults, joints).

From the results of Figure-47 it is evident that the displacement around the tunnel contour in the direction parallel to the Joint network is lower as compared to the direction normal to it, with the maximum displacement reaching around 6m, against the 2.13m of the homogeneous model with no joints.

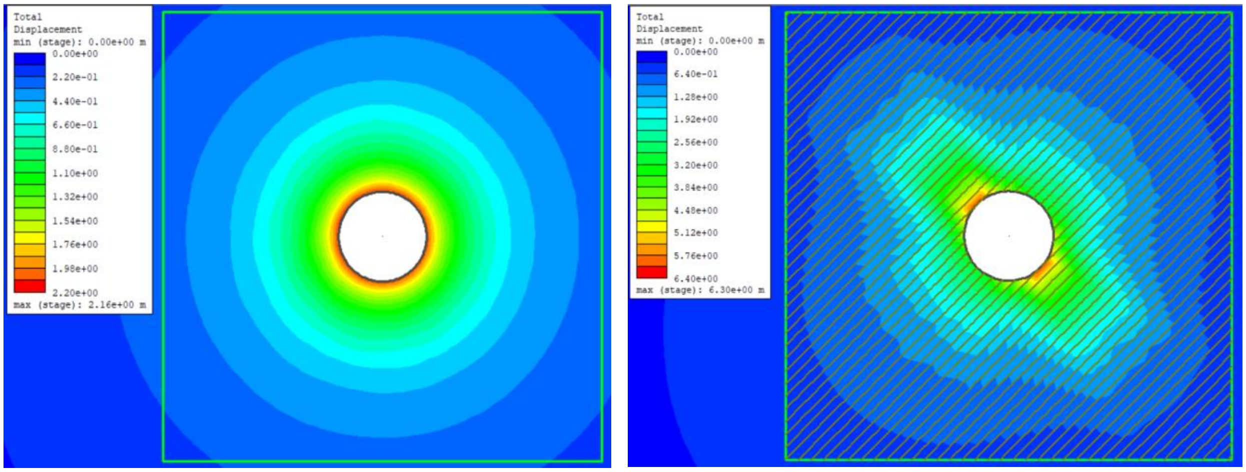

Figure 48- Model for 25% VBP without Joint Network on left and with Joint Network on right showing Total Displacement trend.

The same trend can be observed from the yielding elements in Figure-48 where perpendicular to the schistocity planes the yielding is much higher than it is in the direction parallel to the joints, with the plasticization extending nearly till the end of the domain of interest.

For the case of absence of a Joint network plasticization is almost the same all around the tunnel with an approximate radius of 19m

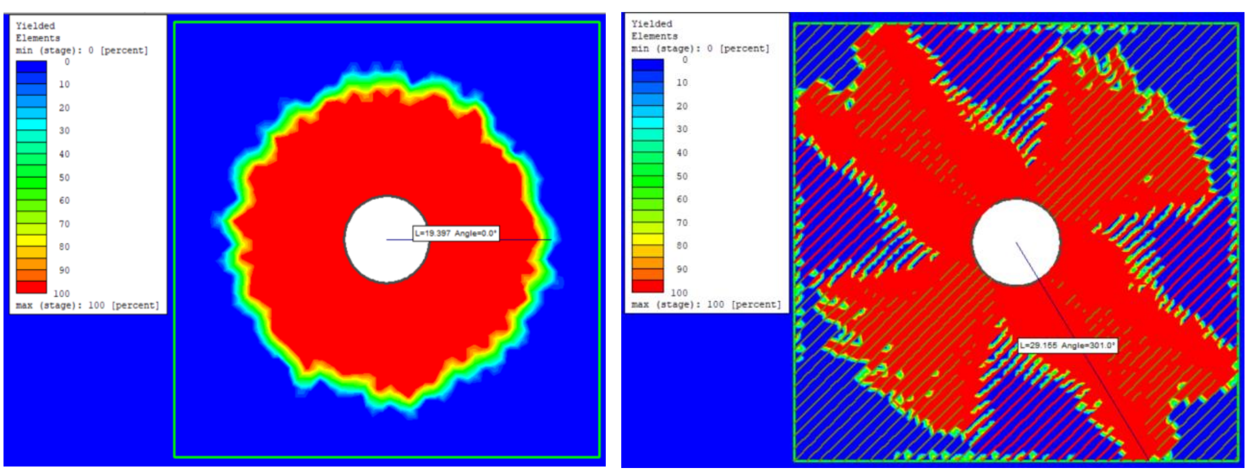

Figure 49- Yielded zone around the tunnel for 25% VBP models without Joint Network (left). On the right the same model with the addition of a Joint Network (yielded joints shown in red)

5.2 Results of 40% VBP models

With the increase of the VBP from 25% to 40% the amount of displacement and the yielding has reduced for both the scenarios with and without the presence of Joints. The radial displacements obtained around the hollow of the tunnel contour for 40% VBP models are shown and compared in Figure-49.

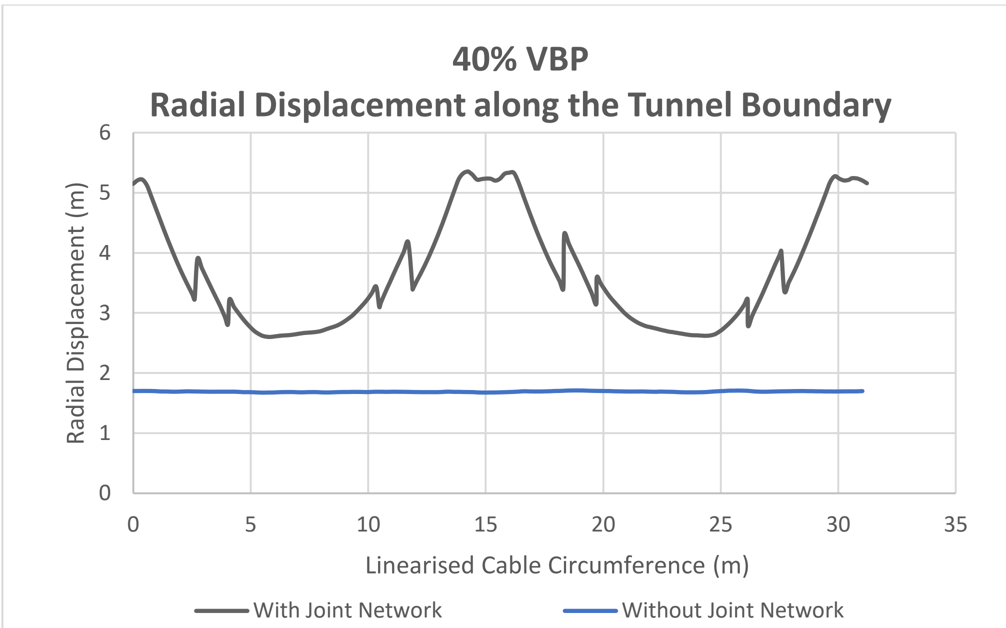

Figure 50- Comparison of the radial displacements on the linearized hollow contour of the tunnel, for the model with strength properties obtained on the basis of the Lindquist empirical approach (Lindquist 1994) with VBP = 40% in the presence of a Joint network and without it.

In the absence of a Joint network an isotropic behavior can be observed where the displacement around the tunnel contour is **1.6 m** approximately, lower than the one obtained in the case of 25% VBP (2.2m).

With the increase of VBP, the displacement around the tunnel contour (Figure-50) has decreased also in the case of a joint network, being lower in the direction parallel to the Joint network and higher in the direction normal to it, with the maximum displacement reaching to around 5.3m.

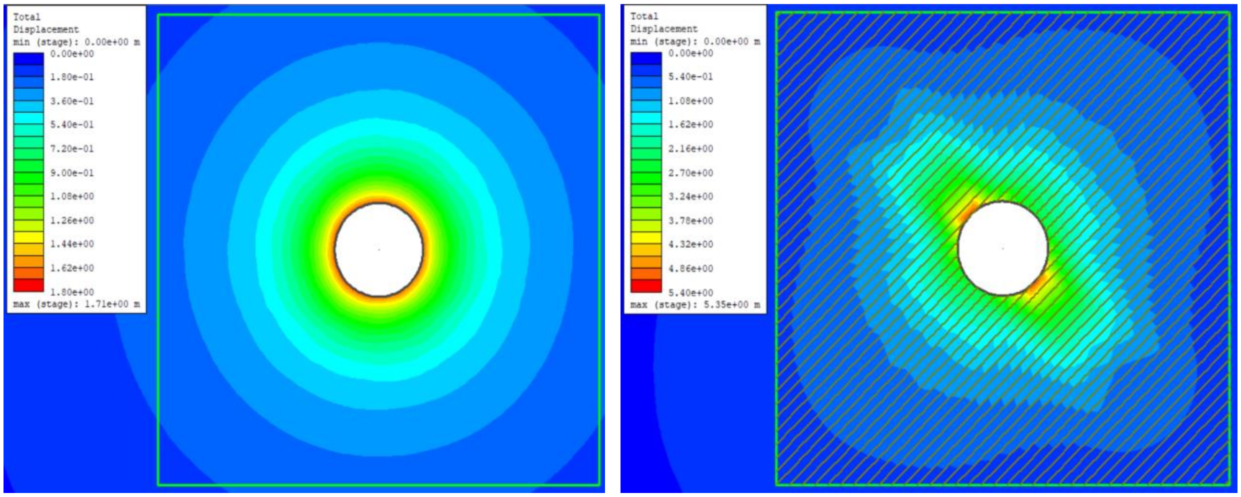

Figure 51- Models for 40% VBP without Joint Network on left and with Joint Network on right showing Total Displacement trend.

The yielding in Figure-51 shows also a decrease in magnitude with the reduction of VBP consistent with the results in case of displacement. The extent of plasticization is less than 25% VBP in both the cases, with and without the Joint network.

A plastic radius of approximate 16 m is observed in the absence of the joint network. For the case with a joint network, the yielding zone does not extend till the edge of the domain of interest but there still is a pronounced difference in yielding in the 2 directions: parallel and normal to the joints.

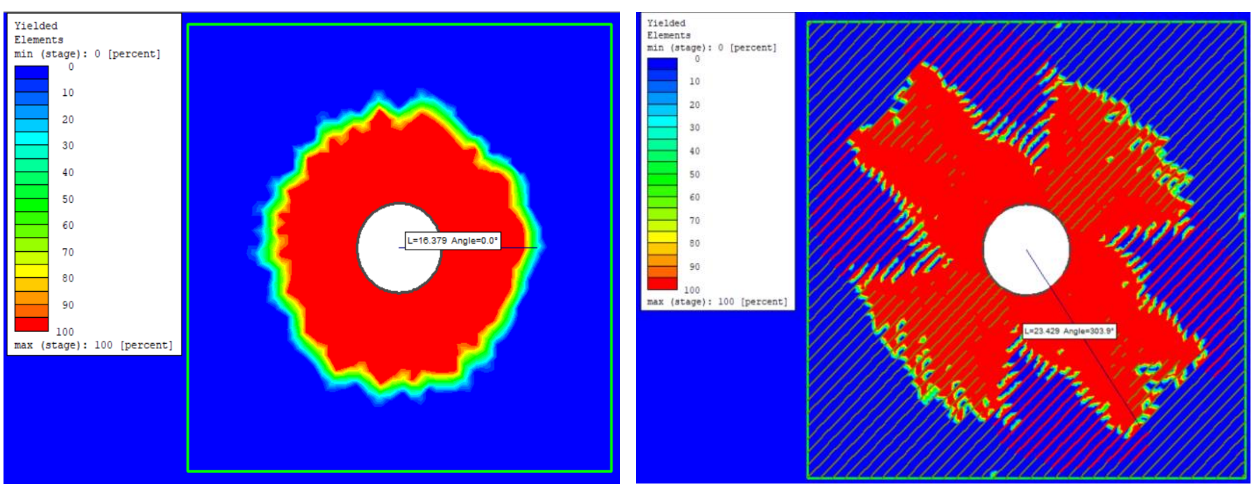

Figure 52- Yielded zone around the tunnel for models of 40% VBP without Joint Network (left). On the right the same model with the addition of a Joint Network (yielded joints shown in red)

5.3 Results of 55% VBP models

A further VBP increase to 55% reduces the amount of displacement and the yielding for both the scenarios with and without the presence of Joints. The radial displacements obtained around the hollow of the tunnel contour for 55% VBP models are shown and compared below in Figure-52:

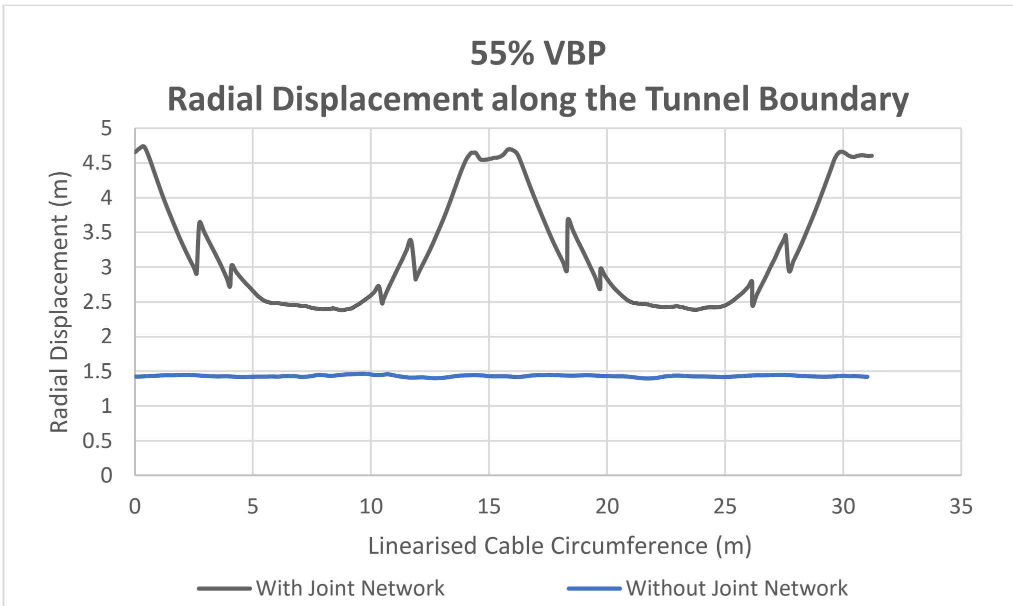

Figure 53- Comparison of the radial displacements on the linearized hollow contour of the tunnel, for the model with strength properties obtained on the basis of the Lindquist empirical approach (Lindquist 1994) with VBP = 55% in the presence of a Joint network and without it.

The behavior in case of displacement (Figure-53) is consistent as for the previous VBPs with an isotropic behavior in the absence of a Joint network showing an average displacement of 1.4 m approximately, still following the decreasing trend with the increase of VBP.

The maximum displacement is about 4.7m in the presence of a Joint network occurring in a direction normal to the Joints. This value is lower than 6m and 5.3m obtained in the previous two cases.

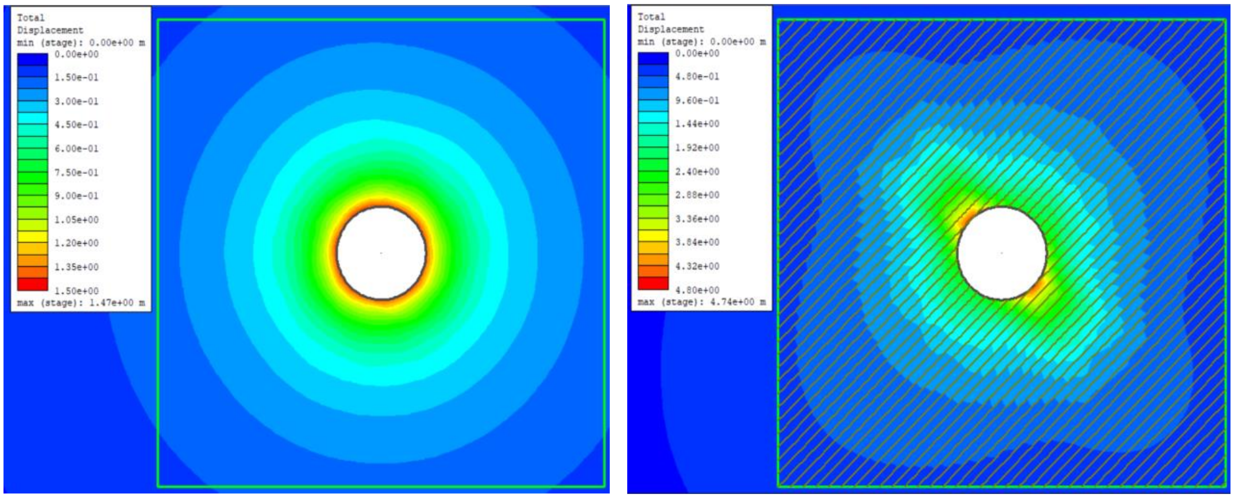

Figure 54- Models for 55% VBP without Joint Network on left and with Joint Network on right showing Total Displacement trend.

The extent of plasticization is less in both the cases with and without the Joint network with the increase of VBP to 55%.

A plastic radius of approximate 14.5 m is observed in the absence of joints in Figure-54. The yielding zone in case of the presence of joints is still extended more in one direction than the other.

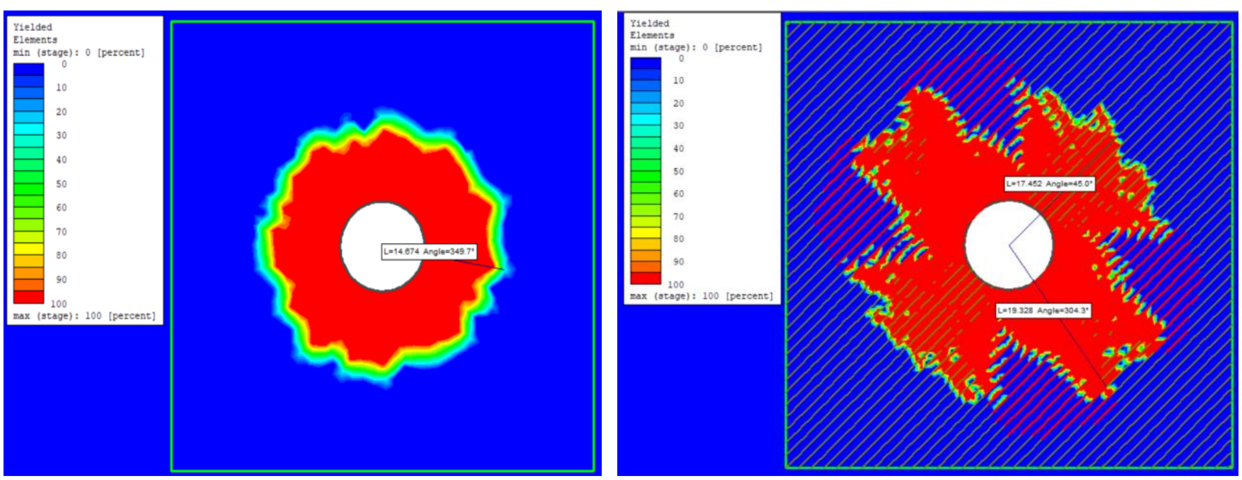

Figure 55- Yielded zone around the tunnel for models of 55% VBP without Joint Network (left). On the right the same model with the addition of a Joint Network (yielded joints shown in red)

5.4 Results of 70% VBP models

The last models for the highest VBP of 70% with and without the presence of Joints yielded the following results with lower displacement with respect to the previous cases (VBP equal to 25%, 40% and 55%). The radial displacements around the hollow of the tunnel contour for 70% VBP models are shown and compared in Figure-55.

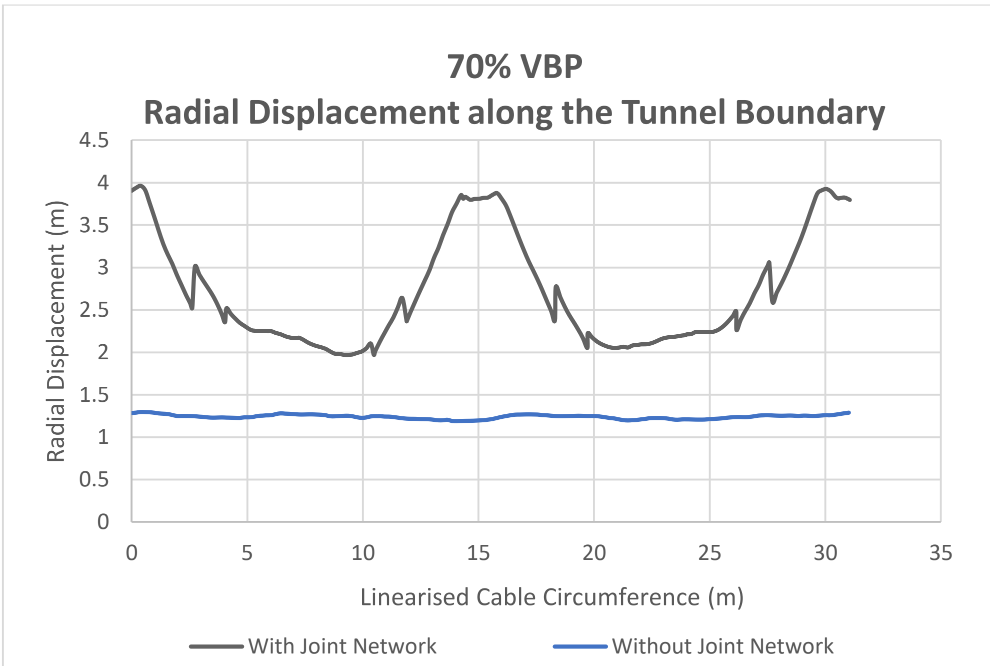

Figure 56- Comparison of the radial displacements on the linearized hollow contour of the tunnel, for the model with strength properties obtained on the basis of the Lindquist empirical approach (Lindquist 1994) with VBP = 70% in the presence of a Joint network and without it.

The trend of displacement (Figure 56) for the model with a joint network is still symmetric with higher displacement occurring in the direction normal to the joint network with a maximum value of 3.9m.

The isotropic behavior in the absence of joints leads to a displacement of 1.2m, which is significantly lower than the other case where the joints have been added.

In both the cases, however, the displacement has decreased (due to the VBP increase), and this is consistent with the results provided by the previous models analyzed.

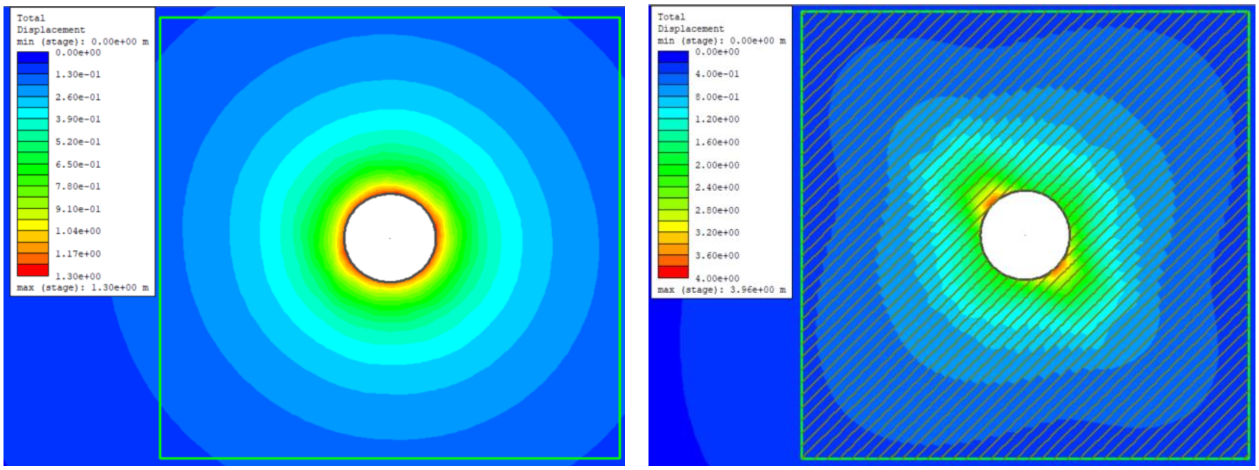

Figure 57- Models for 70% VBP without Joint Network on left and with Joint Network on right showing Total Displacement trend.

For the case of absence of a Joint network plasticization extends to a radius of 13.5m approximately in Figure-57.

The yielding, in case of the presence of the Joint network, reduces as compared to that observed for previous lower VBPs.

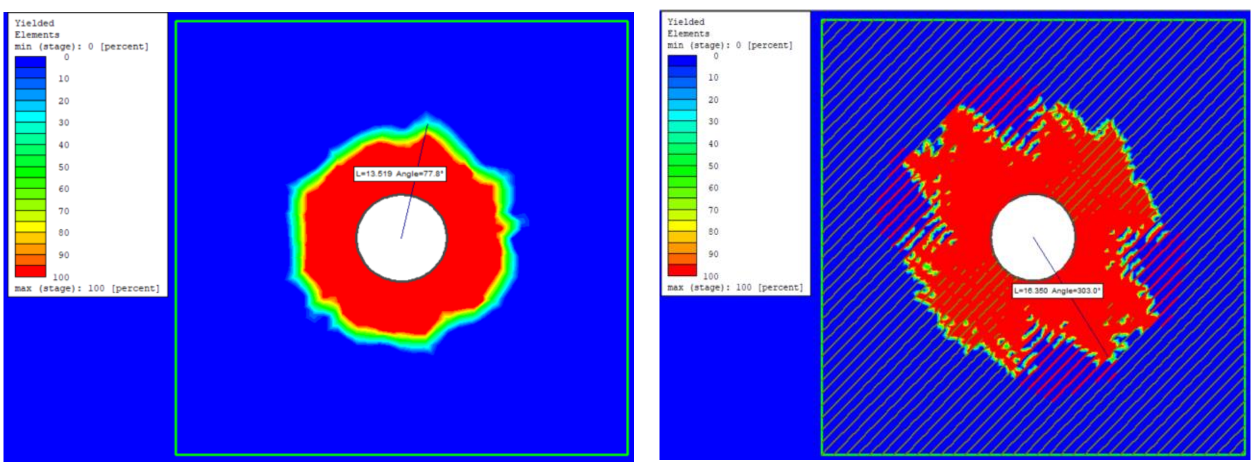

Figure 58- Yielded zone around the tunnel for models of 70% VBP without Joint Network (left). On right the same model with the addition of a Joint Network (yielded joints shown in red)

The results obtained have demonstrated that for high VBPs there is an improvement in the structural response of the material affected by the excavation.

Table-6 compares the results obtained from the Lindquist analysis with Joint network with those obtained from heterogeneous models with joint network. The displacement values are quite high using the Lindquist approach as compared to the heterogeneous models.

	Max Displacement (m) in Joint Network models	
VBP	Lindquist models	Heterogeneous models
25%	6.30	3.63
40%	5.35	1.56
70%	3.96	0.37

Table 7- Comparison of Maximum displacement obtained in the presence of Joint Networks using Lindquist approach and heterogeneous models for each VBP

The empirical method of Lindquist provided an overly cautious solution with very high displacement values and hence, does not appear to be sufficiently capable of predicting the tunnel convergence for excavation in the reference domain examined. In conclusion, the behavior associated with the construction of an underground work in complex formations could not be adequately analyzed using this method.

Conclusions

The dissertation reports a study carried out in order to investigate the differences in the behavior of bimsoils with respect to bimrocks via numerical analyses by introducing an interface at the block-matrix contacts. The interface properties were gradually reduced with respect to that of the matrix in order to simulate Bimsoils and to ultimately study the mechanical and deformation response of a circular tunnel of 10m diameter. The results were then compared with those obtained in a previous work (Dadone, 2018) in which the same underground excavation was simulated in a Bimrock mass, without the presence of any interfaces.

The response of the heterogeneous material was investigated with respect to different volumetric Blocks percentages (VBP), with random arrangement and orientation of the block inclusions embedded in the matrix which were obtained by using a Matlab script that generated random block arrangements.

Analysis was carried out first starting with 25% VBP because below this threshold, the presence of rock blocks does not affect the overall behavior of the soft bimrocks/bimsoils much. Eight random block extractions for 25% VBP were modelled with the presence of rock-matrix interfaces in RS2 FEM software, in which the properties of the interfaces were gradually decreased from 100% to 25% of that of the matrix. It was observed that the presence of interfaces has not a marked effect on the response of the underground excavation, neither on the tunnel convergence nor the plasticization around the tunnels. On comparing these results of bimsoils with those related to bimrocks (Dadone, 2018), where no block-matrix interfaces were inserted, the tunnel response was almost similar.

1 random extraction each for higher VBP (40% and 70%) was also analysed in order to observe if the results changed if the percentage of blocks in the deposit increased, but it was not the case. This led to the conclusion that, when dealing with bimsoils, the simulation of the interfaces via Joint boundaries did not have significant effects on the response of the underground excavation and no notable differences were observed in numerical modelling of bimsoils with reduced interface strength as compared to bimrocks.

The response of the heterogeneous block-in-matrix formations was also studied in the presence of a rock mass with schistosity, by simulating a Joint Network within the matrix material. One model for each VBP considered (25%, 40% and 70%) was anlysed. The same model was then modified to include rock-matrix interface, and the results were compared. With reference to the radial displacements registered along the tunnel contour, for a given VBP, an increase in the overall radial displacement was noticed for models which included both the Joint network and the rock-matrix interface. This difference in the displacements became less pronounced as the VBP increased. We can conclude here that presence of rock-matrix interfaces is comparatively more important while dealing with lower VBPs. For the same Joint conditions, the displacement values decreased in both the cases, with the increasing VBPs.

Lastly, an analysis of the homogeneous approach was carried out based on the Lindquist empirical criterion in which again the effects of the presence of a Joint network was studied over the same range of VBPs (25%, 40%, 55% and 70%). In the absence of a Joint network an isotropic behavior was observed with same convergence all around the tunnel contour and a similar plastic zone which decreased as the VBP increased. The presence of the Joint network simulating schistosity of the matrix, as expected, provided anisotropic results with displacements and plasticization around the tunnel higher in the direction normal to the Joints as compared to the parallel direction. The results still decreased as the VBP increased, consistently with the fact that for high VBPs there is an improvement in the structural response of the material affected by the excavation.

Bibliography

Adam, D. M. (2014). Block-in-Matrix Structure and Creeping Slope: Tunneling in Hard Soil and/or Weak Rock. *Geotech Geol Eng 32*, 1467–1476.

Afifipour, M. M. (2013). Mechanical behavior of bimrocks having high rock block proportion. Int. J. Rock Mech. Min. 40–48.

Afifipour, M. M. (2014). Mechanical behavior of bimrocks having high rock block proportion. *Int. J. Rock Mech. Min. Sci. 65,*, 40–48.

Barbero M., B. M.-B. (2007). Numerical modelling of the mechanical behaviour of bimrock. . *Proc. 11th ISRM*.

Barbero, M. B.-B. (2008). Three-dimensional finite element simulations of compression tests on bimrock. *In Proceedings of the 12th international conference of international association for computer methods and advances in geomechanics (IACMAG), Goa, India*, 631-37.

Barbero, M. B.-B. (2012). Numerical Simulations of Compressive Tests on Bimrock. *EJGE, 17, 3397-3414.*

Button, G. R. (2001). Tunnelling in Tectonic Melanges – Accommodating the Impacts of Geomechanical Complexities and Anisotropic Rock Mass Fabrics. . *Bulletin of Engineering Geology and the Environment*.

Coli N., B. P. (2012). The contribution of geostatistics to the characterisation of some bimrock properties. *Engineering Geology, vol. 137-138:* , 53-63.

Coli, N. B. (2011). In situ non-conventional shear tests for the mechanical characterisation of a bimrock. *Int J Rock Mech Min Sci 48(1):*, 95–102.

Dadone. (2018). Analysis of underground excavations in complex formations. *Master's Degree Thesis*.

Goodman, M. a. (1994.). Estimating the block volumetric proportions of mélanges and similar block-in-matrix rocks (bimrocks), Proceeding, 1st North American Rock Mechanics Symposium, Austin, TX, May .

Goodman, RE, Ahlgren, CS. (2000). Evaluating the safety of a concrete gravity dam on weak rock-Scott Dam. *Journal of Geotechnical and Geoenvironmental Engineering 126*, 429-442.

Irfan, T.Y., Tang, K.Y. (1995). Effect of the Coarse Fractions on the Shear Strength of Colluvium. GEO report No.22. *Hong Kong Geotechnical Engineering Office, Reprinted*, 223.

Kalender A., S. H. (2014). An approach to predicting the overall strengths of unwelded bimrocks. Engineering Geology 183 65-79.

Li, X. L. (2004). In-situ tests and a stochastic structural model of rock and soil aggregate in the three Gorges Reservoir area, China. *Int. J. Rock Mech. Min. Sci., 41, No. 3* , 702-707.

Lindquist, E. (1991). Fractals-Fracture and Franciscan Melange. *Term Paper for CE 280, Rock Mechanics instructor: Prof. R.E Goodman, Dept Civil Engineering, University of California, Berkeley*.

Lindquist, E. (1994). The Strength and Deformation Properties of Melange. . *Ph.D. dissertation, Department of Civil Engineering, University of California, Berkeley.*

Lindquist, E.S., Goodman, R.E. (1994). Strength deformation properties of a physical model melange. *Proceedings 1st North American Rock Mech. Symp., Austin, Texas*, 843-850.

Mandelbrot. (1983). Geometric Implementation of Hypercubic Lattices with Noninteger Dimensionality by Use of Low Lacunarity Fractal Lattices.

Medley E. (1999). Systematic characterization of melange bimrocks and other chaotic soil/rock mixtures. Felsbau 17. *No.3.*

Medley E. (2007b). Bimrocks Article Part 2: Case Histories and Practical Guidelines. Newsletter of HSSMGE, No. 8, April.

Medley, E. (1994). The engineering characterization of melanges and similar block-in-matrix rocks (bimrocks). *Dept of Civil Engineering, University of California, Berkley, California, PhD diss., UMI Diss. Svc., Ann Arbor, NI.*

Medley, E. (1997). Uncertainty in estimates volumetric proportions in melange bimrocks. *Proceedings of International Symposium on Engineering Geology and the Environment, Athens, 23-27 June 1997, eds P.G Marinos et al.,*, 267-272.

Medley, E. (1999). Systematic characterization of melange bimrocks and other chaotic soil/rock mixtures. Febuary 17. *No.3*.

Medley, E. (2001). Orderly Characterization of Chaotic Franciscan Melanges. Felsbau Rock and Soil Engineering. *Journal for Engineering Geology, Geomechanics and Tunneling 19*, 4.20-4.21.

Medley, E. (2002). Estimating Block Size Distributions of Melanges and Similar Block-in Matrix Rocks (Bimrocks). *Proceedings of 5th North American Rock Mechanics Symposium (NARMS), Toronto,*, 509-606.

Medley, E. (2004). Observations on tortuous failure surface in bimrocks. *Felsbau Vol.22*, 35-43.

Medley, E. (2007a). Bimrocks-Part 1 Introduction. *Newsletter of the Hellenic Society of Soil Mechanics and Geotechnical Engineering, February 2007, No. 7, pp 17-21 with Errata*.

Medley, E. (July 2002). Estimating Block Size Distributions of Melanges and Similar Block-in Matrix Rocks (Bimrocks). . *Proceedings of 5th North American Rock Mechanics Symposium (NARMS), Toronto*, 509-606.

Medley, E. S. (2004). Characterization of Bimrocks (Rock/Soil Mixtures) with Application to Slope Stability Problems. *Proceedings Eurock 2004 53rd Geomechanics Colloquium Salzburg, Austria October*.

Medley, E., Lindquist, E.S. (1995). The engineering significance of the scale independence of some Franciscan melanges in California, USA. *Proceedings of the 35th US Rock Mechanics Symposium, Reno*, 907-914.

Medley, E., Sanz Rehermann, P.F. (2004). Characterization of Bimrocks (Rock/Soil Mixtures) with Application to Slope Stability Problems. *Proceedings Eurock 2004 53rd Geomechanics Colloquium Salzburg, Austria October*.

Medley, EW and Goodman, RE,. (1994). Estimating the block volumetric proportions of mélanges and similar block-in-matrix rocks (bimrocks). *Proceeding, 1st North American Rock Mechanics Symposium, Austin, TX, May*.

Napoli, M. B. (2018). A stochastic approach to slope stability analysis in bimrocks. . *International Journal of Rock Mechanics and Mining Sciences, 101*, 41-49.

Napoli, M. B. (2021). Tunneling in heterogeneous rock masses with a block-in-matrix fabric. *International Journal of Rock Mechanics and Mining Sciences, Vol 138*.

Pan, Y. M. (2008). Mechanical Properties of virtual block-inmatrix colluvium. *In: Proceedings of ARMA 2008, American Rock Mechanics Association, 42nd U.S. Rock Mechanics Symposium, San Francisco, USA, ARMA08-51, 8*.

Peitgen, H. J. (1992). Length, Area and Dimension: Measuring Complexity and Scaling Properties. . *Chaos and Fractals*, 183-228.

Riedmueller G., F. B. (2001). Engineering Geological Characterization of Brittle Faults and Classification of Fault Rocks, Felsbau Rock and Soil Engineering. *Journal for Engineering Geology, Geomechanics and Tunneling, Vol. 19, No. 4*, 13-18.

S. Kahraman, M. A. (2006). Estimating unconfined compressive strength and elastic modulus of a fault breccia mixture of weak blocks and strong matrix. *International Journal of Rock Mechanics and Mining Sciences Volume 43, Issue 8*, 1277-1287.

Sonmez, H. A. (2006a). Considerations in Developing an Empirical Strength Criterion for Bimrocks. *Proceedings 4th Asian Rock Mechanics Symposium (ARMS 2006), November 6-10, Singapore*.

Sonmez, H. E. (2016.). Predicting uniaxial compressive strength and deformation modulus of volcanic bimrock considering engineering dimension. Int. Jour. Rock Mech. Min. Sci. 86, . 91-103.

Sonmez, H. G. (2004a). Relationships Between Volumetric Block Proportions and Overall UCS of a Volcanic Bimrock. Felsbau Rock and Soil Engineering. *Journal for Engineering Geology, Geomechanics and Tunneling 22(5)*, 27-32.

Sonmez, H. G. (2006b). Estimating the Uniaxial Compressive Strength of a Volcanic Bimrock. *Int. Jour. Rock Mech. Min. Sci. 43,* , 554-561.

Sonmez, H. K. (2009). A conceptual empirical approach for the overall strength of unwelded bimrocks. *In ISRM Regional Symposium, Rock Engineering in Difficult Ground Condition, Soft Rock and Karst, Dubrovnik, Croatia*.

Sonmez,, H., T. E. (2004b). Models to predict the uniaxial compressive strength and the modulus of elasticity for Ankara Agglomerate. *Int. Jour. Rock Mech. Min. Sci. 41*, 717–729.

Turcotte, D. (1986). A Fractal Model for Crustal Deformation. . *Tectonophysics, 132*, 261-269.

Xu, W. W. (2016). Discrete element modelling of a soil-rock mixture used in an embankment dam. *International Journal of Rock Mechanics and Mining Sciences, 86*, 141-156.

Xu, W. Y. (2008). Study on the mesostructure and mesomechanical characteristics of the soil–rock mixture using digital image processing based finite element method. . *Int. J. Rock Mech. Min. Sci., 45,749–62*.

Annex A

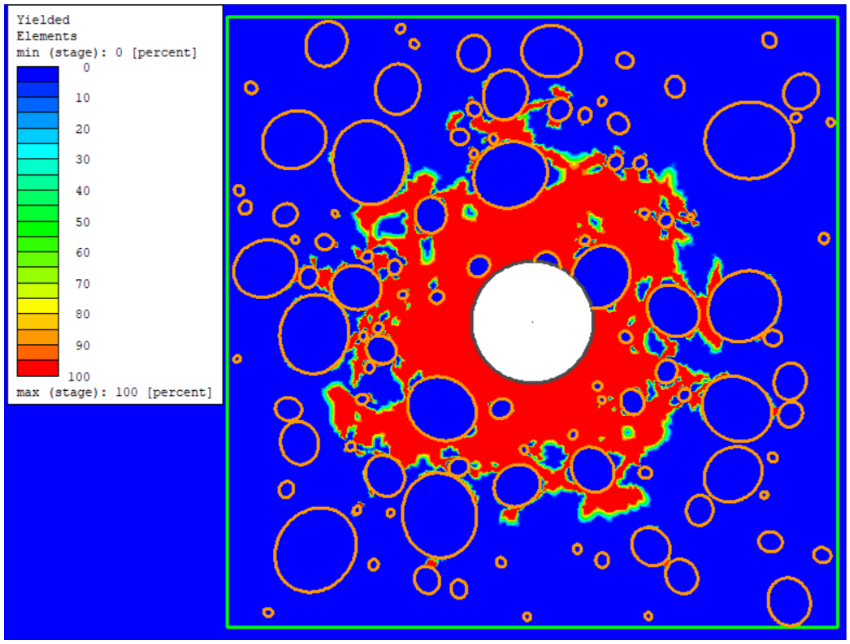

Figure 59- Plasticization around the tunnel at total relaxation associated with extraction 2 for 25%VBP with 25% of matrix properties of the interface. Model 0.25_2_0.25

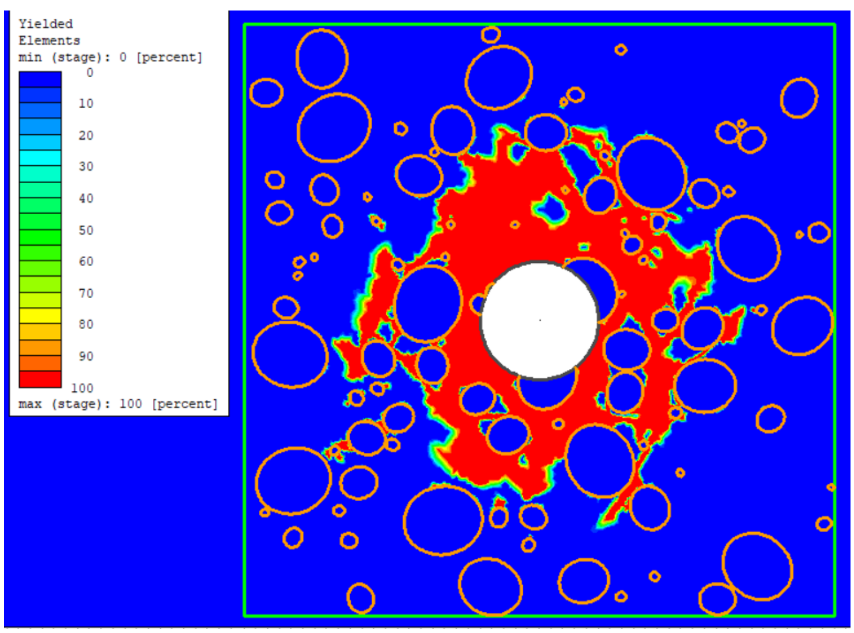

Figure 60- Plasticization around the tunnel at total relaxation associated with extraction 4 for 25%VBP with 25% of matrix properties of the interface. Model 0.25_4_0.25

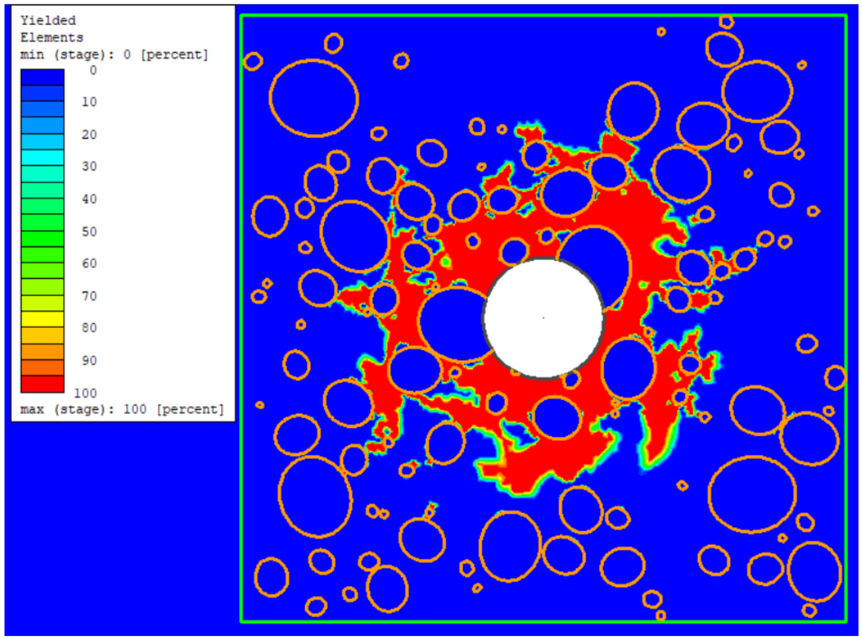

Figure 61- Plasticization around the tunnel at total relaxation associated with extraction 5 for 25%VBP with 25% of matrix properties of the interface. Model 0.25_5_0.25

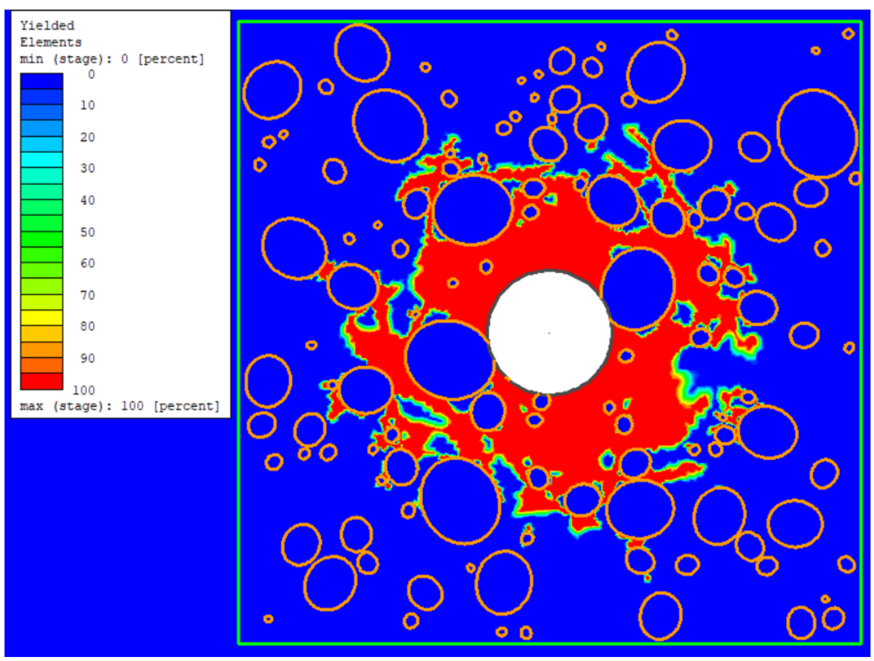

Figure 62- Plasticization around the tunnel at total relaxation associated with extraction 6 for 25%VBP with 25% of matrix properties of the interface. Model 0.25_6_0.25

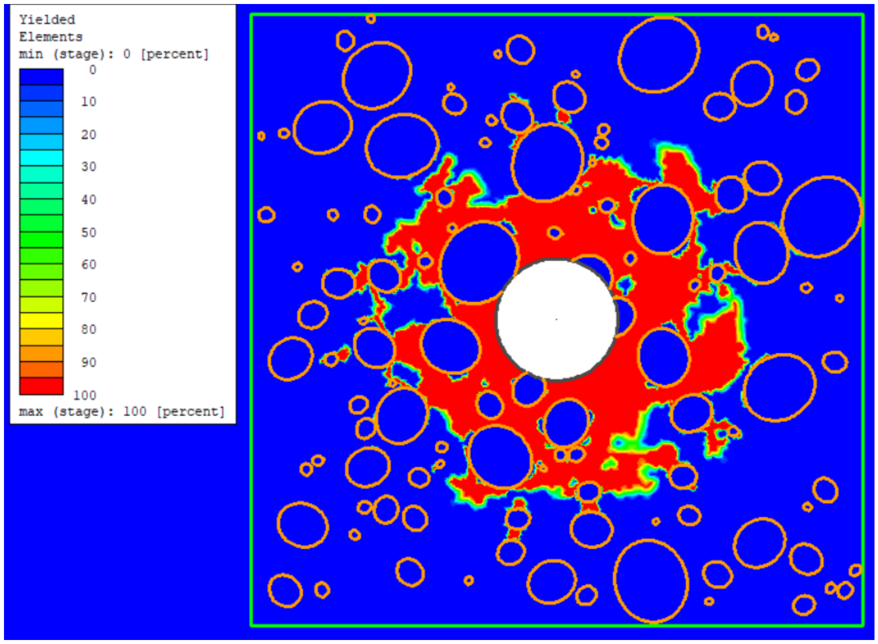

Figure 63- Plasticization around the tunnel at total relaxation associated with extraction 7 for 25%VBP with 25% of matrix properties of the interface. Model 0.25_7_0.25

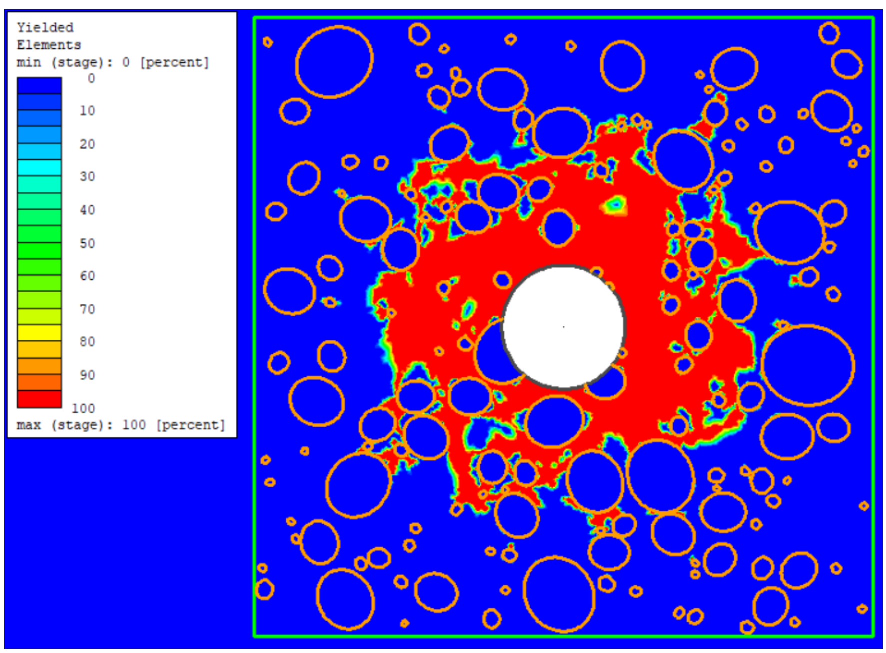

Figure 64- Plasticization around the tunnel at total relaxation associated with extraction 8 for 25%VBP with 25% of matrix properties of the interface. Model 0.25_8_0.25

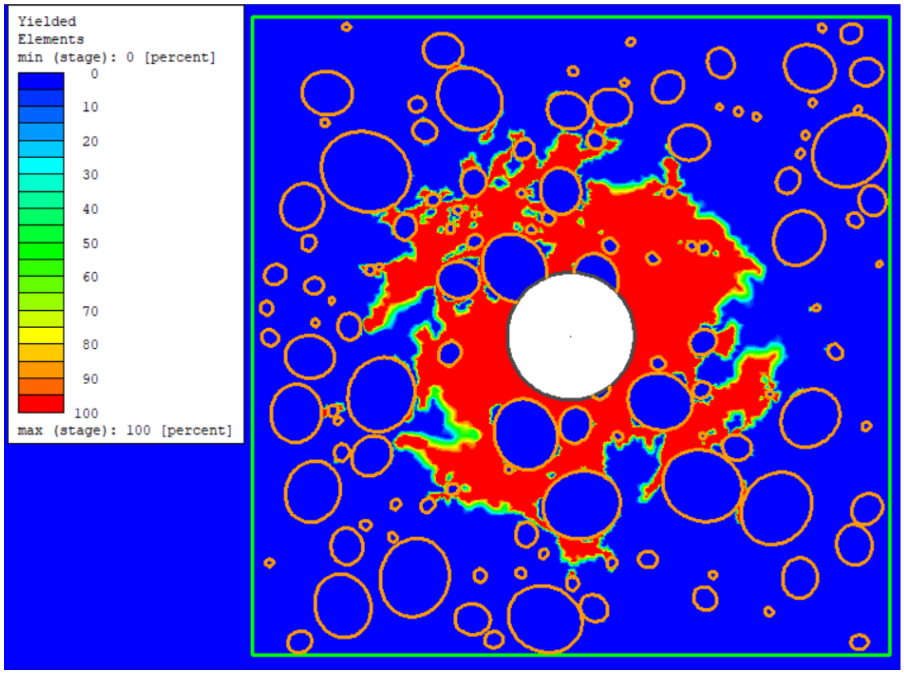

Figure 65- Plasticization around the tunnel at total relaxation associated with extraction 9 for 25%VBP with 25% of matrix properties of the interface. Model 0.25_9_0.25

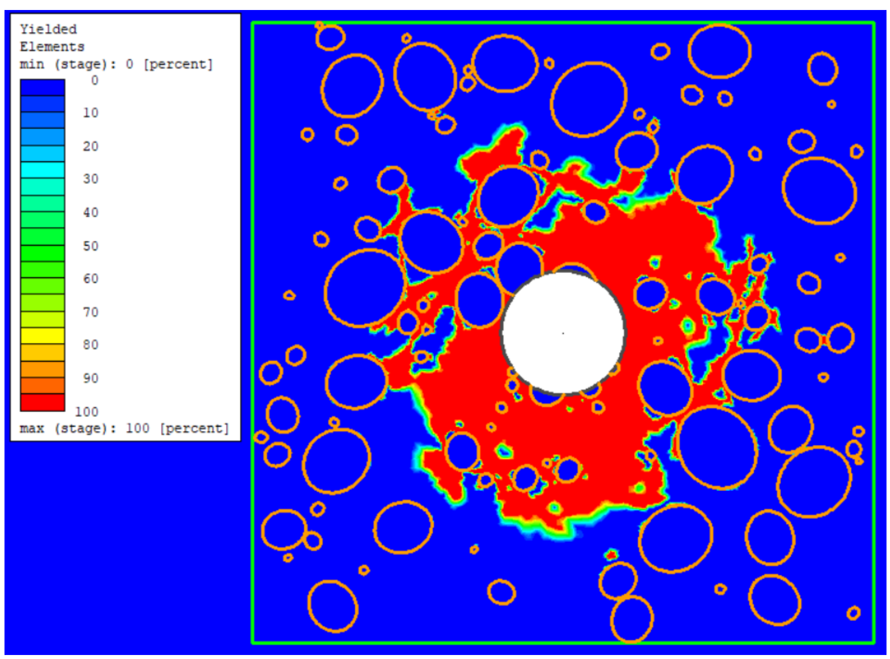

Figure 66- Plasticization around the tunnel at total relaxation associated with extraction 10 for 25%VBP with 25% of matrix properties of the interface. Model 0.25_10_0.25

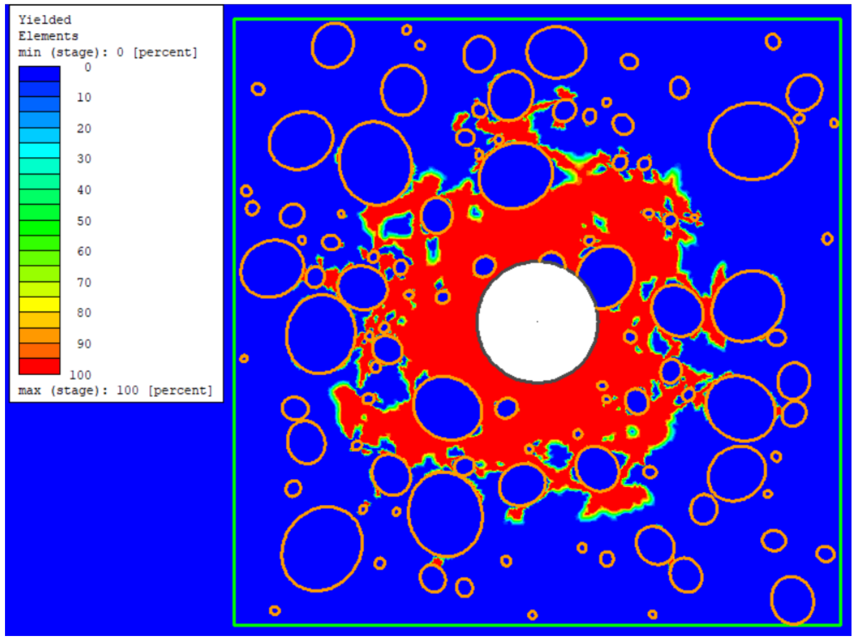

Figure 67- Plasticization around the tunnel at total relaxation associated with extraction 2 for 25%VBP with 50% of matrix properties of the interface. Model 0.25_2_0.5

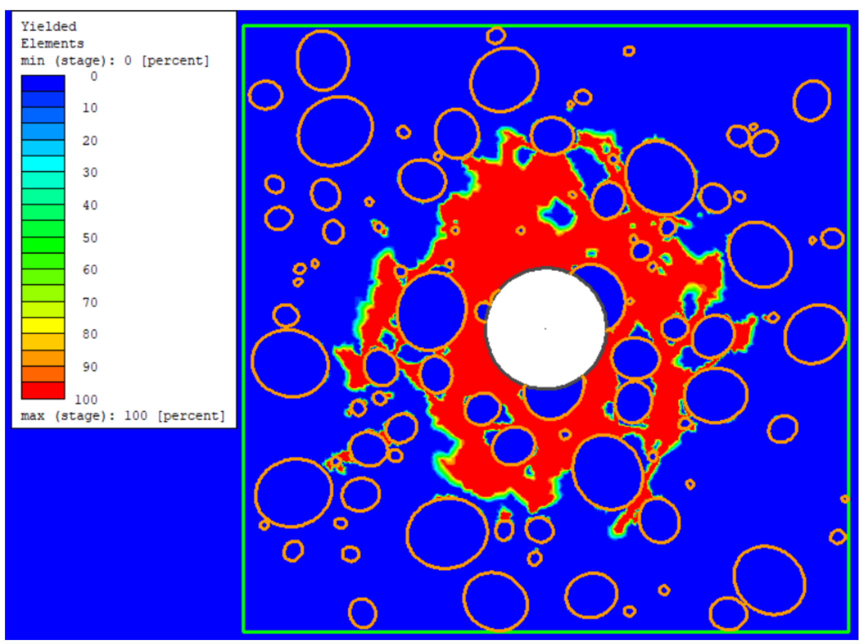

Figure 68- Plasticization around the tunnel at total relaxation associated with extraction 4 for 25%VBP with 50% of matrix properties of the interface. Model 0.25_4_0.5

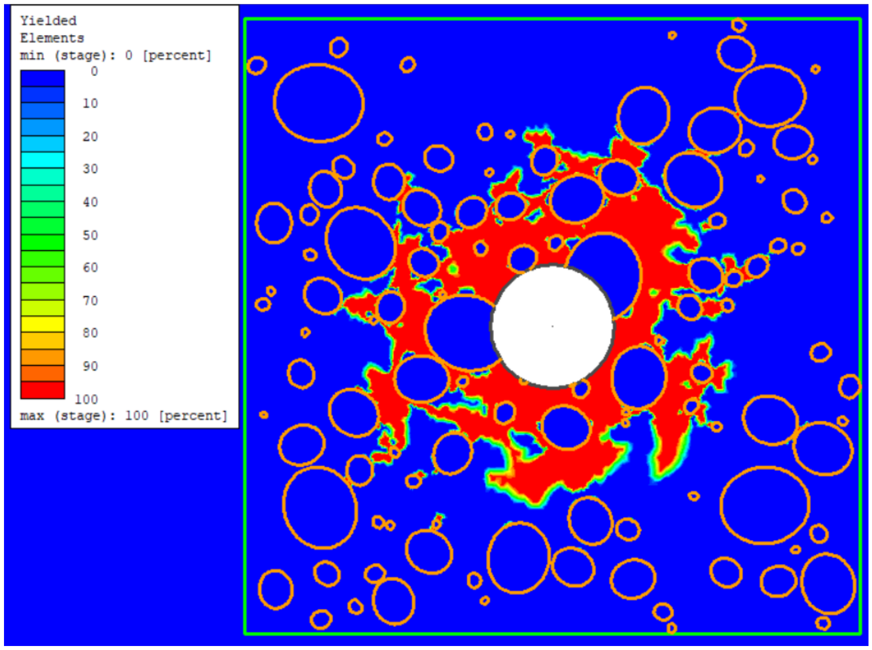

Figure 69- Plasticization around the tunnel at total relaxation associated with extraction 5 for 25%VBP with 50% of matrix properties of the interface. Model 0.25_5_0.5

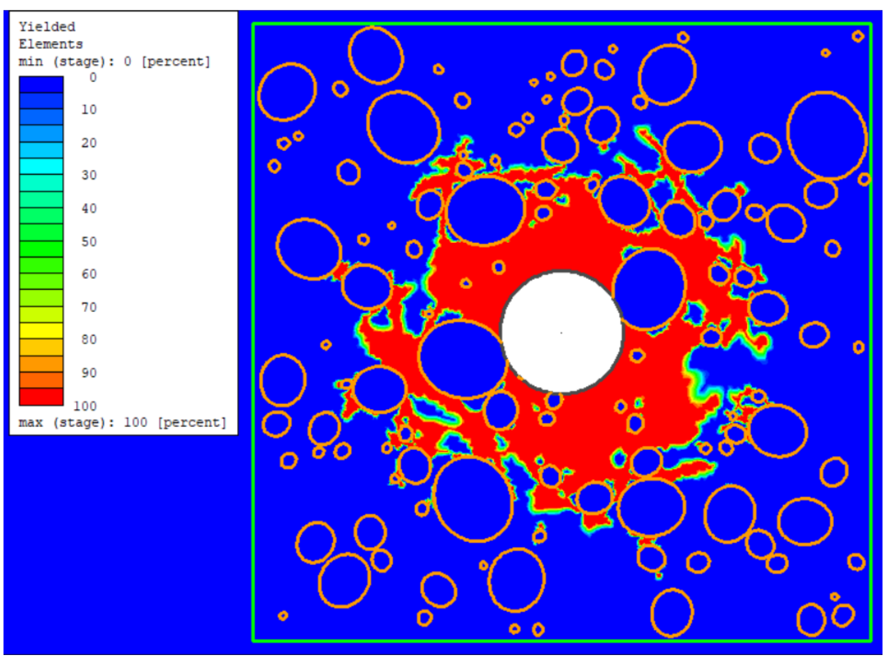

Figure 70- Plasticization around the tunnel at total relaxation associated with extraction 6 for 25%VBP with 50% of matrix properties of the interface. Model 0.25_6_0.5

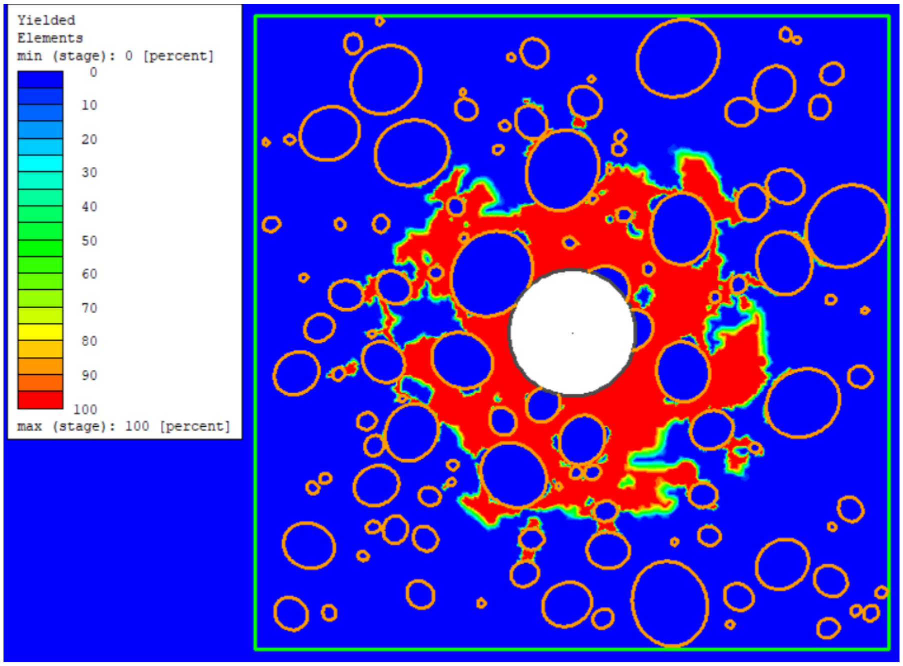

Figure 71- Plasticization around the tunnel at total relaxation associated with extraction 7 for 25%VBP with 50% of matrix properties of the interface. Model 0.25_7_0.5

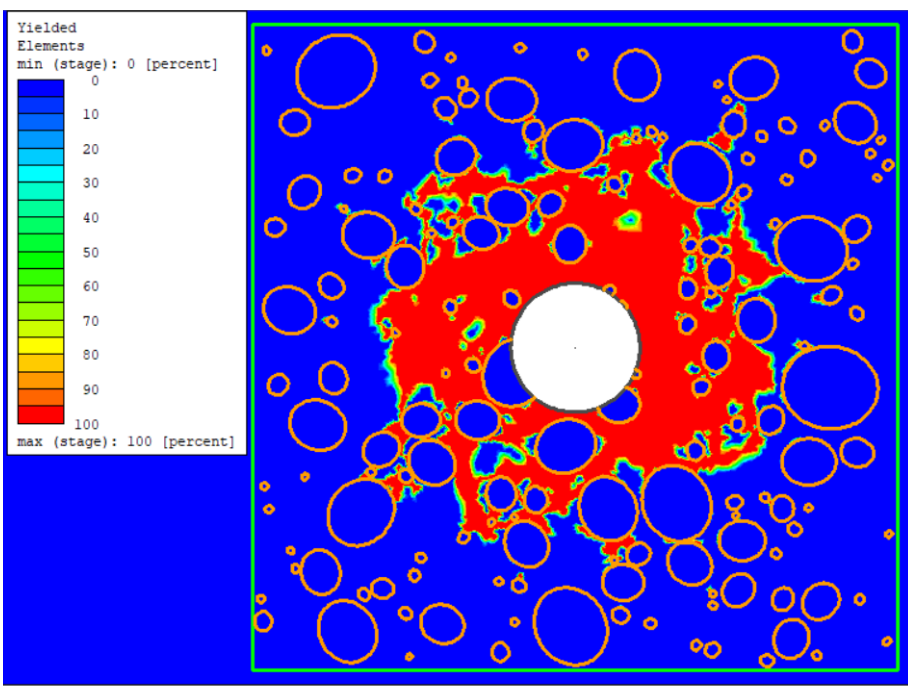

Figure 72- Plasticization around the tunnel at total relaxation associated with extraction 8 for 25%VBP with 50% of matrix properties of the interface. Model 0.25_8_0.5

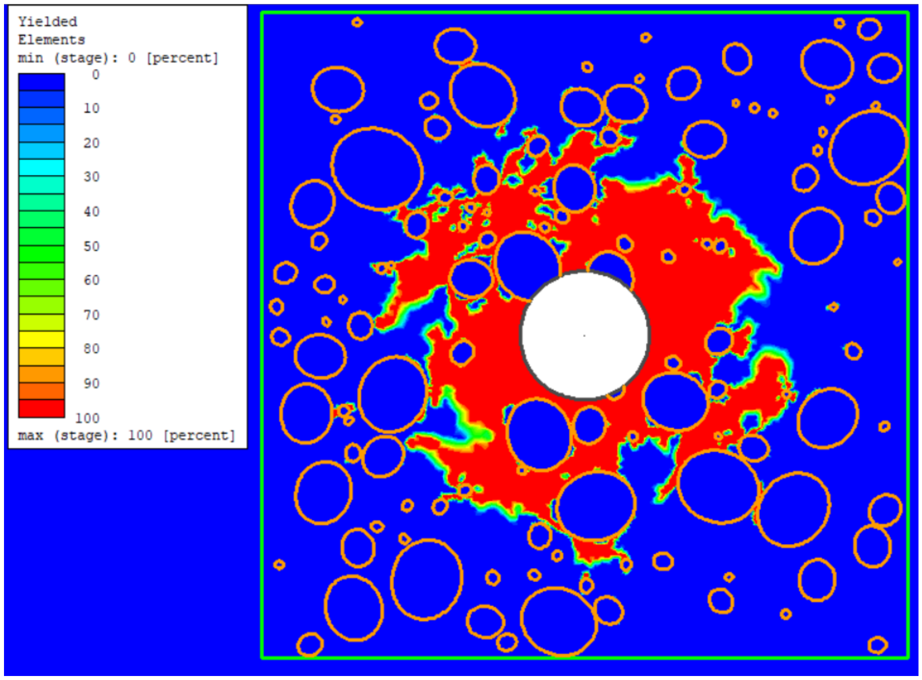

Figure 73- Plasticization around the tunnel at total relaxation associated with extraction 9 for 25%VBP with 50% of matrix properties of the interface. Model 0.25_9_0.5

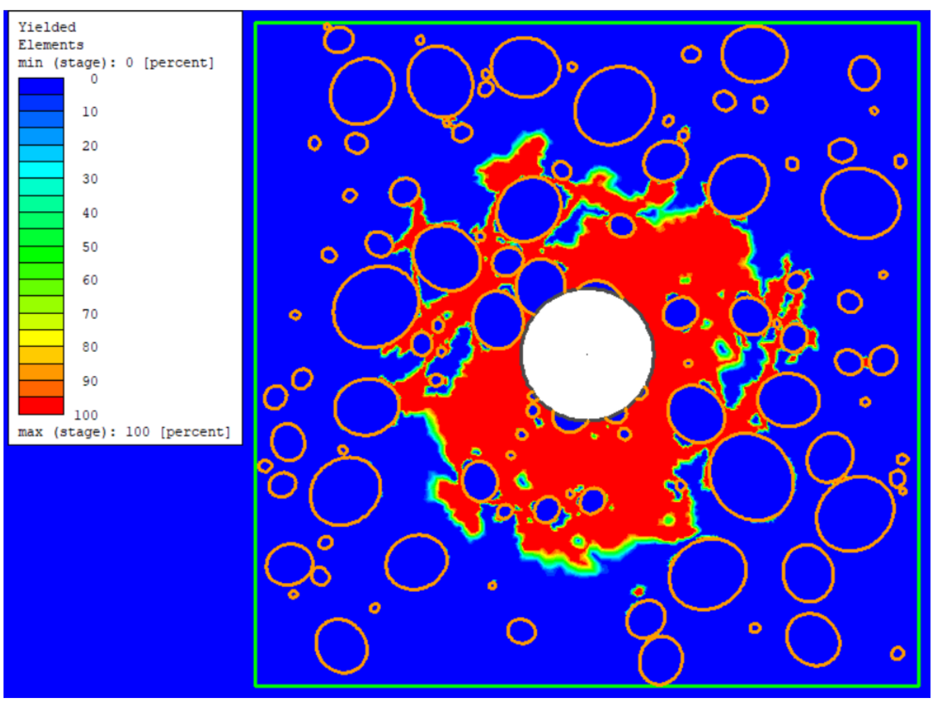

Figure 74- Plasticization around the tunnel at total relaxation associated with extraction 10 for 25%VBP with 50% of matrix properties of the interface. Model 0.25_10_0.5

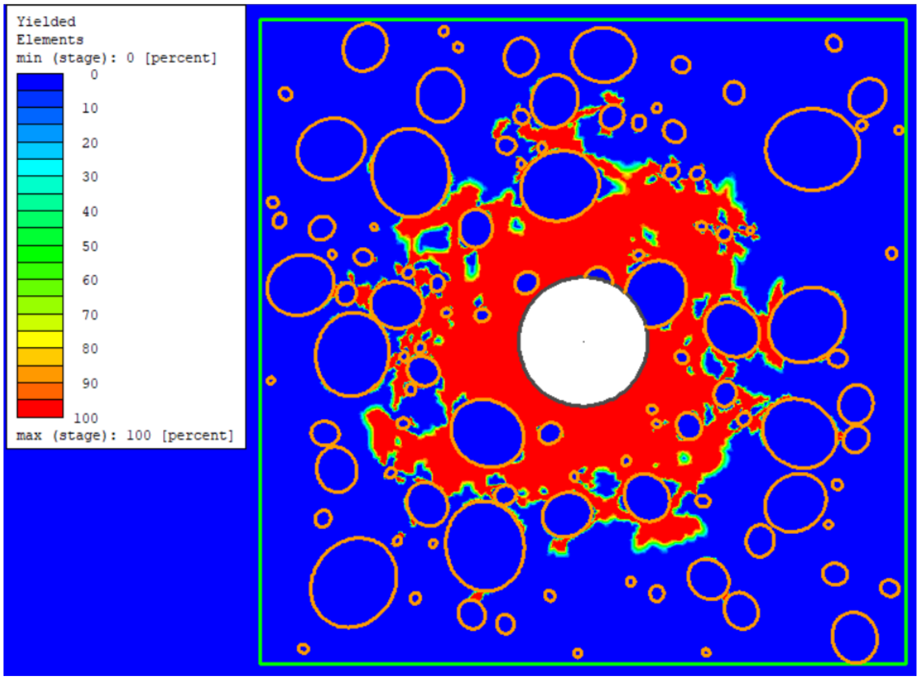

Figure 75- Plasticization around the tunnel at total relaxation associated with extraction 2 for 25%VBP with 75% of matrix properties of the interface. Model 0.25_2_0.75

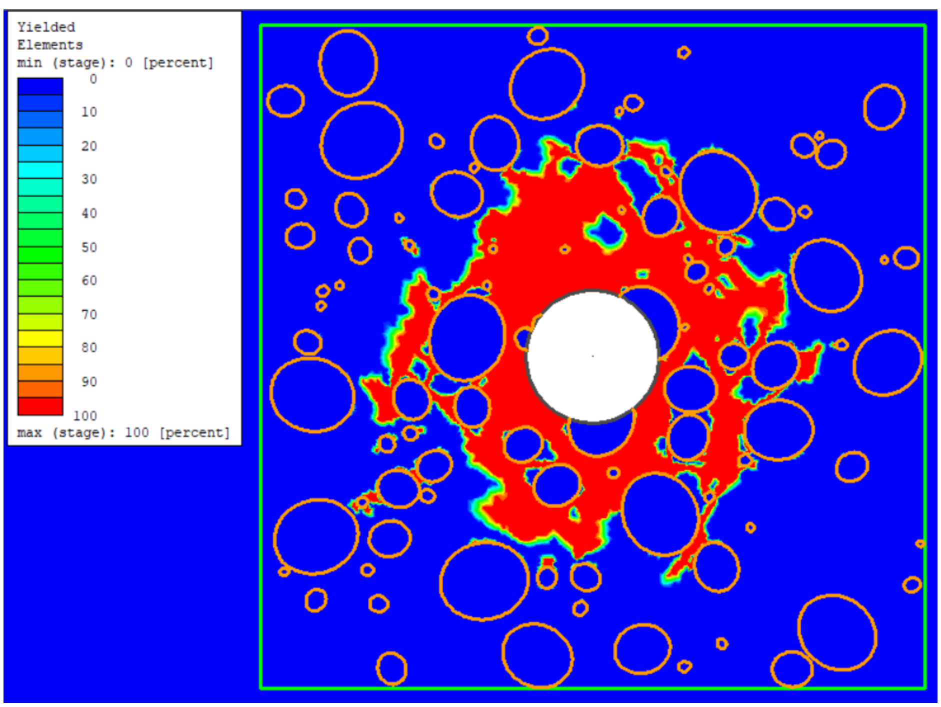

Figure 76- Plasticization around the tunnel at total relaxation associated with extraction 4 for 25%VBP with 75% of matrix properties of the interface. Model 0.25_4_0.75

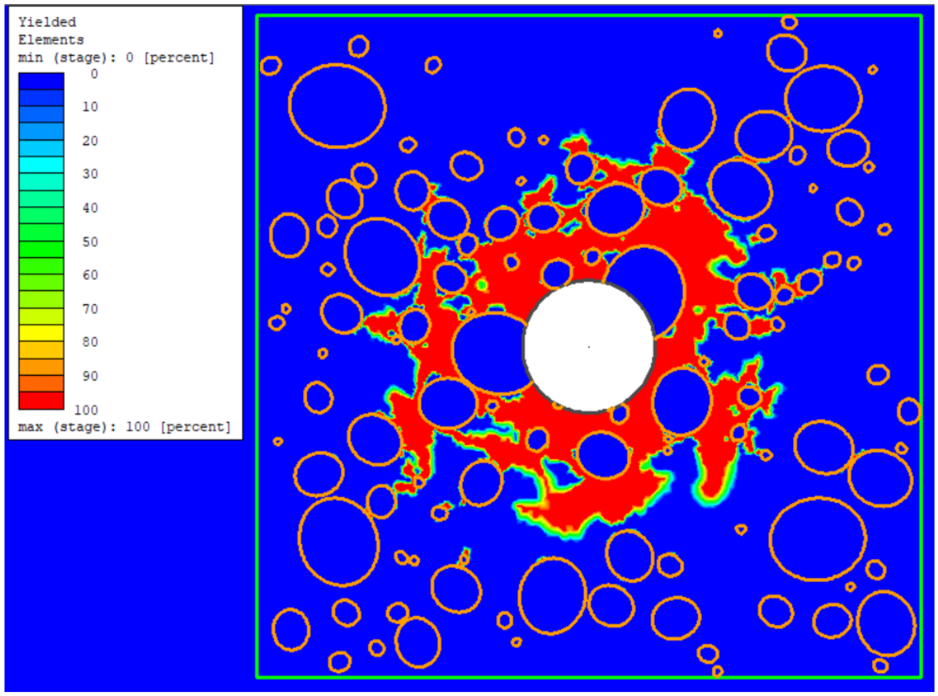

Figure 77- Plasticization around the tunnel at total relaxation associated with extraction 5 for 25%VBP with 75% of matrix properties of the interface. Model 0.25_5_0.75

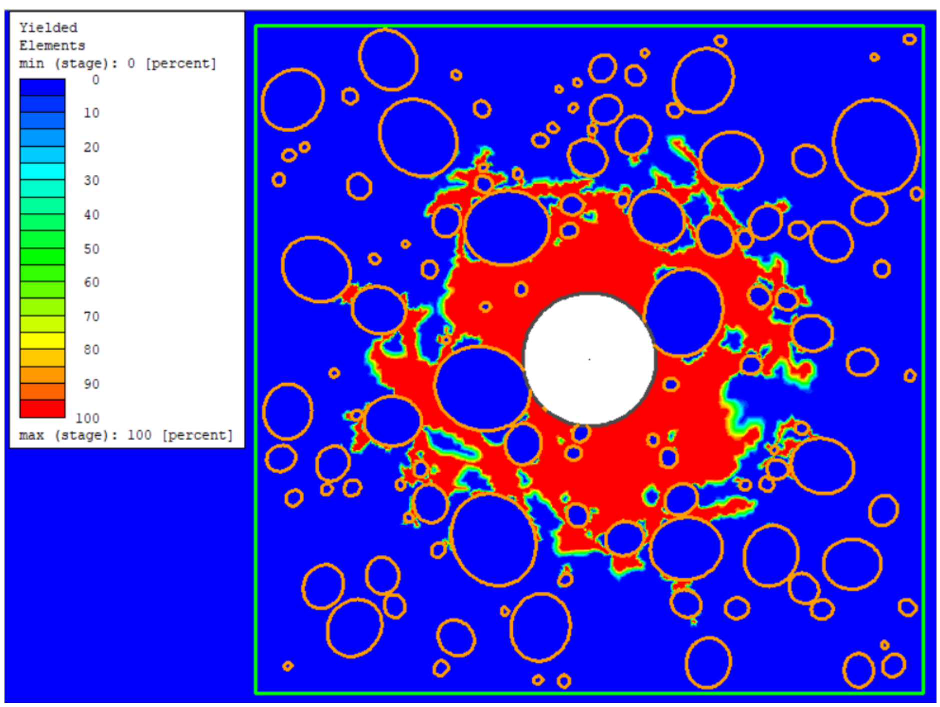

Figure 78- Plasticization around the tunnel at total relaxation associated with extraction 6 for 25%VBP with 75% of matrix properties of the interface. Model 0.25_6_0.75

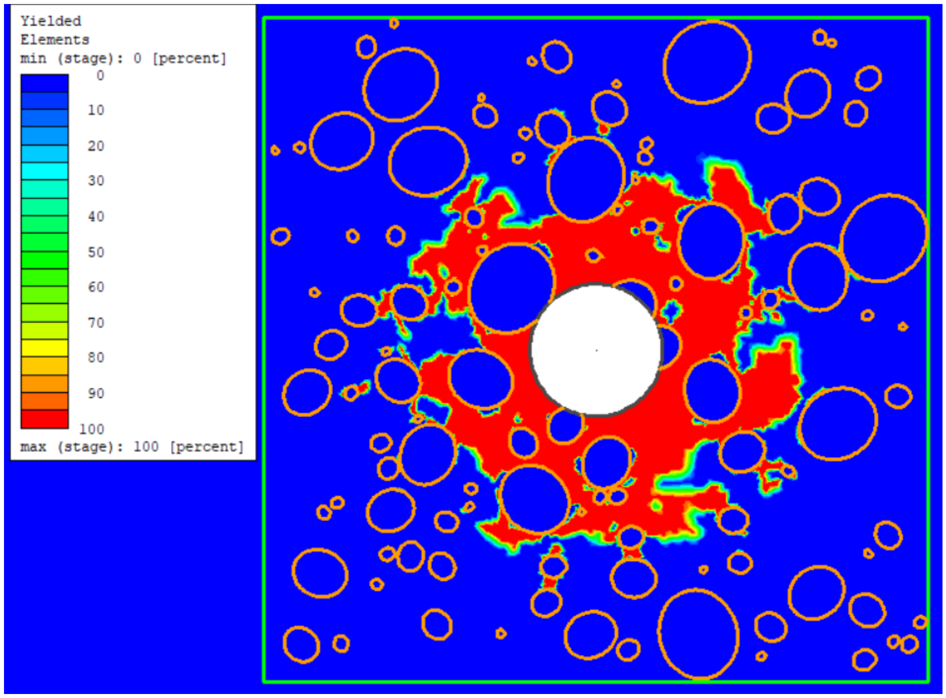

Figure 79- Plasticization around the tunnel at total relaxation associated with extraction 7 for 25%VBP with 75% of matrix properties of the interface. Model 0.25_7_0.75

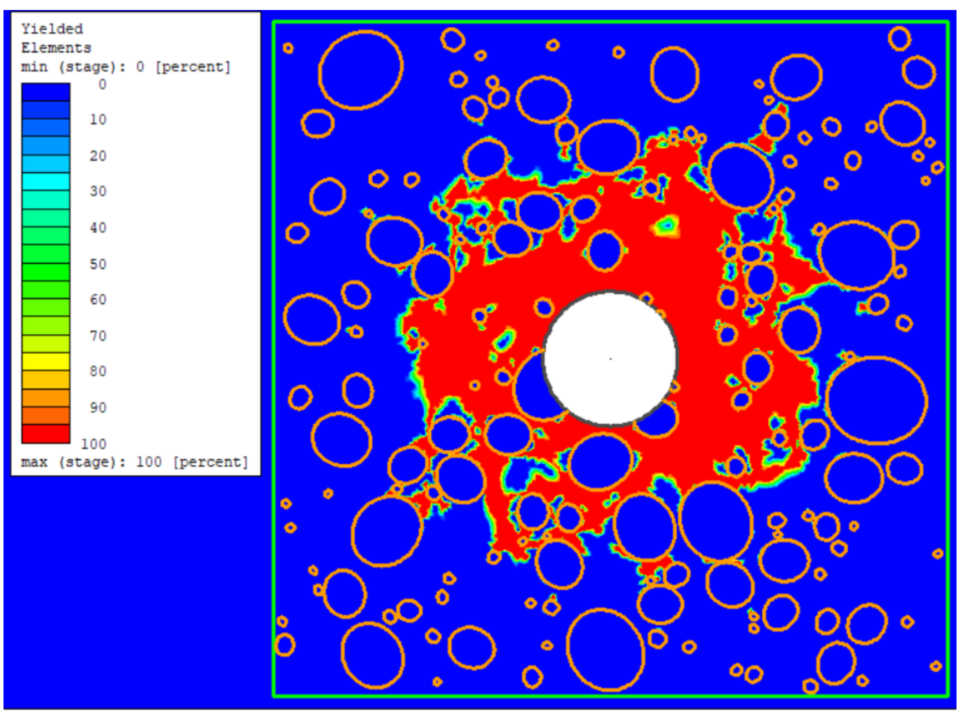

Figure 80- Plasticization around the tunnel at total relaxation associated with extraction 8 for 25%VBP with 75% of matrix properties of the interface. Model 0.25_8_0.75

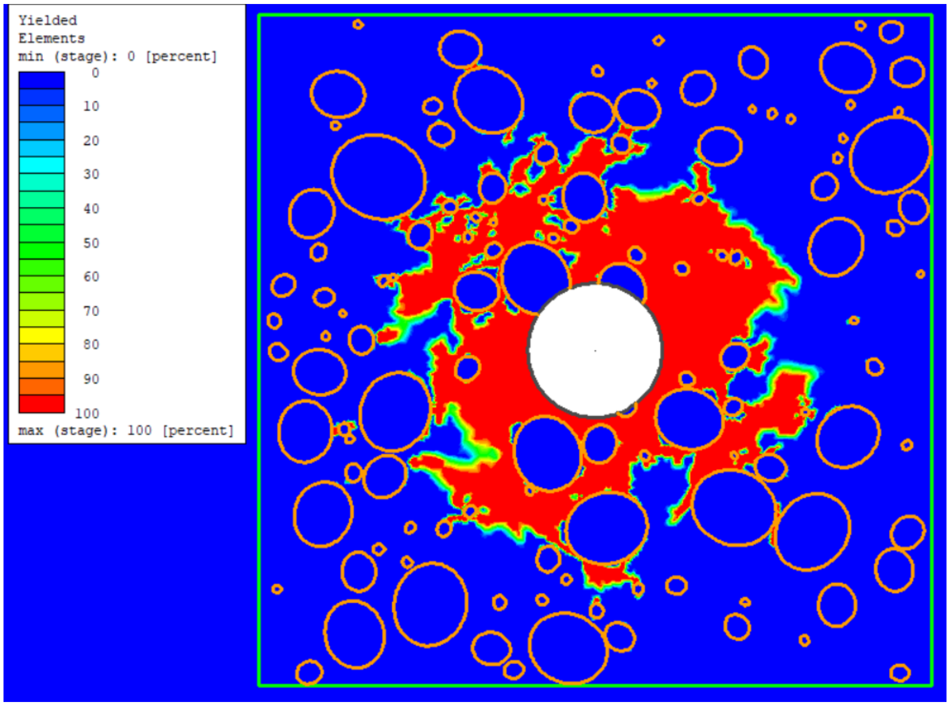

Figure 81- Plasticization around the tunnel at total relaxation associated with extraction 9 for 25%VBP with 75% of matrix properties of the interface. Model 0.25_9_0.75

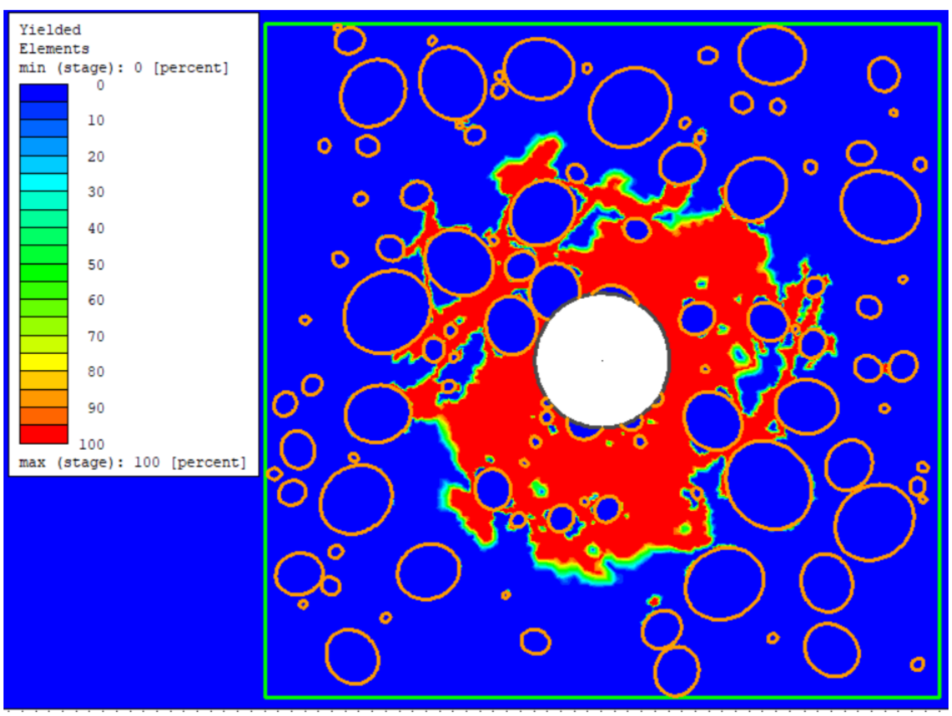

Figure 82- Plasticization around the tunnel at total relaxation associated with extraction 10 for 25%VBP with 75% of matrix properties of the interface. Model 0.25_10_0.75

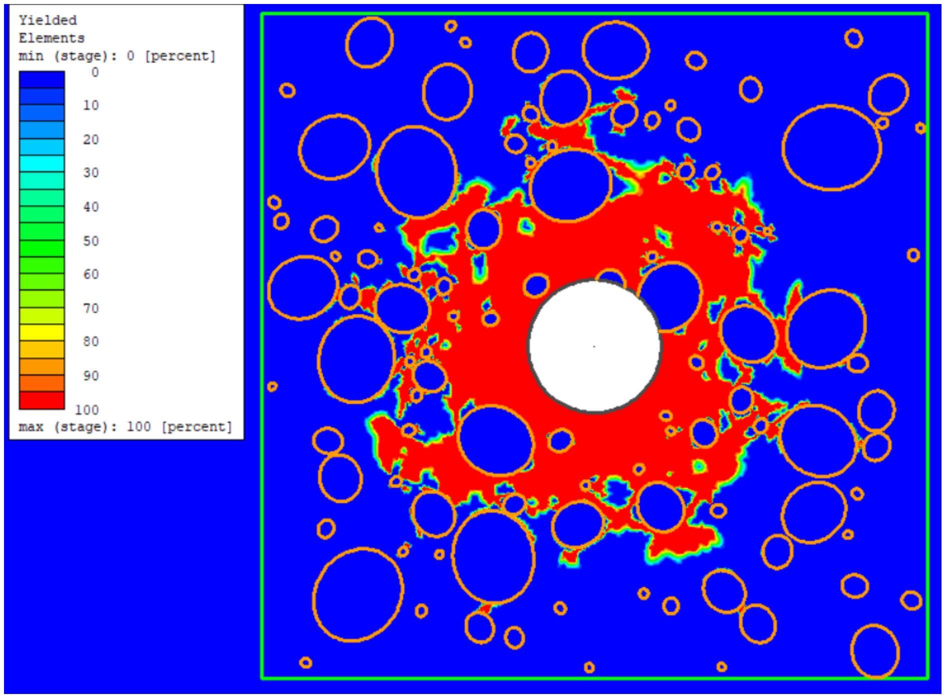

Figure 83- Plasticization around the tunnel at total relaxation associated with extraction 2 for 25%VBP with 100% (same as) matrix properties of the interface. Model 0.25_2_1.0

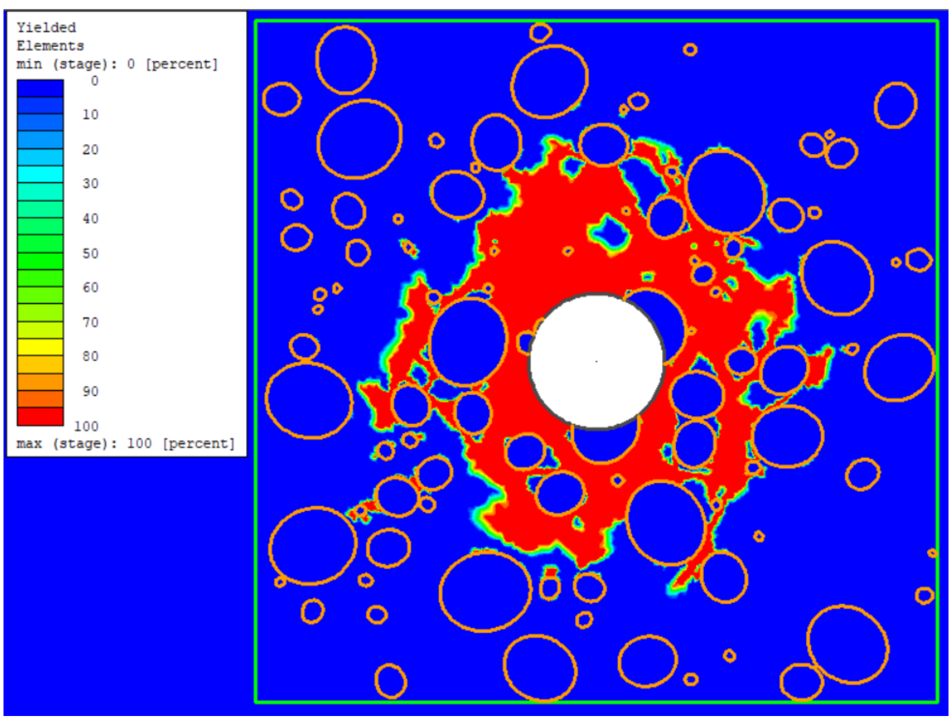

Figure 84- Plasticization around the tunnel at total relaxation associated with extraction 4 for 25%VBP with 100% (same as) matrix properties of the interface. Model 0.25_4_1.0

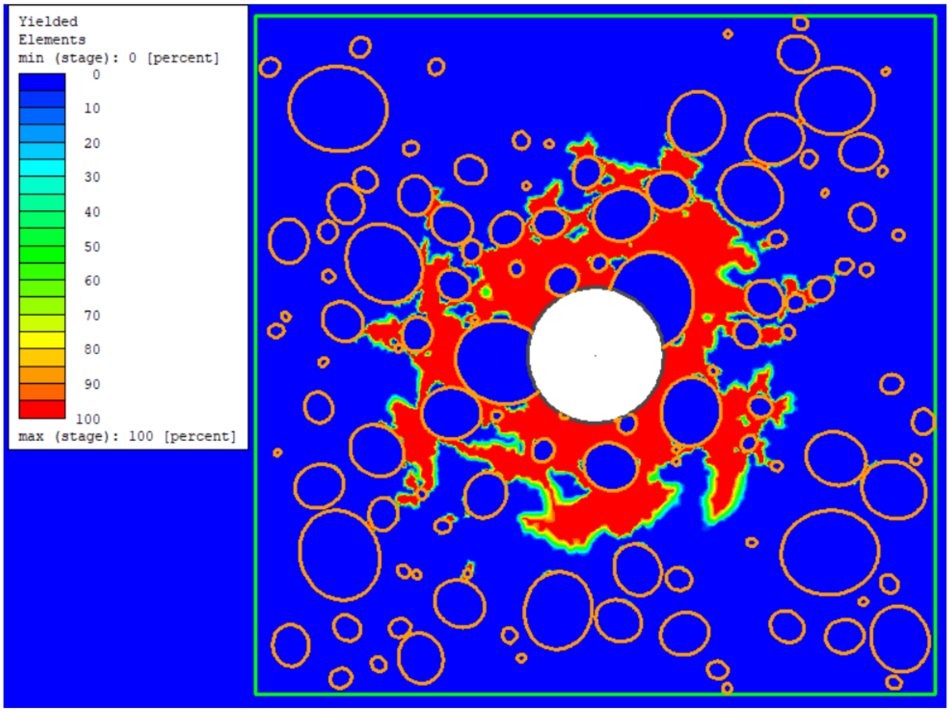

Figure 85- Plasticization around the tunnel at total relaxation associated with extraction 5 for 25%VBP with 100% (same as) matrix properties of the interface. Model 0.25_5_1.0

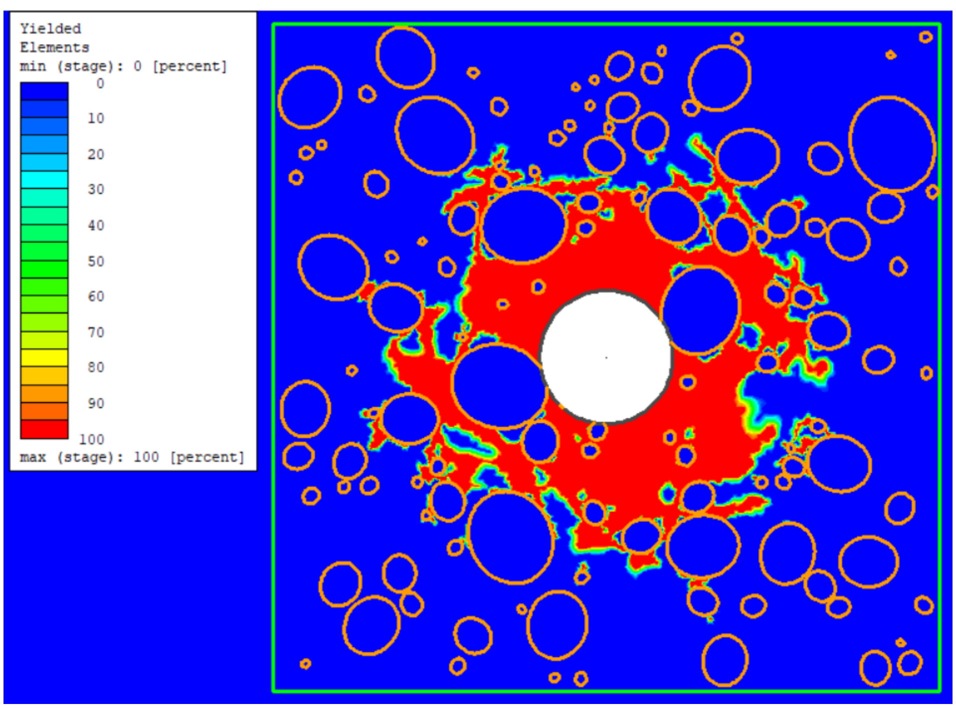

Figure 86- Plasticization around the tunnel at total relaxation associated with extraction 6 for 25%VBP with 100% (same as) matrix properties of the interface. Model 0.25_6_1.0

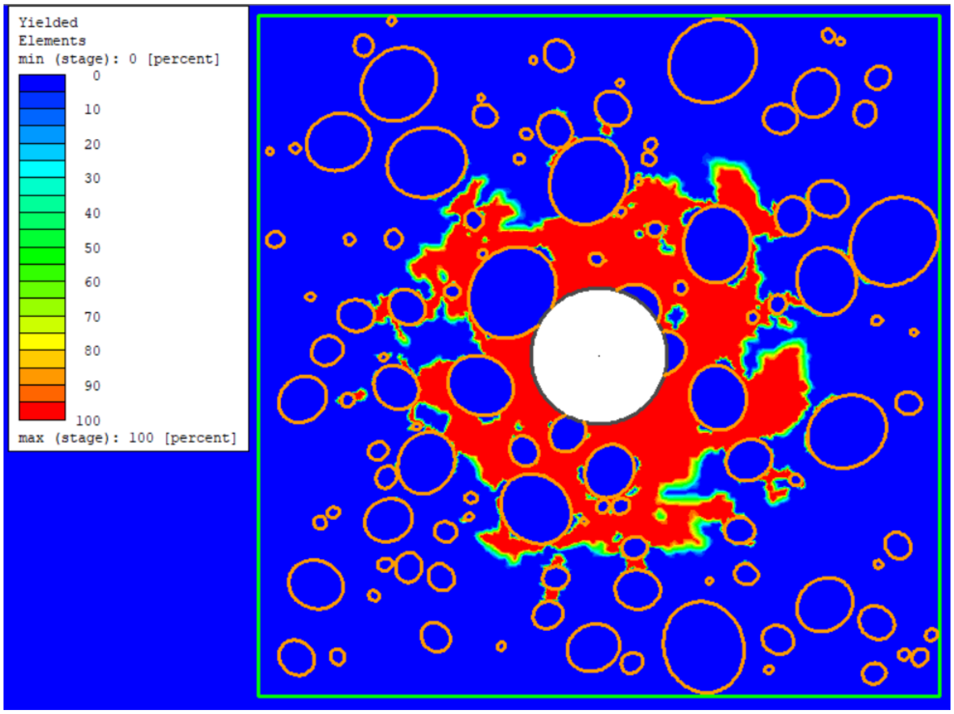

Figure 87- Plasticization around the tunnel at total relaxation associated with extraction 7 for 25%VBP with 100% (same as) matrix properties of the interface. Model 0.25_7_1.0

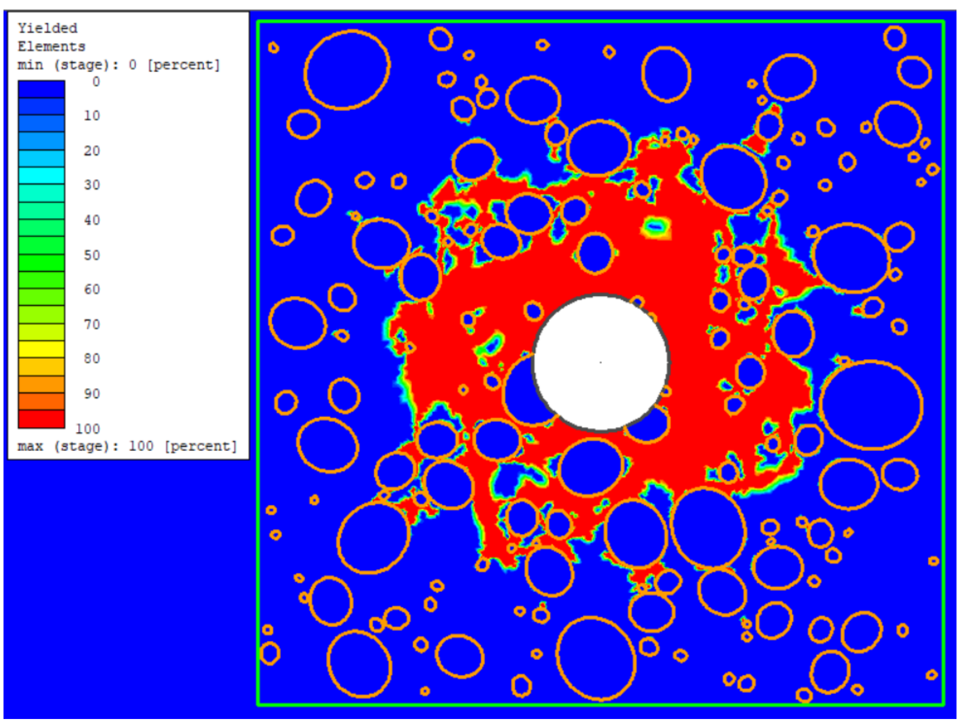

Figure 88- Plasticization around the tunnel at total relaxation associated with extraction 8 for 25%VBP with 100% (same as) matrix properties of the interface. Model 0.25_8_1.0

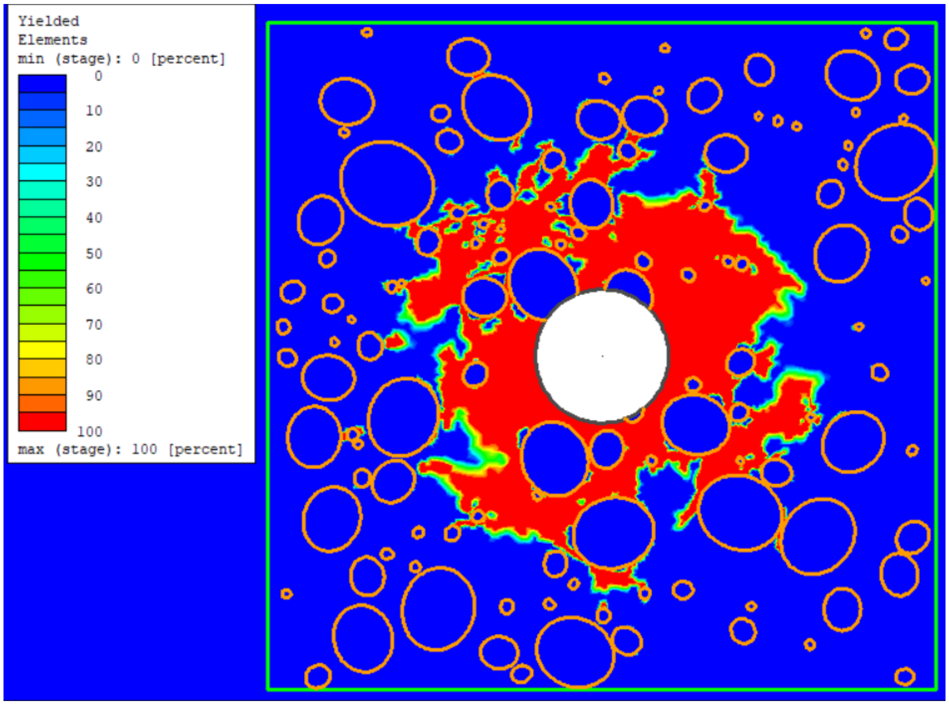

Figure 89- Plasticization around the tunnel at total relaxation associated with extraction 9 for 25%VBP with 100% (same as) matrix properties of the interface. Model 0.25_9_1.0

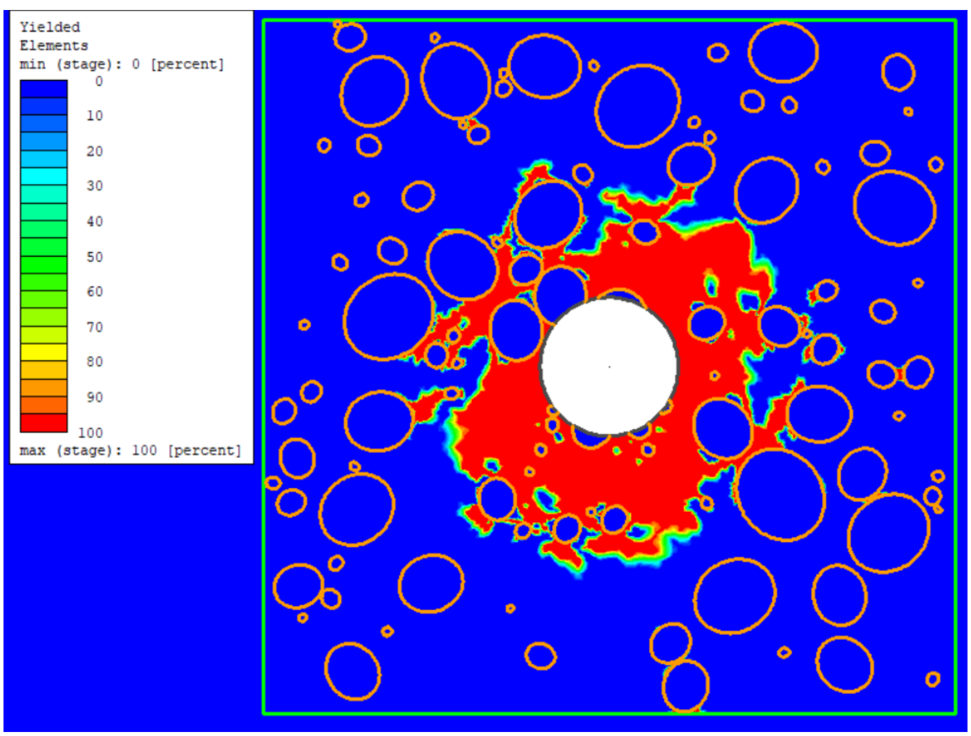

Figure 90- Plasticization around the tunnel at total relaxation associated with extraction 10 for 25%VBP with 100% (same as) matrix properties of the interface. Model 0.25_10_1.0

Annex B

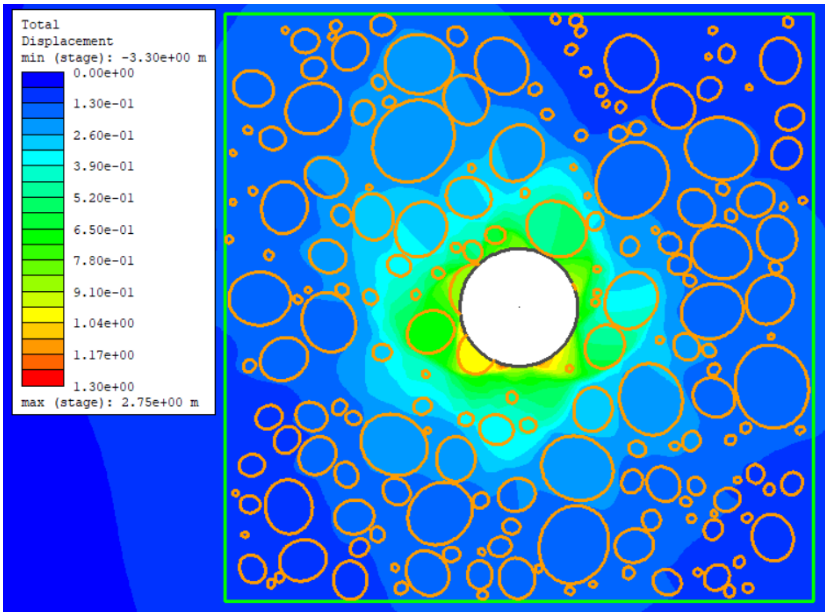

Figure 91- Model 0.40_4_0.25 (4th random draw of block orientation with VBP = 40% with properties equal to 25% of the matrix), Trend of radial displacement, Definition of Joint Boundaries in orange

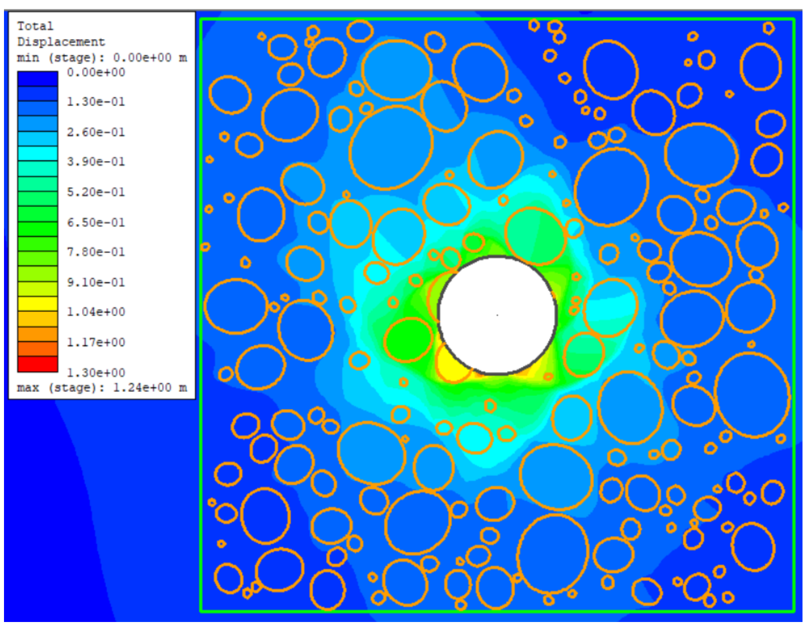

Figure 92- Model 0.40_4_0.5 (4th random draw of block orientation with VBP = 40% with properties equal to 50% of the matrix), Trend of radial displacement, Definition of Joint Boundaries in orange

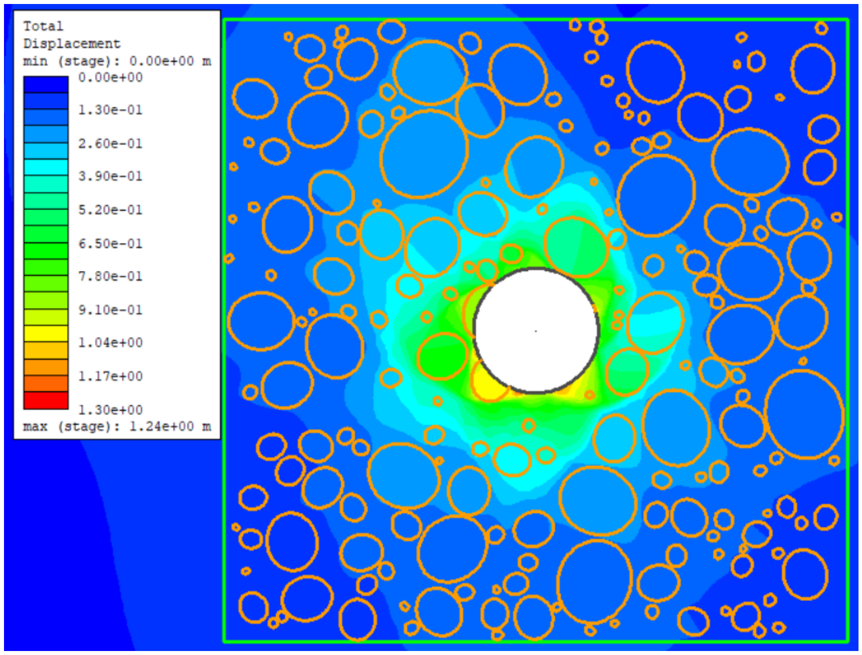

Figure 93- Model 0.40_4_0.75 (4th random draw of block orientation with VBP = 40% with properties equal to 75% of the matrix), Trend of radial displacement, Definition of Joint Boundaries in orange

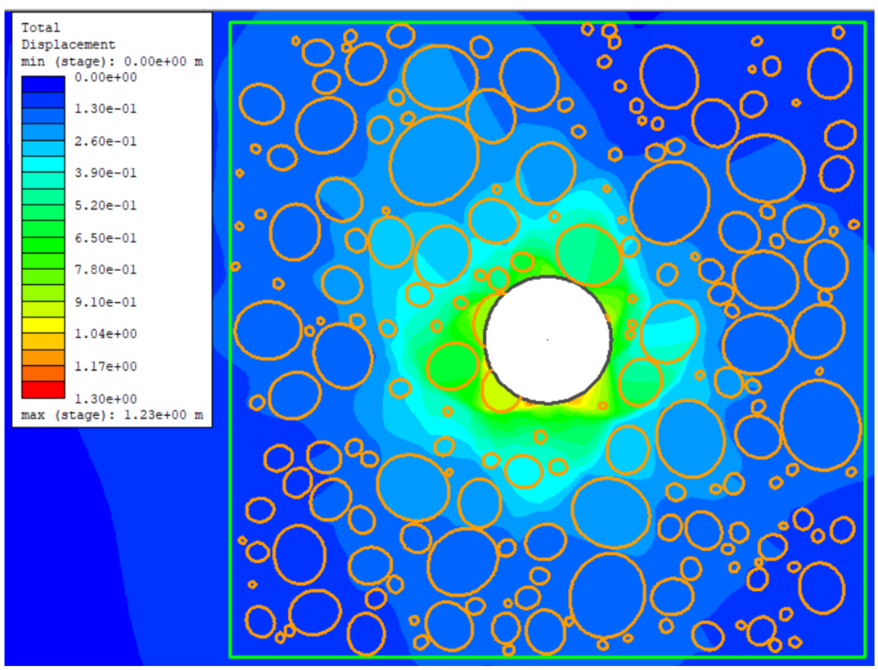

Figure 94- Model 0.40_4_1.0 (4th random draw of block orientation with VBP = 40% with properties equal to that of the matrix), Trend of radial displacement, Definition of Joint Boundaries in orange

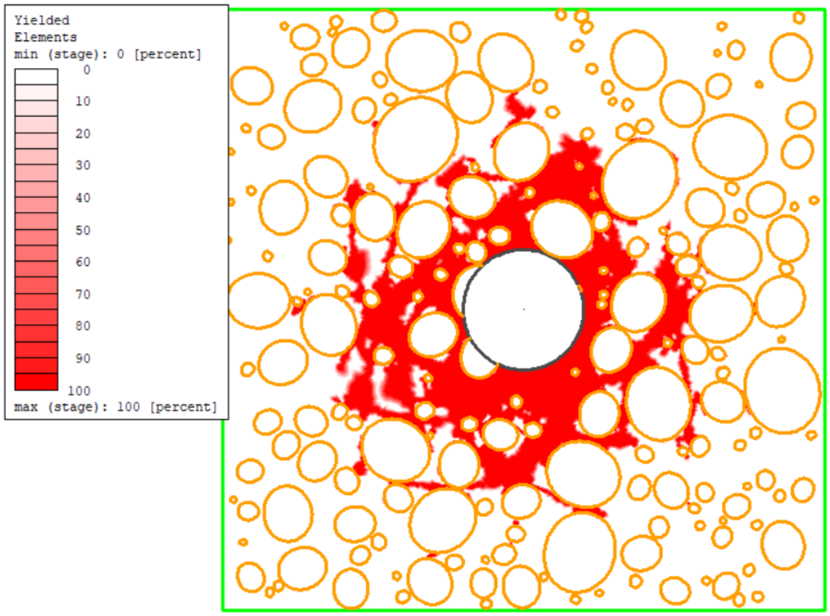

Figure 95- Model 0.40_4_0.25 (4th random draw of block orientation with VBP = 40% with properties equal to 25% of the matrix), Trend of yielding zones

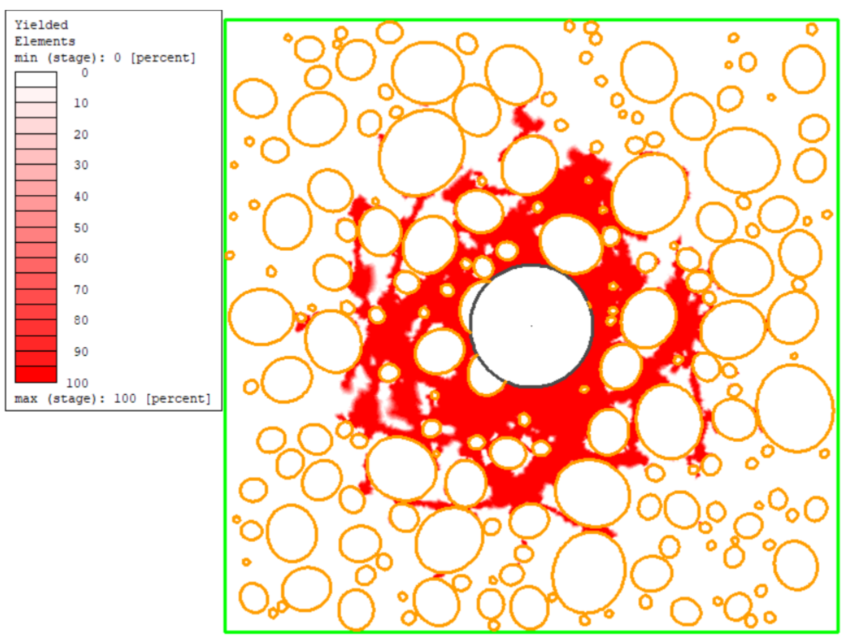

Figure 96- Model 0.40_4_0.50 (4th random draw of block orientation with VBP = 40% with properties equal to 50% of the matrix), Trend of yielding zones

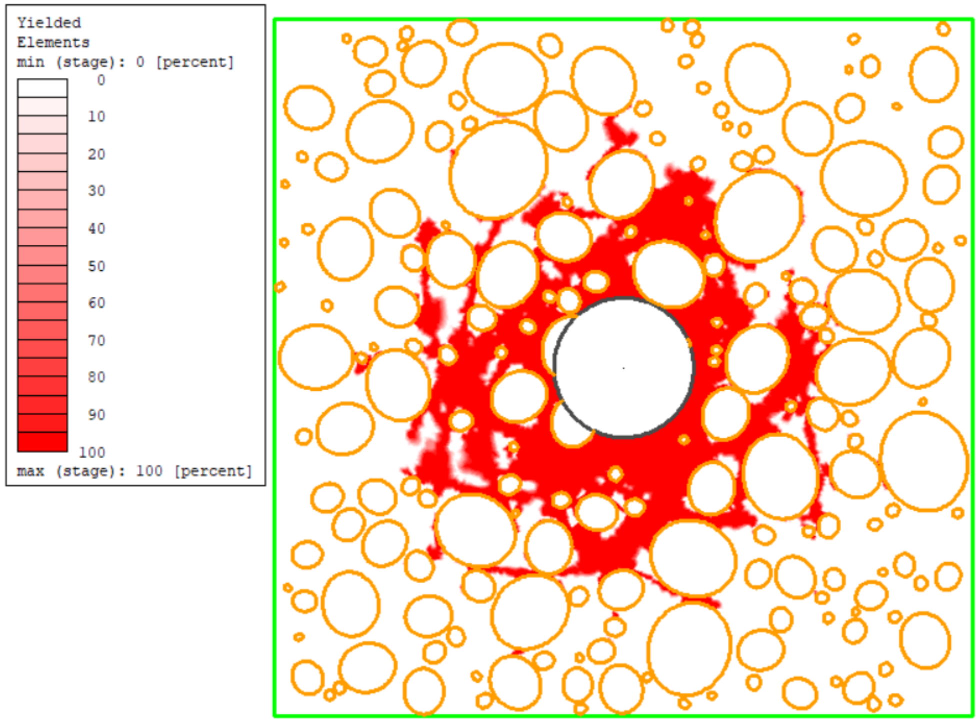

Figure 97- Model 0.40_4_0.75 (4th random draw of block orientation with VBP = 40% with properties equal to 75% of the matrix), Trend of yielding zones

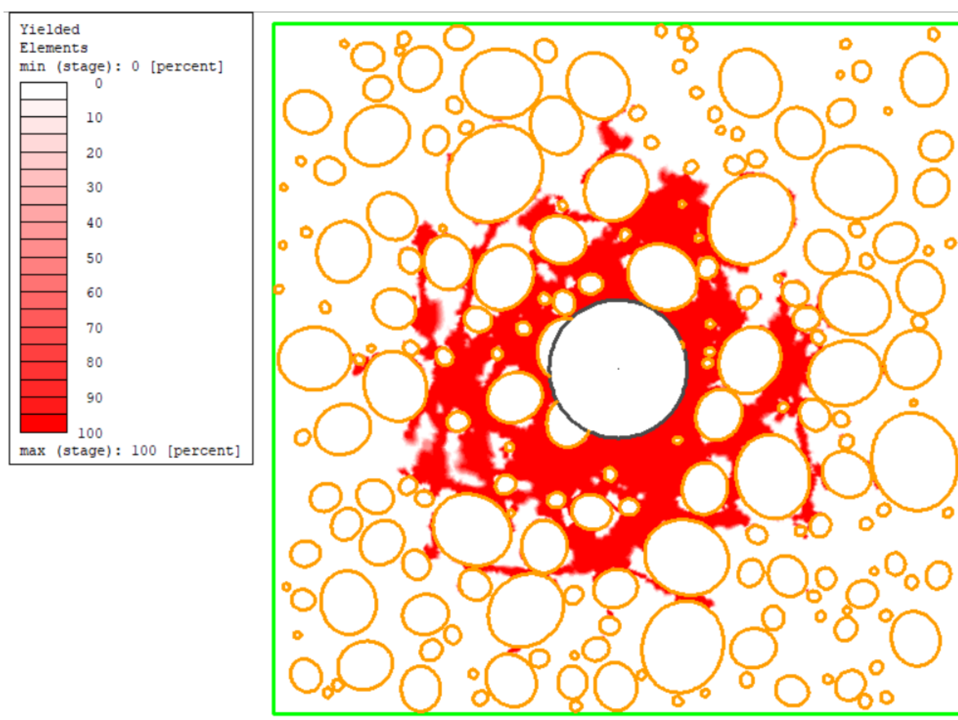

Figure 98- Model 0.40_4_1.0 (4th random draw of block orientation with VBP = 40% with properties equal to that of the matrix), Trend of yielding zones

Annex C

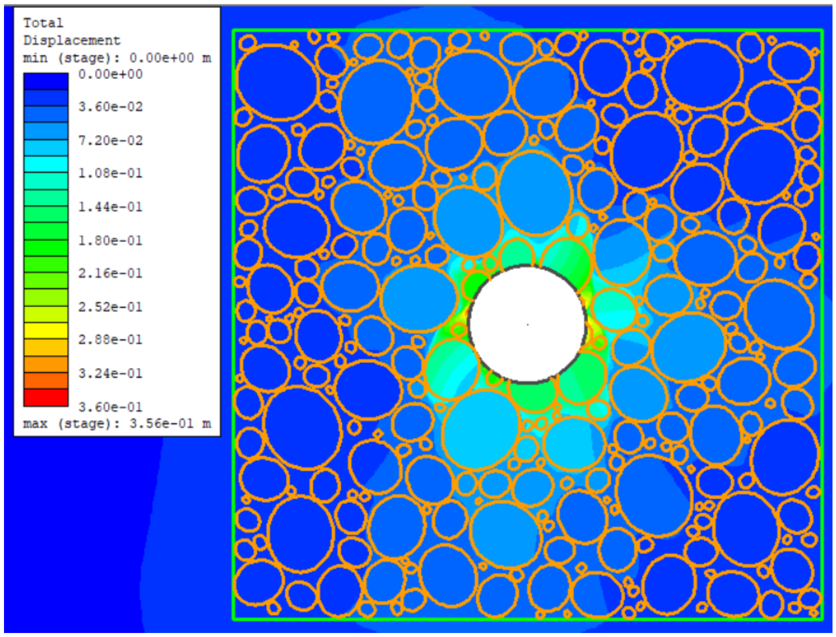

Figure 99- Model 0.70_1_0.25 (1st random draw of block orientation with VBP = 70% with properties equal to 25% of the matrix), Trend of radial displacement, Definition of Joint Boundaries in orange

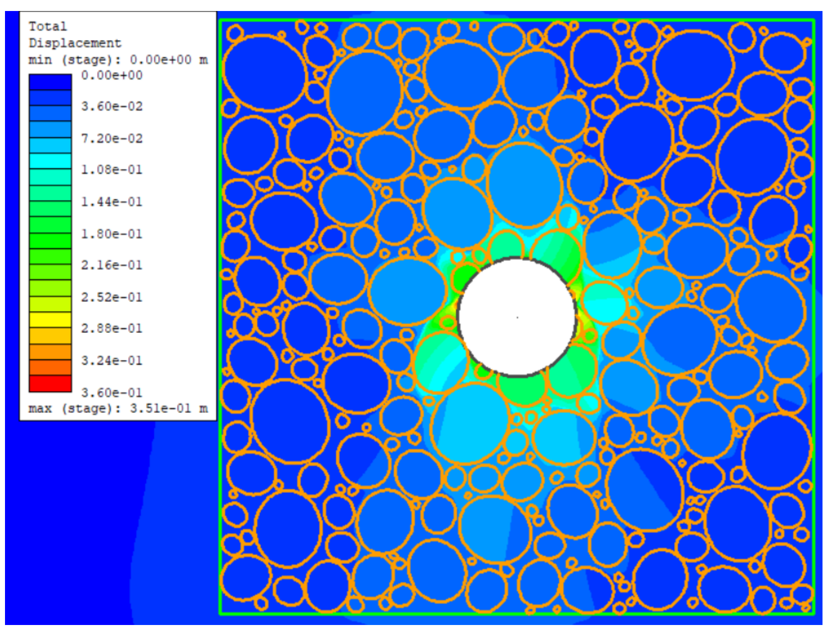

Figure 100- Model 0.70_1_0.5 (1st random draw of block orientation with VBP = 70% with properties equal to 50% of the matrix), Trend of radial displacement, Definition of Joint Boundaries in orange

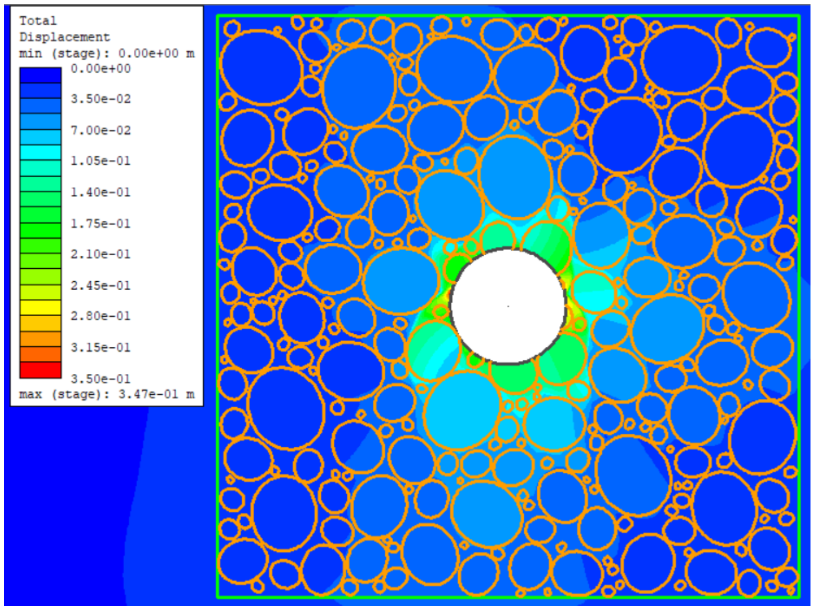

Figure 101- Model 0.70_1_0.75 (1st random draw of block orientation with VBP = 70% with properties equal to 75% of the matrix), Trend of radial displacement, Definition of Joint Boundaries in orange

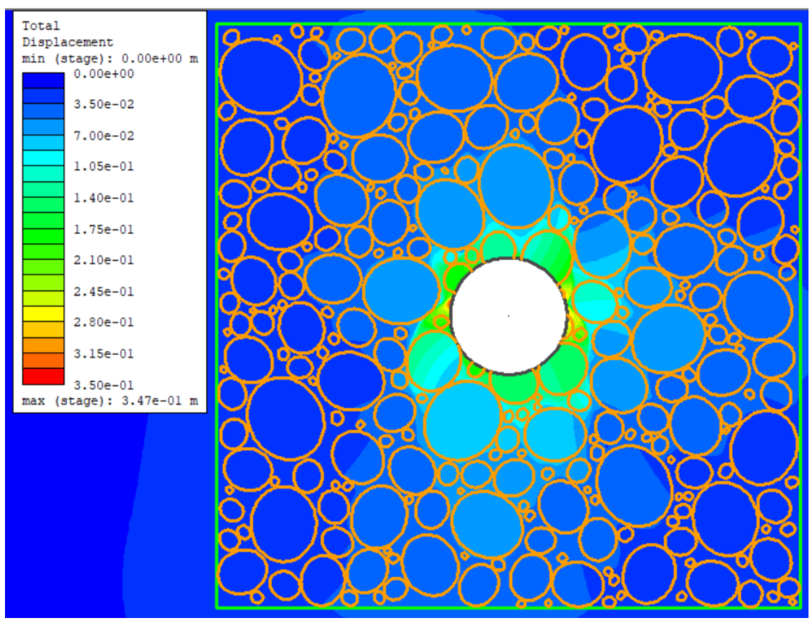

Figure 102- Model 0.70_1_1.0 (1st random draw of block orientation with VBP = 70% with properties equal to 100% of the matrix), Trend of radial displacement, Definition of Joint Boundaries in orange

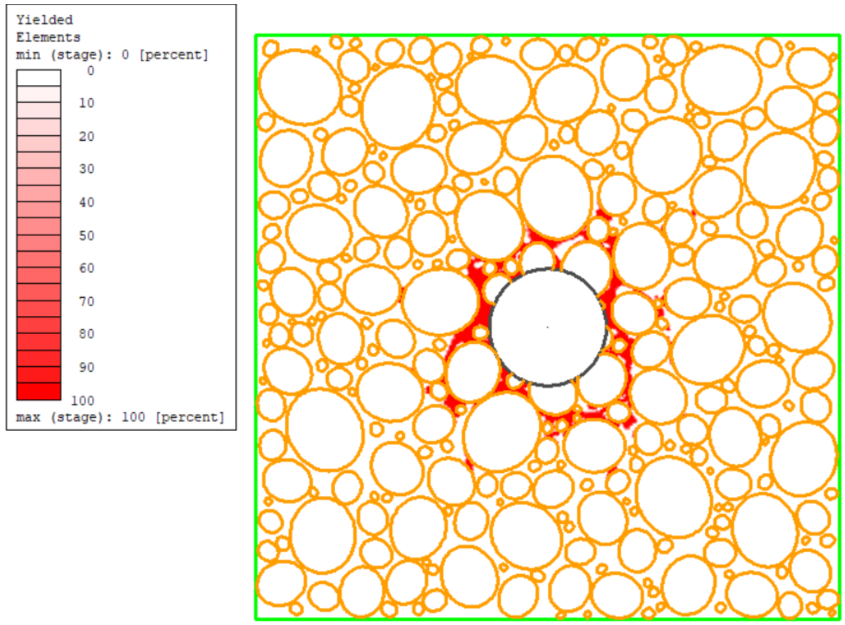

Figure 103- Model 0.70_1_0.25 (1st random draw of block orientation with VBP = 70% with properties equal to 25% of the matrix), Trend of yielding zones

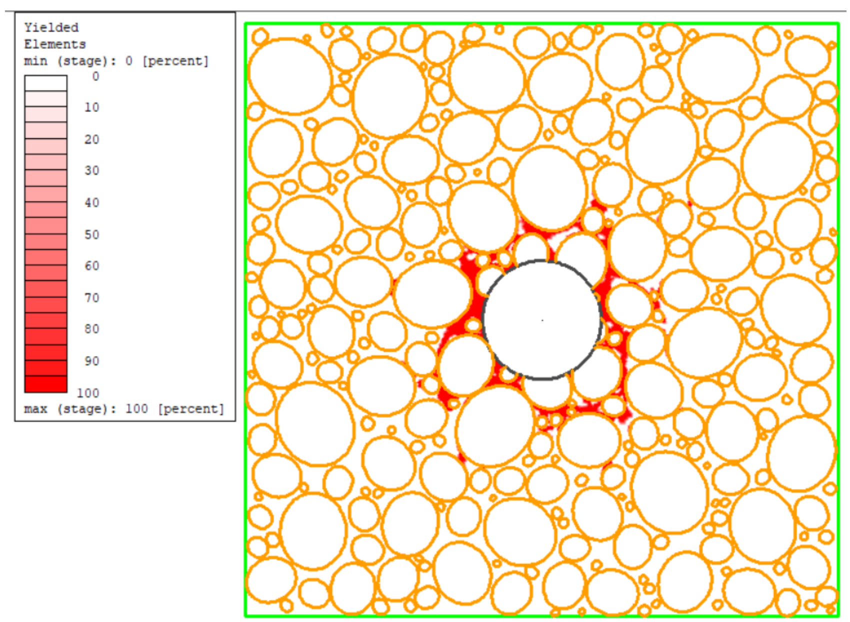

Figure 104- Model 0.70_1_0.5 (1st random draw of block orientation with VBP = 70% with properties equal to 50% of the matrix), Trend of yielding zones

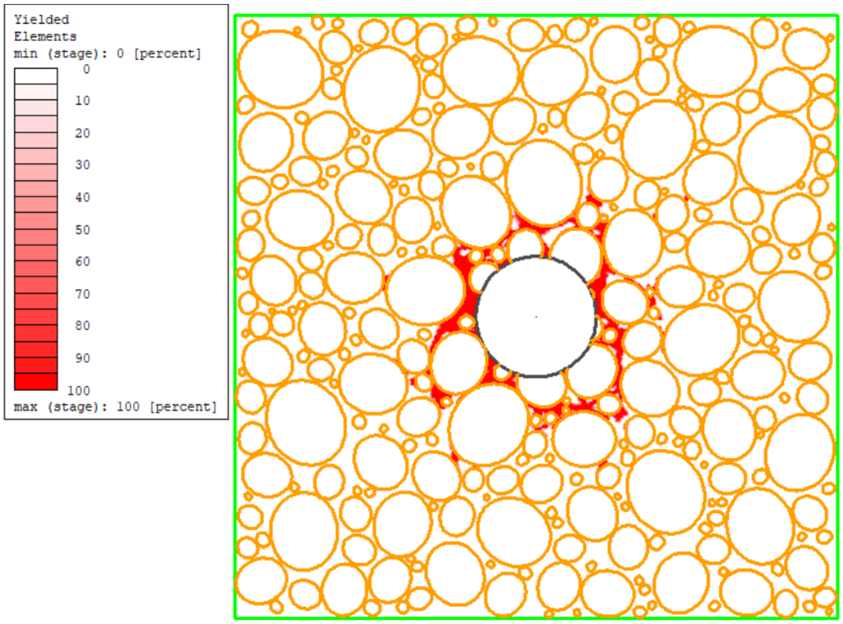

Figure 105- Model 0.70_1_0.75 (1st random draw of block orientation with VBP = 70% with properties equal to 75% of the matrix), Trend of yielding zones

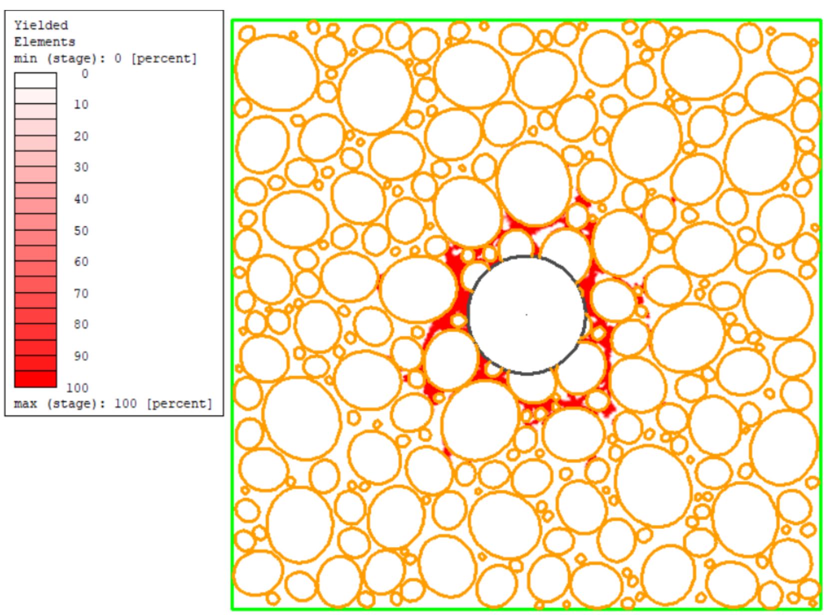

Figure 106- Model 0.70_1_1.0 (1st random draw of block orientation with VBP = 70% with properties equal to 100% of the matrix), Trend of yielding zones